Taras Shevchenko National University of Kyiv
Astronomical Observatory

Astronomy and Space Physics in the Kyiv University

Book of Abstracts

International Conference
dedicated to the 175th of the Astronomical Observatory of Taras Shevchenko National University of Kyiv

May 27 – 29, 2020
Kyiv, Ukraine

Scientific Organizing Committee

Chair: L. Hubersky (Ukraine)
Vice-chairs: O. Zhylinska (Ukraine), V. Efimenko (Ukraine), V. Ivchenko (Ukraine)
Conference Secretary: I. Luk'yanyk (Ukraine)

Scientific Committee Members:

Antonio Del Popolo (Italy), Bohdan Novosyadly (Ukraine), Bohdan Hnatyk (Ukraine), Gennadi Milinevsky (Ukraine), Igor Karachentsev (Russia), Mykola Gordovsky (United Kingdom), Peter Berczik (Ukraine), Piotr Homola (Poland), Roman Kostyk (Ukraine), Sergiy Andrievsky (Ukraine), Sergiy Parnovsky (Ukraine), Vadym Kaydash (Ukraine), Valery Shulga (Ukraine), Valery Zhdanov (Ukraine), Vera Rosenbush (Ukraine), Vsevolod Lozitsky (Ukraine), Yaroslav Yatskiv (Ukraine), Yury Izotov (Ukraine)

Local Organizing Committee

Chair: V. Efimenko (Ukraine)
Vice-chair: I. Luk'yanyk (Ukraine)
Secretary: V. Danylevsky (Ukraine)
E-mail: **conference@observ.univ.kiev.ua**, **aoconf@ukr.net**

Local Committee Members:

O. Mozgova, R. Hnatyk, S. Zaichenko, V. Ponomarenko, I. Izotova, O. Sergienko, I. Yakovkin

Place of the meeting (Web-conference on zoom-platform)
Astronomical observatory of the Taras Shevchenko national university of Kyiv, Observatorna str., 3

CONTENTS

SYSTEM

ПЛЕНАРНА СЕСІЯ

PLENARY SESSION

175 YEARS OF THE ASTRONOMICAL OBSERVATORY OF THE KYIV UNIVERSITY

V.M. Efimenko, V.M. Ivchenko

Taras Shevchenko National University of Kyiv, Kyiv, Ukraine
efim@observ.univ.kiev.ua

In 2020, the Astronomical Observatory celebrates its 175th anniversary. The first director of the Observatory was Professor Vasyl Fedorovich Fedorov. Under his leadership, a place for the Observatory was chosen, a project was developed (architect V. Beretti), the main building was built, and the main astronomical instruments of the Observatory were ordered. He also prepared and taught basic courses in astronomy and geodesy for university students. After him, the position of professor of astronomy and director of the Astronomical Observatory in the Observatory was held by famous astronomers A.P. Shidlovsky, M.F. Khandrikov, R.P. Vogel, S. D. Chornyi.

Shortly before the Second World War, the Observatory and the Department of Astronomy were headed by Professor S. K. Vsekhsvyatsky, whose name is associated with the beginning of systematic large-scale research in cometary, solar and solar-terrestrial physics. Under his leadership, university heliophysicists, beginning in the late 1940s, performed a series of high-quality observations of the solar corona, equipping numerous expeditions to areas of total solar eclipses. It was at the University that the nature of the solar corona was first closely understood: in the late 1950s, the concept of a dynamic corona (E. A. Ponomarev) was developed, which, according to Yu. Parker (USA), was called the "solar wind".

University astronomers have been involved in ground-based space missions to Halley's Comet (VEGA) and to Mars (FOBOS). Scientists at the university discovered two comets (Churyumov-Gerasimenko, 1969 and Churyumov-Solodovnikov, 1986). According to the decision of the European Space Agency, the ROSETTA spacecraft was sent to one of them (67P / Churyumov – Gerasimenko). This is the first comet to which the spacecraft flew (August 6, 2014), became its satellite and accompanied it through the entire inner part of the solar system until September 30, 2016, when the spacecraft ended its active existence on the comet's surface, transmitting scientific material to Earth. According to the heads of the European Space Agency, the scientific project "ROSETTA" has become one of the most significant scientific projects in recent years.

Kyiv University was the initiator and organizer of Ukraine's accession to the International Scientific Program CTA (Cherenkov Teleskop Array). The STA project is extremely important for the development of not only high-energy astrophysics, but also the physics of fundamental interactions, as its issues include both astrophysical problems and searches for dark matter particles, verification of Lorentz invariance, search for gamma rays from gravitational wave sources, etc.

Over the past 175 years, university astronomers have made important contributions to research in various areas of astronomical science, training of qualified personnel. Thus, in the years after the Second World War, the university graduated 737 astronomers, among the graduates of the department 38 doctors of sciences, 184 candidates, 2 academicians of NASU (Steshenko, Izotov), 1 corresponding member NASU (Churyumov), 13 laureates of the State Prizes in the field of science and technology of the Ukraine. University astronomers receive important scientific results that are highly valued by the world scientific community. Today, the Astronomical Observatory is a world-renowned scientific institution with modern scientific areas, a qualified team of scientists capable of solving current scientific problems of modern astronomy.

Aerosol investigation in the Earth atmosphere from the Aerosol-UA orbital mission

I. Syniavskyi[1], Ya. Yatskiv[1], M. Sosonkin[1], V. Danylevsky[2], Ye. Oberemok[2], G. Milinevskyi[1,2], A. Bovchaliuk[1], Zh. Dlugach[1], I. Fesianov[2], Yu. Ivanov[1], Yu. Yukhymchuk[1]

[1]Main Astronomical Observatory of the NAS of Ukraine, Kyiv, Ukraine
[2]Taras Shevchenko National University of Kyiv, Kyiv, Ukraine
syniavskyi@gmail.com

The purpose of the Aerosol-UA experiment is to carry out high precision photopolarimetric measurements in order to perform the qualitative and quantitative study of the aerosol characteristics in the Earth's atmosphere on regional and global scale. The key elements of the report are: (1) the use of modern algorithms and software for modeling characteristics of electromagnetic radiation scattered by complex aerosol particles; (2) the theoretical description of the space measurement methods and design used for orbital aerosol monitoring; (3) the technical improvement and data validation based on the AERONET aerosol network. The last has already been supported by the considerable practical results obtained in determining

the effects of aerosol on local climate conditions.

The Aerosol-UA remote sensing concept is based on using two onboard instruments: (1) the multispectral Scanning Polarimeter (ScanPol) and (2) the MultiSpectral Imaging Polarimeter (MSIP). Being installed at the YuzhSat satellite platform, these two polarimeters are designed to carry out high precision radiance and polarization measurements. The ScanPol (MSIP) allow measuring three Stokes parameters *I*, *Q* and *U* of the sunlight scattered by the atmospheric aerosols and the earth surface from about 200 (15) viewing directions. The MSIP imager provides the aerosol parameter measurements and aerosol/clouds separation with wide angle swath, which is important for the ScanPol data corrections. The ScanPol and MSIP, combined together, allow multi-angular measurements of the polarized radiance. The ScanPol allows the both instruments cross-calibration procedure since the overlapping of fields of view for two instruments. The further work will be concentrated both on study of the effects of complex morphology of aerosol particles on their scattering characteristics and development of the algorithms for calculation the intensity and polarization of reflected radiation for realistic models of the Earth's atmosphere.

The second task of the study is the theoretical description for space monitoring hardware including the engineering and computer simulation of the new hardware. The improvement of existing facilities, development of networks and conducting on their basis local monitoring of the composition and quantity of aerosols also are discussed. The orbital-based polarimetry allows to develop realistic model of the spatial distribution of aerosols across the globe over several hours/days. Theoretical conclusions about the effects of the morphology of aerosol particles on the values of the intensity and polarization of the scattered sunlight will help to provide the evaluation of the optimal composition of equipment for the aerosol space monitoring and can improve the understanding of the estimated levels of measurement accuracy and polarimetric efficiency of the space orbital equipment.

Gravitational lensing in the era of Gaia

J. Surdej and the GraL collaboration(*)

Space Science, Technologies and Astrophysics Research (STAR) Institute, Université de Liège, Institut d'Astrophysique et de Géophysique, Liège, Belgium

(*) L. Delchambre, A. Krone-Martins, O. Wertz, C. Ducourant, L. Galluccio, J. Klüter, F. Mignard, R. Teixeira, S.G. Djorgovski, D.

Stern, M.J. Graham, U. Bastian, J. Wambsganss, J.-F. Le Campion, E. Slezak, S. Scarano, A. Drake

After recalling the basic principles underlying the formation of atmospheric and gravitationally lensed mirages, we shall describe a simple optical lens experiment which accounts for all types of image configurations observed among presently known gravitational lens systems.

We shall then give a detailed report on a recent systematic search for multiply imaged quasars based upon observations carried out with Gaia. Using the Singular Isothermal Sphere (SIS) and Singular Isothermal Ellipsoid (SIE) lens models, we shall first present the numbers of multiply imaged quasars expected in the Gaia survey. Based upon the non-singular isothermal ellipsoid lens model in the presence of an external shear (nSIEγ), we shall after describe the technique used to identify in the second data release of Gaia (DR2) the candidates and will finally present first observational results obtained with the Keck, VLT, NTT and Gemini telescopes.

A brief update on the 4m International Liquid Mirror Telescope project also aimed at the detection of multiply imaged quasars will be shortly presented.

Recent Progress in Understanding Type II Spicules Based on data from the Goode Solar Telescope

Vasyl Yurchyshyn

Big Bear Solar Observatory ,Center for Solar Research. New Jersey Institute
of Technology, New Jersey, USA

Solar spicules are dynamic jet-like chromospheric structures that have been observed since 1877 and yet we still do not have clear understanding of this phenomenon. Things became more complicated with the discovery of a new sub-class of spicules called type II spicules, which are thought to have a driving mechanism different from that driving the well known "classical" spicules.

The interest to those events is fuelled by two major science questions. The first one is related to solar magnetism and is concerned with the process of emergence of small-scale magnetic fields and the transfer of injected magnetic energy into the large-scale coronal fields. Understanding the formation mechanism of solar spicules would helps us to better understand

the small-scale solar magnetism. The second question isrelated to the coronal heating. Are these small-scale energy release events capable of heating the solar corona? If so, how the needed energy is stored, transported and released?

In this presentation I will review recent progress in the study of type II spicules. Three different formation mechanisms were advocated in various studies basedon high resolution data obtained by the Goode Solar Telescope (GST). These are mainly based on the idea of magnetic reconnection although each of them suggested different magnetic configurations involved inthe process.

Opposition effect of asteroids: our knowledge after 65 years of investigations

I.N. Belskaya[1], V.G. Shevchenko[2,1]

[1]Institute of Astronomy, V.N. Karazin Kharkiv National University
[2]Department of Astronomy and Space Informatics of V. N. Karazin Kharkiv National University
irina@astron.kharkov.ua

The opposition effect in the magnitude phase dependence of an asteroid was first measured in 1955 by T. Gehrels, who introduced the term “opposition effect” to define a pronounced nonlinear increase in brightness close to opposition. Further observations showed that this is a typical phenomena for atmosphereless bodies, which was explained by shadowing effect in the regolith layer. The discovery of a narrow opposition surge for high-albedo asteroids and satellites, which was impossible to explain by the shadowing effect, led to introduce the coherent-backscattering mechanism explaining this phenomenon. With increasing number of observational data, it was shown that the opposition effect amplitude depends on albedo in non-monotonic way. This was explained by a combined influence of shadow hiding and coherent backscattering. Both mechanisms contribute to the moderate albedo surfaces, while shadow hiding dominates for the dark surfaces, and the coherent backscattering dominates for the bright surfaces. Although physical nature of opposition phenomena is well-known, its interpretation in terms of surface physical properties is ambiguous. Over the last twenty years, high-quality magnitude dependencies were measured for asteroids of main composition types and different dynamical classes. We will discuss recent progress in study of opposition effect of asteroids and the

relationships between phase-curve parameters and physical properties of asteroids.

Polarization of comets: Clues to understanding the microphysics of their dust

E. Zubko

Humanitas College, Kyung Hee University, 1732 Deogyeong-daero, Yongin-si, Gyeonggi-do 17104, Republic of Korea

Interaction of unpolarized solar radiation with cometary dust particles produces linearly polarized scattered radiation. The polarimetric response is dependent on the phase angle α, which subtends from the Sun to the observer, with the comet at its vertex. The angular profile of polarization consists of two branches, the negative polarization (i.e., electric field vector is coincident with the scattering plane) near backscattering ($\alpha < 30°$) and positive polarization (i.e., electric field vector lies perpendicular to the scattering plane) at larger phase angles ($\alpha > 30°$). Polarization measured in various comets in the visible ranges between $P_{min} = –6\%$ that occurs at $\alpha_{min} = 10–15°$ and $P_{max} = 35\%$ predominantly appearing at $\alpha_{max} > 90°$. The latter fact unambiguously suggests presence of at least two types of dust particles having significantly different material absorption. In one of them imaginary part of refractive index is constrained to $\mathrm{Im}(m) \leq 0.02$ that is consistent with Mg-rich silicates; whereas, in another one to $\mathrm{Im}(m) > 0.3$, that is representative of various organics and amorphous carbon. It is worth noting that both these components have been found in comets *in situ*. Vast majority of polarimetric observations can be fitted using those two end-members. Within such approach, significant dispersion of P_{max} in comets can be explained in terms of different relative abundance of the silicate and carbonaceous particles. For instance, coma of comets with low P_{max} is largely dominated (up to 100%) with silicate particles; whereas, in the high-P_{max} comets their volume fraction is about 25% or less. This approach also suggests that temporal variations of polarization that have been observed in some comets could indicate changing relative abundance of the silicate and carbonaceous particles in their coma. Finally, one needs to note that the two-component model of coma also explains fast and dramatic temporal variations of the photometric color that were observed in some comets. More details on performance of the two-component model could be found in: https://doi.org/10.1093/mnras/stu480;

https://doi.org/10.1016/j.pss.2015.09.020;
https://doi.org/10.1093/mnras/stx1004;
https://doi.org/10.1093/mnras/stz669; and
https://doi.org/10.1016/j.icarus.2019.113471.

Багатоканальна астрономія: сьогодення та майбутнє (пленарний)

О. Сергієнко

Астрономічна обсерваторія Київського національного університету імені Тараса Шевченка,
Київ, Україна

Багатоканальна астрономія на сьогоднішній день є наймолодшим розділом астрономії. Спостереження 1940-х років вказали на сонячне походження частини космічних променів, у 1987 році детектовані нейтрино від спалаху наднової SN 1987A, однак ще 5 років тому практично вся астрономічна інформація отримувалась за допомогою електромагнітних хвиль різної довжини. Детектування у вересні 2015 року першого гравітаційно-хвильового джерела GW150914 та у серпні 2017 року першого гравітаційно-хвильового джерела з електромагнітним відповідником GW170817, а також ідентифікація у вересні 2017 року можливого електромагнітного відповідника джерела нейтринної події IceCube-170922A ознаменували початок епохи багатоканальних спостережень. Ми обговорюємо сьогоднішній стан та перспективи багатоканальної астрономії у найближчі 2 десятиліття.

Prediction of solar activity with the solar background magnetic field and exploration of its links with solar-terrestrial processes

V.V. Zharkova

Northumbria University, Newcastle, UK

In this talk I will overview the prediction of solar activity using a new proxy –solar background magnetic field. I will explain how to distil the main parameters of dynamo waves with Principal Component Analysis (PCA) from the full disk solar background magnetic field observed in cycles 21-23 by Wilcox Solar Observatory. This PCA process acts on

magnetic waves of the Sun similar to the separation with a glass prism of electromagnetic waves of different wavelengths from white light emission. This PCA analysis allowed us to detect magnetic waves in the Sun to appear in pairs, with the first pair of Principal Components accounting for 40% of the data variance, or 67% by standard deviation. The both magnetic waves travel from the opposite hemispheres to the Northern hemisphere (odd cycles) or to Southern hemisphere (even cycles), with the phase shift between the waves increasing with a cycle number.

Using the symbolic regression analysis based on Hamiltonian invariance, we managed to derive the fundamental mathematical formulae describing the both waves. The summary curve of the two waves is shown to closely fit average sunspot numbers in cycles 21-24 and predict with high accuracy the solar activity in cycle 24.

These two magnetic waves were interpreted with double dynamo model arising from the background (poloidal) magnetic field combined with the sunspot (toroidal) magnetic field induced by dipole magnetic sources in two layers of the solar interior showing ballpark fit to the derived wave patterns. This model was expanded by adding the next set of magnetic waves generated by quadruple magnetic sources which improved the fit of summary curve to the current index of solar activity defined by average sunspot numbers.

Using the derived formulae for summary curve we extrapolated the solar activity model forward by 1200 and backward by 3000 years. This allowed us to discover grand solar cycle of 350-400 years caused by beating effect of two waves, which are separated by grand solar minima, e.g. Maunder, Wolf, Oort or Homeric minima. This approach predicts the occurrence modern grand solar minimum in cycles 25-27 (2020-2053) with the properties of Maunder minimum.

The restoration of the solar irradiance during the last 400 year shows its strong decrease during the period of the Maunder Minimum by a magnitude of about 3 W/m^2. This amount of the solar radiance reduction was converted into reduction of the average temperature of the Earth. In particularly, in England the average temperature in 17 century dropped to ~8.5C versus 10.5C in 20^{th} century. This drop of temperature led to freezing rivers and lakes in England, and all over the Europe.

Furthermore, I present the baseline oscillations of solar background magnetic field with a period of 2100 years that is close to the 2200 years period of oscillations (Hallstatt's cycle) detected in the terrestrial carbon ^{14}C isotope abundances and confirmed with the wavelet analysis of solar irradiance in the past 12 millennia. I will show that solar inertial motion

(SIM) can cause these millennial variations because of a change of the distance between the Sun and Earth using the mathematical properties of elliptical orbits. Using the current JPL ephemeris for reducing aphelion and increasing perihelion distances I will demonstrate that the S-E distances averaged by time or by arc are decreasing in the current millennium until 2700. The current decrease started from the Maunder minimum reducing by 0.00027 au per 100 years, or by 0.0027 au per 1000 years. We present the estimation of solar irradiance variations caused by these variations of the S-E distance, which are comparable with the observed variations of the solar irradiance measured by the different satellites.

We also estimate the baseline temperature variations since Maunder Minimum caused by the increase of solar irradiance caused by the recovery from grand solar minimum and by reduction of the S-E distance caused by SIM. These estimations show that the Sun will still continue moving towards the Earth in the next 700 years that will result in the increase of the baseline terrestrial temperature by to 2.5-3.0°C in 2700. These variations of solar irradiance will be over-imposed by the variations of solar activity of 11 cycles and the two grand solar minima occurring in 2020-2053 and 2370-2415 caused by the double dynamo actions inside the Sun.

Since cycle 25 still have about 80% of solar activity of cycle 24, I will also explore acceleration of particles during their passage through reconnecting current sheets with magnetic islands occurring in the solar corona and interplanetary space using particle-in-cell approach. I will demonstrate that current sheets with multiple X-nullpoints are very effective accelerator of energetic particles. I will consider coalescent and squashed magnetic islands formed in the current sheets with different thicknesses, ambient density and mass ratios for different magnetic field topologies, and simulate energy, density and pitch-angle distributions of accelerated particles. I will show that distinct populations of two groups of particles, transit and bounced ones have very different energy and asymmetric pitch-angle distributions associated with the magnetic field parameters. I will demonstrate the simulated pitch angle distributions of accelerated particles for a few cross-sections of the spacecraft paths through the current sheets with magnetic islands and compare the outcomes with the in-situ observations of solar wind particles. This comparison detects locally generated suprathermal electrons, which account for the counter-streaming 'strahls' often observed in the pitch-angle distribution spectrograms of the satellites crossing local current sheets in the heliosphere.

АСТРОФІЗИКА, ГРАВІТАЦІЯ І КОСМОЛОГІЯ

ASTROPARTICLE PHYSICS, GRAVITATION AND COSMOLOGY

Higher dimensional massive Brans-Dicke gravity in the weak-field limit: observational constraints

O. Akarsu[1], A. Zhuk[2], A. Chopovsky[2], E. Yalcinkaya[1]

[1]Department of Physics, Istanbul Technical University, Maslak, Istanbul, Turkey
[2]Astronomical Observatory, Odessa National University, Odessa, Ukraine

We consider higher-dimensional massive Brans-Dicke theory with Ricci-flat internal space. The background model is perturbed by a massive gravitating source which is pressureless in the external (observable space) but has an arbitrary equation-of-state parameter Ω in the internal space. We obtain the exact solution of the system of linearized equations for the perturbations of the metric coefficients and scalar field. For a massless scalar field, relying on the fine-tuning between the Brans-Dicke parameter ω and Ω, we demonstrate that the model does not contradict gravitational tests relevant to the parameterized post-Newtonian parameter γ, and (ii) the scalar field is not ghost in the case of nonzero $\Omega \sim O(1)$ along with the natural value $|\omega| \sim O(1)$. In the general case of a massive scalar field, the metric coefficients acquire the Yukawa correction terms, where the Yukawa mass scale m is defined by the mass of the scalar field. For the natural value $\omega \sim O(1)$, the inverse-square-law experiments impose the following restriction on the lower bound of the mass: $m \geq 10{-}11$ GeV. The experimental constraints on γ requires that Ω must be extremely close to $-1/2$.

New estimation of supermassive black hole mass in NGC 1068

N.A. Akerman[1], E.Yu. Bannikova[1,2], A.V. Sergeyev[1,2], P.P. Berczik[3], M.V. Ishchenko[3]

[1]V.N. Karazin Kharkiv National University, Kharkiv, Ukraine
[2]Institute of Radio Astronomy of National Academy of Sciences of Ukraine, Kharkiv, Ukraine
[3]Main Astronomical Observatory, National Academy of Sciences of Ukraine,
Kyiv, Ukraine

ALMA observations of the Sy2 galaxy NGC~1068 have revealed a structure in its nucleus that can be associated with a dusty torus.

Observational velocity maps demonstrate orbital motion in the torus, while distribution non-uniformity in dispersion maps is an indirect proof of its clumpy structure. To explain the observational data we provide numerical N-body simulations in the framework of a clumpy torus model. We obtain the supermassive black hole mass for NGC~1068 $5\times 10^6 M_\odot$ from velocity maps having taken the self-gravity of the torus and obscuration of clouds into account. This mass is consistent with bolometric luminosity and is larger than the one obtained from the suggestion of keplerian disk motion only. Temperature distribution maps are obtained for the dusty torus in NGC~1068. They demonstrate that the hot component of the active galactic nucleus central region, which was derived from spectral density flux modeling, can be explained by the emission of the inner edge (throat) of the torus.

Geometry of the tangent bundle of space-time, adapted to local observations

A.N. Alexandrov

Astronomical Observatory, Taras Shevchenko National University of Kyiv, Kyiv, Ukraine

In the General Relativity, reference systems (RS) of a local (single) observer are called such RSs in which the coordinates of events are determined directly relative to the point observer. The basis of such RSs is the use of geodesic lines of space-time *M* as an analog of straight lines of Minkowski space. Locally observable quantities depend on the world coordinates of two points − the observed event and the position of the observer. Thus, they are functions that are defined in areas of direct product $M \times M$. Taking into account the observer's own movement, the transition to the description in terms of local observables corresponds to the mapping of the manifold $M \times M$ onto the tangent bundle *TM*. We consider the geometry of *TM*, which is induced by such transition. Based on the metric and connection defined on *M*, expressions for the metric tensor and connection coefficients of *TM* are constructed using the derivatives of the exponential mapping. It is shown that in the system of equations for geodesics of space *TM* a subsystem is split off that describes the geodesic movement of the observer. Moreover, the second part of the system is the equation of relative dynamics of geodesics (Aleksandrov, Piragas, 1979).

Testing Einstein's formula for gravitational deflection of light using observations of Galactic microlensing

A.N. Alexandrov, V.I. Zhdanov, V.M. Sliusar

Astronomical observatory, Taras Shevchenko National University of Kyiv, Kyiv, Ukraine

The General Theory of Relativity has a strong experimental and observational base, which includes a number of relativistic gravity tests. Nevertheless, it is natural that the emergence of new observational capabilities stimulates new such tests. In this report we discuss the potential of the gravitational microlensing for testing the Einstein's formula for the gravitational light deflection. For this purpose, the lens mapping is modified by introducing parameter ε, which characterizes the deviation from this formula; this model must be compared with the observational data on the Galactic microlensing. An example of such deviation from the General Relativity described by a simple power law is analyzed. We formed a sample of 100 microlensing light curves using the data of the Optical Gravitational Lensing Experiment (OGLE) for 2018. We treated these light curves using three methods which differ in the choice of weighs. The resulting ε value does not contradict the General Relativity within errors. See arXiv:2004.07522 for more details.

Super-critical accretion regime in the Q2237+0305 quasar?

L.A. Berdina[1,2], V.S. Tsvetkova[1,2], V.M.Shulga[1,3]

[1]Institute of Radio Astronomy, National Academy of Sciences of Ukraine, Kharkiv, Ukraine,
[2]Institute of Astronomy of V. N. Karazin Kharkiv National University, Kharkiv, Ukraine
[3]The International Center of Future Science, Jilin University, Changchun, China

We continued interpreting our measurements of the inter-band time lags between the flux variations of the Q2237+0305 quasar in the V, R and I spectral bands. As has been shown earlier, the values of the time lags for filter pairs R-V, I-R and I-V turned out to be significantly larger than those predicted by the standard accretion disk model by Shakura and Sunyaev. To explain the discrepancy, the idea of a supercritical (super-Eddington)

accretion regime in the quasar disk is involved. Such a regime has been considered in 1973 by Shakura and Sunyaev to result in emerging a scattering envelope on the accretion disk periphery. The envelope efficiently scatters and re-emits the radiation from the accretion disk thus making an apparent disk size larger. We have made use of analytical expressions for the envelope radius and temperature derived by Shakura and Sunyaev to show that our results are consistent with the existence of such an envelope for certain values of the angular momentum transport efficiency and a ratio of energy losses in Compton processes to those in free-free transitions. We have built a map of these two parameters distribution for several values of the black hole mass, for which the supercritical accretion regime is possible. The idea of a supercritical regime is also capable of interpreting a behavior of the inter-band time lags in wavelengths, namely, the unexpectedly low value for the interval between filters R and I (235.6 nm and 326.4 nm in the source plane)

Absence of a fundamental acceleration scale in galaxies

A. Del Popolo

Catania University, Department of Physics, Catania, Italy

There is much strong indirect evidence that supports dark matter existence, but there is yet no sign of a direct detection. Moreover, at the scale of galaxies, there is tension between the theoretically expected dark matter distribution and its indirectly observed distribution. Therefore, phenomena associated with dark matter have a chance of serving as a window towards new physics. The radial acceleration relation confirms that a non-trivial acceleration scale a_0 can be found from the internal dynamics of several galaxies. The existence of such a scale is not obvious as far as the standard cosmological model is concerned, and it has been interpreted as a possible sign of modified gravity. Here, we consider 193 high-quality disk galaxies and, using Bayesian inference, show that the probability of existence of a fundamental acceleration is essentially 0: the null hypothesis is rejected at more than 10σ. We conclude that a0 is of emergent nature. In particular, the modified Newtonian dynamics theory is a well known alternative to dark matter based on the existence of a fundamental acceleration scale or any other theory that behaves like it at galactic scales, is ruled out as a fundamental theory for galaxies at more than 10 sigma .

Machine Learning methods for binary morphological classification of SDSS-galaxies and their problem point

D. Dobrycheva[1], I. Vavilova[1], M. Vasylenko[1,2], A. Elyiv[1], O. Melnyk[1]

[1]Main astronomical observatory of National academy of sciences of Ukraine, Kyiv, Ukraine
[2]Institute of Physics of the National Academy of Sciences of Ukraine, Kyiv, Ukraine

We investigated the effectiveness of the Machine Learning methods for binary morphological classification of SDSS-galaxies into early (E) and late (L) types. The target sample included 316031 SDSS-galaxies at z<0.1. We used scikit-learn library for Python and following classification methods: Naive Bayes, Random Forest, Support Vector Machines, Logistic Regression, and k-Nearest neighbors algorithm. Training sample include 6163 galaxies with visually identified morphological type (E - 4147, L - 2016). To study the classifier, we used different absolute magnitudes, color indices, and inverse concentration index to the center R50/R90. We identified problematic galaxies with the following characteristics: interacting galaxies; background galaxy; the disk covered by the star; artifacts; red spirals; bright nucleus (spiral galaxies are defined as elliptical); dim objects (poor signal-to-noise ratio). Nevertheless, it turned out that the method of Support Vector Machines provides the highest accuracy of 96.4% (E - 96.1%, L - 96.9%). The accuracy of the other mentioned methods from 90% to 95%. We were able to classify 316031 galaxies from the SDSS DR9 with unknown morphologies. Eventually, we found 141211 E and 174820 L types among them.

Spherically-symmetric R and T-solutions of the 5-dimensional Kaluza-Klein theory equations

V.D. Gladush

Oles Honchar Dnipro National University, Dnipro, Ukraine

The paper considers 5-dimensional (5D) spherically-symmetric models of the Kaluza-Klein (KK) theory. 5D, the Einstein-Hilbert variational principle after dimensional reduction is reduced to four-dimensional. Subsequent orthogonalization and conformal mapping reduces the action to an Einstein form describing gravitational, electromagnetic, and scalar interacting fields.

We restrict ourselves to the construction and study of 5D models, the geometry of which depends only on the radial (R-solution) or time (T-solution) coordinate. Note that we consider more general models depending on the discrete parameter α. When α =1, we are dealing with the 5D KK theory. In the case α =1, we obtain the configuration of the general relativity with gravitational, electromagnetic, and scalar fields.

For each R and T solution, canonical formalisms are considered in which the radial coordinate is used as the evolution parameter for the R-solution, and the time coordinate is used for the T-solution. The transition to configuration spaces with the corresponding metrics is carried out. The actions in the configuration space and the Einstein-Hamilton-Jacobi equations are constructed.

Using these equations, the metrics and fields of the models under consideration are found and some of their geometric and physical properties are investigated. Note that the spaces, their topology, are significantly different for R and T-solutions.

The T-solution corresponds to a Kantovsky-Sachs-type cosmological model with the topology of a hypercylinder with scalar and electromagnetic fields interacting in a contact manner. To find the fields and the metric, the Cauchy problem is actually solved here with the initial data on the surface of a hypercylinder with extreme radius. On the other hand, with the appropriate choice of integration constants, they correspond to the solution for the inner part of the black hole 5D theory.

Unlike the T-solution, the class of 5-dimensional models based on R-solutions is much richer. Here, the properties of the models and the type of solutions differ significantly depending on the relationship between the separation constants in the corresponding Hamilton-Jacobi equation. Therefore, naturally the need arose to construct a classification of the obtained set of solutions. Among the possible solutions, we note an interesting class of configurations with a removable electric charge. In these models, using a linear coordinate transformation (x0, x4), which at infinity reduces to a Lorentz type transformation in the plane of variables (x0, x4), we can turn out the electric charge to zero.

Search for Supernova remnant and magnetar wind nebula connected with SGR 1900+14

B. Hnatyk[1], R. Hnatyk[1], V. Zhdanov[1], V.Voitsekhovskyi[2]

[1]Astronomical Observatory of Taras Shevchenko National University of Kyiv,

Kyiv, Ukraine
[2]Faculty of Physics, Taras Shevchenko National University of Kyiv, Kyiv, Ukraine

Magnetar wind nebulae created by new-born millisecond magnetars and magnetar giant flares are potential sources of ultrahigh energy ($E > 10^{18}$ eV) cosmic rays (UHECRs). Promising signatures of acceleration processes should be nonthermal high energy (HE) and very high energy (VHE) gamma-ray emission from magnetar outskirts. We investigate whether HE and VHE gamma-ray emission from the vicinity of the magnetar SGR 1900+14 can be explained by cosmic rays accelerated in Supernova remnant of magnetar progenitor Supernova or/and in magnetar wind nebula. We simulate the observed high energy (E > 100 MeV, extended Fermi-LAT source 4FGL J1908.6+0915e) and very high energy (E > 100 GeV H.E.S.S. extended source candidate HOTS J1907+091) gamma-ray emission flux spatially coincident with the magnetar SGR 1900+14 in the frame of hadronic and leptonic models. We show that the observed gamma-ray emission of Fermi-LAT 4FGL J1908.6+0915e and H.E.S.S. HOTSJ1907+091 sources may be explained or at least considerably contributed by (still undetected) magnetar-connected Supernova remnant and/or magnetar wind nebula with reasonable assumptions about model parameters.

The Shapley Supercluster: high energy processes and multimessenger observations

R. Hnatyk[1], V. Voitsekhovskyi[2]

[1]Astronomical Observatory, Taras Shevchenko National University of Kyiv, Kyiv, Ukraine
[2]Faculty of Physics, Taras Shevchenko National University of Kyiv, Kyiv, Ukraine

The Shapley Supercluster (SSC) or the Shapley Concentration (redshift z = 0.046, total mass $M_{tot} = 1.34 \cdot 10^{16}\ h^{-1}\ M_{sun}$ of SSC central part R < 12.4 h^{-1} Mpc) is the largest and richest structure of the cosmic web in the nearby Universe ($z \leq 0.1$). Due to dominant contribution of the dark matter to the total mass and violent dynamical processes in its collapsed central part SSC is a unique laboratory of high energy astrophysics. We estimate expected multimessenger signatures of high-energy processes in SSC – cosmic ray

acceleration at accretion and merger shocks, AGN activity, WIMP dark matter decay/annihilation, gamma-ray bursts and tidal disruption events.

Inner structure of planetary nebulae and their emission line spectra

M.D. Kasheba, B. Ya. Melekh

Ivan Franko National Univerity of Lviv, Lviv, Ukraine

The grid of photoionization models of planetary nebulae (PNe) envelopes along the evolutionary tracks of their nuclei for two types of dust grains (carbonates and silicates) and various masses of progenitor stars was calculated using code Cloudy 17.01. Two types of the chemical abundances averaged over ones of PNe in Large Magellanic Clouds (LMC) and Milky Way (MW) correspondingly were adopted. We applied three different types of density distribution (Golovatyi-Malkov semi-empirical law, hydrodynamical and uniform). Main aim of this study is search of dependence between emission line intensities as well as ratios between them on inner structure of PN envelope. Also, we compare the observed emission line spectra of PNe with modelling ones.

On the reliability of popular indicators to determine the star formation rate

I.O. Koshmak, B.Ya. Melekh, O.S. Buhajenko

Ivan Franko National University of Lviv, Lviv, Ukraine

We represent the results on checking of the reliability for star formation rate (SFR) indicators by Kennicutt and Calzetti obtained by us on the two kinds of models of nebular environment in dwarf galaxies with active star formation: the first one represents the multicomponent photoionization modeling (MPhM) of spherically symmetrical models based on the models of superwind cavity described by models Chevalier, Clegg (1985) and Weaver, McCray, Castor (1977), and the second one corresponds to the MPhMs calculated by us in 2D geometry on the base evolutionary chemodynamical simulations by Recchi & Hensler (2013) of these objects. For models the evolutionary population synthesis models for continuous star formation regions with different star formation rate were calculated. Synthetic spectra from such modeling were used to determine of SFR using Kennicutt's and Calzetti's indicators and the obtained values were

compared with ones assumed in our models.

Magnetic Field in Young Supernova Remnants

T. Kuzyo, O. Petruk

Pidstryhach Institute for Applied Problems of Mechanics and Mathematics, Lviv, Ukraine

The evolution of supernova remnants (SNRs) starts with the release of massive amount of energy (of order 10^{51} erg) into the circumstellar medium (CSM). At early stages the dynamics of the shock front and the distribution of the post-shock parameters (density, pressure, velocity, etc.) are mainly defined by the explosion energy, stellar ejecta mass and its density profile as well as by the structure of CSM. A common approach to the SNR evolution at these times is solving just hydrodynamic equations.

The structure of magnetic field in young SNRs is an important factor in the acceleration of cosmic rays and features of its non-thermal emission. We employ a full magneto-hydrodynamic approach to supernova remnants on pre-Sedov stages of evolution in order to identify properties of the magnetic field for different explosion scenarios: type Ia, Ic and IIP events.

Influence of variability in height of generation of secondary cosmic rays on registered muon flux

N. Lozitska

Astronomical observatory, Taras Shevchenko National University of Kyiv, Kyiv, Ukraine

In number of works the dependence of the muon flux, corrected for temperature, on solar activity was found. A positive statistical relationship between the muon flux and the sunspot index cannot be caused by primary cosmic rays whose intensity is in opposite with solar activity. When calculating the temperature coefficients by the mass-average temperature method, it is assumed that there is a strong positive correlation between the temperature and the height of the isobaric surfaces - the higher the temperature, the higher the isobaric levels. To identify the causes of instability of effective temperature coefficients over long periods, a study was made of changes in temperature and height of the main isobaric

surfaces in the regions where the detectors of the Yakut complex of muon telescopes (Russia) and the muon detector Borexino (Italy) are located. A positive relationship between the height of the isobaric levels of 200 and 300 hPa, where muons are generated, with temperatures at the levels of 500, 700, 850 and 995 hPa is observed. The ratio changes to negative for temperature at the tropopause level. During maxima of solar activity, heating of the stratosphere by ozone leads to a decrease in the height of isobaric surfaces of 200 and 300 hPa, which explains the increase in the muon flux due to a decrease in ionization and decay losses, and not because of a real increase in temperature coefficients.

Cosmological perturbations in the Universe with interacting dark energy

R.G. Neomenko, B.S. Novosyadlyj

Astronomical Observatory of Ivan Franko National University of Lviv, Lviv, Ukraine

The evolution of cosmological perturbations is analyzed in the Universe where additional non-gravitational interaction between dark energy and dark matter (DE-DM interaction) is present. As for dark energy with constant equation of state (EoS) parameter the non-adiabatic instabilities arise at scales much larger then Hubble horizon in the radiation dominated epoch, we are studying the model of dynamical dark energy which allows to avoid such problem. The three component Universe is considered which consists of dark components and electromagnetic radiation which are described by ideal fluid approximation. The DE-DM interaction is set up as the function of Hubble parameter and densities of interacting components, so the three types of this interaction are studied: independent on the densities of dark components, proportional to the density of dark energy and proportional to the density of dark matter. Using the property of our dark energy model that EoS parameter of which is almost constant at early epoch and later it began to evolve in time significantly the solutions of cosmological perturbation equations in radiation dominated epoch were obtained. The stability conditions of these solutions were derived for all three types of DE-DM interaction at early epoch. Using these solutions as initial conditions for numerical integration of the system of cosmological perturbation equations for different values of interaction parameter the evolution of perturbations of dark components was analyzed. The modification of evolution of dark energy perturbations is strongly

dependent on the type of dark energy (quintessence or phantom), type of DE-DM interaction and strength of this interaction. The modification of evolution of dark matter perturbations for all mentioned above cases is similar: after entering in the Hubble horizon they grow faster and closer to modern epoch they grow slower in compare with non-interacting case.

Emission of dark ages and cosmic dawn halos in the rotational lines of the first molecules

B.S. Novosyadlyj[1,3], Yu.A. Kulinich[1], V.M. Shulga[2,3]

[1]Ivan Franko National University of Lviv, Lviv, Ukraine,
[2]Institute of Radio Astronomy of NAS of Ukraine, Kharkiv, Ukraine
[3]International Center of Future Science of Jilin University, P.R.China

The emission from dark ages and cosmic dawn halos in the lines of transitions between lowest rotational levels of hydrogen molecule H_2, hydrogen deuteride molecule HD and helium hydride ion HeH^+ is analyzed. It is assumed that in the Dark Ages these molecules to be excited by CMB and collisions with hydrogen atoms and electrons. The physical parameters of halos and number density of molecules are precalculated in assumption that halos formed from the cosmological density perturbations in the four-component Universe with post-Planck cosmological parameters. The differential brightness temperatures and differential spectral fluxes in the rotational lines of molecules are computed for two phenomena: luminescence and resonant scattering of CMB radiation. The results show that expected maximal values of differential brightness temperature of the warm dark ages halos (T_K~200-800 K) are at the level of nanokelvins, are comparable for both phenomena, and are below sensitivity of modern sub-millimeter radio telescopes. For the hot dark ages halos (T_K~2000-5000 K) the thermal emission of hydrogen molecules dominates and the differential brightness temperatures for them are at the microkelvin level in the frequency range 300-600 GHz. At the end of the Dark Ages epoch, at the Cosmic Dawn, the light of the first stars becomes the dominant perturber of H_2, HD, and HeH^+ rotational levels, due to which their brightness temperatures increase significantly, so they can be detected using new generation telescopes such as ALMA and SKA. In the Cosmic Dawn epoch the halos are brighter in the lines of helium hydride ion HeH^+ than in the lines of hydrogen molecules H_2 and HD. At the end of the Dark Ages epoch, at the Cosmic Dawn, the light of the first stars becomes the dominant perturber of H_2, HD, and HeH^+ rotational levels, due to which their

brightness temperatures increase significantly, so they can be detected using new generation telescopes such as ALMA and SKA. In the Cosmic Dawn epoch the halos are brighter in the lines of helium hydride ion HeH^+ than in the lines of hydrogen molecules H_2 and HD. Their detection and identification will be a source of unique information about the epoch of the formation of the first stars.

Two types of the initial luminosity function from astronomical observations

S.L. Parnovsky[1], I.Yu. Izotova[1]

[1]Astronomical Observatory, Taras Shevchenko National University of Kyiv, Kyiv, Ukraine

We discuss some key points on the determination of the initial luminosity function of compact star-forming galaxies. We use a sample of galaxies with derived luminosity L_i in some spectral line or in continuum, and the starburst age T_i. The initial luminosity function can be determined using these data.

The Hα luminosities L(Hα) of compact star-forming galaxies rapidly decrease by more than two orders of magnitude on a time scale of 10 Myr because they are produced by ionizing radiation of the most massive stars. The far ultraviolet luminosities decrease as well, but more slowly, because they are produced by less massive stars. Our goal is to construct the initial luminosity function for galaxies, i.e. luminosity function at zero starburst age $T = 0$, immediately after the instantaneous starburst. We show that this technique is ambiguous because one needs to choose between two possibilities for determining this initial luminosity function.

Consider a sample of galaxies at zero starburst age $T = 0$ that satisfy certain criteria, including a requirement that the galaxy emission flux is greater than a certain threshold value. This requirement is needed just to be able to observe the galaxy and to determine its parameters. We denote it as a sample A. However, the galaxies are observed at different starburst ages T_i. The fluxes from some galaxies fall below the threshold value because of the luminosity decreasing with increasing of the starburst age, and therefore they are not included in the sample, which we will call as a sample B. This is the sample obtained by selecting of the real astronomical objects. It is

clear that all objects from the sample B are included in the sample A, but not visa versa.

It is easy for galaxies from the sample B to determine the luminosities L_i at zero starburst age adopting some temporal evolution of the galaxy luminosities L(T), and to study their initial luminosity function. But it differs from the luminosity function of the sample A. This difference can be obtained by solving the integral equation linking the initial and observed luminosity functions.

Two resulting types of the initial luminosity functions obtained from the same set of observational data, and their differences are discussed.

Warm dark matter could resolve inconsistencies in Hubble constant values obtained from high- and low-redshift observations

S.L. Parnovsky[1]

[1]Astronomical Observatory, Taras Shevchenko National University of Kyiv, Kyiv, Ukraine

The tensions between the values of Hubble constant obtained from the early and the late Universe data could be eliminated if we use the ΛWDM cosmological model with dark energy, cold baryonic matter and warm dark matter (WDM). We consider two limiting cases. In the first the WDM temperature is constant with characteristic velocities about 16% of the speed of light and a pressure is equal to its energy density multiplied by factor 0.009.

In the second limiting model the WDM temperature drops as quickly as possible. The characteristic WDM velocities in this case are falling from ~0.44c in the era of recombination to 4000 km/s now. It can be assumed that all reasonable variants of the evolution of the WDM density lie within the range limited by these two models. The pressure of WDM practically does not affect its manifestation in the late Universe except for the processes of structure formation.

Toward a reconstruction of 3-D morphology of Tycho SNR

O.Petruk[1], V.Marchenko[2], T.Kuzyo[1], M.Patrii[3]

[1]Institute for Applied Problems in Mechanics and Mathematics, Lviv, Ukraine
[2]Astronomical Observatory, Jagiellonian University, Cracow, Poland
[3]Ivan Franko National University of Lviv, Lviv, Ukraine

Remnant of the supernova event observed by Tycho Brahe in 1572 is an important object observed in great details in radio and X-ray bands. We use these observations in order to reconstruct morphology of the remnant as well as ambient medium. In particular, we determine the direction of the ambient density gradient, orientation of interstellar magnetic field and its gradient in vicinity of the remnant. We also perform detailed studies of the Doppler effect for two most prominent X-ray lines over the whole surface with goal in mind to reconstruct the structure of the stellar ejecta in three dimensions.

Acceleration and non-thermal emission of cosmic rays in Vela Jr. Supernova remnant.

P. Plotko[1], B. Hnatyk[2] I. Sushch[3,4], R. Brose[3,5]

[1]Faculty of Physics, Taras Shevchenko National University of Kyiv, Kyiv, Ukraine
[2]Astronomical Observatory, Taras Shevchenko National University of Kyiv, Kyiv, Ukraine
[3] DESY, Zeuthen, Germany
[4] Astronomical Observatory of Ivan Franko National University of Lviv, Lviv, Ukraine
[5] Institute of Physics and Astronomy, University of Potsdam, Potsdam, Germany

Supernova remnants (SNRs) are the most likely sources of Galactic cosmic rays. Vela Jr. SNR (RX J0852.0-4622) is powerful gamma-ray source, detected by Fermi-LAT and H.E.S.S. and therefore, is promising candidate for cosmic PeVatrons – CR accelerators with energies above 10^{15} eV (1 PeV). Low level of thermal X-ray emission from Vela Jr. SNR favors low density of interstellar medium (ISM) and leptonic processes for gamma-ray emission. But density enhancements (molecular clouds etc.) in the SNR

shock vicinity can result in hadronic CR- ISM interactions as a main contributor to the observed gamma-ray emission of Vela Jr. SNR. We propose a dense shell of SN progenitor wind bubble as a target for hadronic mechanism of gamma-ray emission from Vela Jr. SNR. To this end we calculate the time evolution of the spectrum and non-thermal radiation of CRs accelerated at the shock of Vela Jr. SNR. The PLUTO and RATPaC software were modified for this case. We take into account a complex structure of the ISM environment around the SNR, including stellar wind bubble, by performing 1-D hydrodynamic simulations of a massive progenitor star evolution. We calculate the spectrum of downstream and upstream cosmic rays and compare their non-thermal radiation with the Vela Jr. SNR observations.

Strong spin-gravity repulsion and additional attraction

R.M. Plyatsko, M.T. Fenyk

[1]Pidstryhach Institute for Applied Problems in Mechanics and Mthematics, Lviv, Ukraine

The effects of highly relativistic spin-gravity coupling in the Schwarzschild and Schwarzschild –de Sitter backgrounds that follow from the Mathisson-Papapetrou equations are considered. The physical reason that determines the specific of highly relativistic motions of a spinning particle on these backgrounds is connected with the fact that in the proper system of reference such a particle feels the strong action of the gravitomagnetic components of the gravitational field in general relativity (we use the definition of these components by K. Thorne). This action is repulsive or attractive depending on the correlation between the particle's spin and orbital velocity. The corresponding analytical estimations are obtained for different orbits in the Schwarzschild –de Sitter background, both in the equatorial and non-equatorial planes. The role of the cosmological constant is emphasized. It is shown that generally speaking a highly relativistic velocity of the particle is a necessary condition of motion along these orbits, with an exception of orbits locating close to the position of the static equilibrium, where low velocities are possible as well.

Using computer calculation we investigated the dependence of the contribution of the spin-gravity coupling to the particle's energy on its tangential velocity relative to the Schwarzschild source: this contribution significantly depends on this velocity in the highly relativistic region. Depending on the correlation of the spin orientation and the particle's

orbital velocity the value of the spinning particle energy is much larger or less than the corresponding values for the spinless particle.

Optical monitoring results of selected active galactic nuclei in 2018-2020

V. Ponomarenko, I. Izviekova, A. Simon, V. Vasylenko, K. Kulish

Taras Shevchenko National University of Kyiv, Kyiv, Ukraine

The results of systematical monitoring of AGN BL Lacertae, 1ES 1011+496, PKS 1222+216, 1ES 1426+428, PKS 1510-089, Markarian 501 from the Cherenkov Telescope Array optical checklist, started in January 2018 are presented. The observations are carried out with the AZT-8 (D = 70 cm, F = 2.8 m) telescope of the observation station Lisnyky of Astronomical Observatory of Taras Shevchenko National University of Kyiv. The AZT-8 equipped with the PL4710-1-BB-E2V CCD (1027x1048 pixels, 13x13 μm/pixel, the scale is 0.95 "/pixel, the field of view is 16.2 angular minutes) and broadband Johnson/Bessel UBVRI filters. The telescope Zeiss-600 of Pik Terskol Observatory operated by the International Center for Astronomical, Medical and Ecological Research of the NAS of Ukraine was also used for observation.

The fluxes of energy from the objects of research have been turned into visible stellar magnitudes with the help of standard stars. Light curves for objects BL Lacertae, 1ES 1011+496, PKS 1222+216, 1ES 1426+428, PKS 1510-089, Markarian 501 were plotted. The analysis of long-term variability (LTV), short-term variability (STV) and internal daily variability (IDV) in the optical range was made. As a result of processing the observational material, significant changes in the brightness of the objects of study were detected. In addition, the variability of color indexes with time was investigated. The results were analysed and the errors were estimated (the total error is $\Delta_\Sigma \approx 0.06$-$0.1$ magnitude). Also, the correlation in the changes of brightness between the optical range and the gamma-range was detected.

Model-independent constraints in inflationary magnetogenesis

Yu.V. Shtanov[1,2], M.V. Pavliuk[3]

[1]Bogolyubov Institute for Theoretical Physics, Kyiv, Ukraine
[2]Astronomical Observatory, Taras Shevchenko National University of Kyiv,

Kyiv, Ukraine
[3]Department of Physics, Taras Shevchenko National University of Kyiv, Kyiv, Ukraine

We derived a simple model-independent upper bound on the strength of magnetic fields obtained in inflationary and post-inflationary magnetogenesis taking into account back-reaction and Schwinger effect. The model contains both kinetic and chiral coupling to electromagnetism. The general bound for the present comoving magnetic field is found to be [1]

$$B_0 \lesssim 10^{-30} g_r^{-1/6} \left(\frac{M_P}{T_r}\right)^{1/3} \frac{\mathrm{Mpc}}{\lambda}\ \mathrm{G},$$

where g_r is the number of relativistic degrees of freedom in thermal equilibrium after reheating ($g_r \approx 100$ in the Standard Model), T_r is the reheating temperature, and M_P is the Planck mass.

This upper bound allows one to appreciate the difficulty in producing sufficiently large magnetic fields on large spatial scales. Indeed, the lowest possible temperature of reheating lies in the MeV range, and even for such low reheating temperature, one gets $B_0 \leq 10^{-23}$ G on the megaparsec scale.

Somewhat higher upper bound is obtained if one assumes that some unknown mechanism suppresses the Schwinger effect in the early universe:

$$B_0 \lesssim 10^{-31} g_r^{-1/3} \frac{M_P}{T_r} \frac{\mathrm{Mpc}}{\lambda}\ \mathrm{G}.$$

This would allow one to obtain $B_0 \leq 10^{-15}$ G on the megaparsec scale by choosing $T_r \sim 10^2$ GeV. Incidentally, we have corrected (reduced) our previous estimates [2] for this case.

[1] Yuri Shtanov, Mykhailo Pavliuk, "Model-independent constraints in inflationary magnetogenesis," arXiv:2004.00947.

[2] Yuri Shtanov, "Viable inflationary magnetogenesis with helical coupling," JCAP **10** (2019) 008, arXiv:1902.05894.

Impact of scalar field dark energy on neutron stars

M. Tsizh[1,2], S. Smerechynskyi[1], B. Novosyadlyj[1]

[1]Ivan Franko National University of Lviv, Lviv, Ukraine
[2]Abto software Ltd., Lviv, Ukraine

We study the density distribution of the minimally-coupled scalar field type dark energy inside a neutron star. The dark energy is considered in hydrodynamical representation as a perfect fluid with a linear equation of

state and has three free parameters (background density, equation of state, and effective sound speed). The neutron star matter is modeled with three unified equations of state, developed by the Brussels-Montreal group. With the calculated density distribution of the dark energy inside a neutron star (and its dependence on the dark energy parameters) we investigate how its presence impacts the macroscopic characteristics and the value of the mass limit for neutron stars. From this impact we derive possible constrains on the effective speed of sound of dark energy with the help of maximal known masses of observed neutron stars. With this approach, we have found, that the effective speed of sound can not be smaller than $\sim 10^{-2}$ in units of speed of light.

Inferring of morphological properties of SDSS-galaxies at z<0.1 using deep similarity learning

M.Yu. Vasylenko[1], V. Khramtsov[2], D.V. Dobrycheva[1], I.B. Vavilova[1], A.A. Elyiv[1]

[1]Main Astronomical Observatory of the NAS of Ukraine, Kyiv, Ukraine
[2]Institute of Astronomy, V. N. Karazin Kharkiv National University, Kharkiv, Ukraine

We present the method of morphological parameters determination for the galaxies using deep learning approach. We show the performance of our method on the redshift-limited (z<0.1) sample of ~300 000 SDSS-galaxies. The galaxies were classified into five visual types (completely rounded, rounded in-between, smooth cigar-shaped, edge-on, and spiral) using a convolutional neural network. The training process was based on the images of galaxies from the target sample, matched in the Galaxy Zoo 2 dataset. In the presence of a pronounced difference of visual parameters between galaxies from the training sample, and galaxies without known morphological parameters, we applied novel procedures, which allowed us to get rid of this difference. Using the adversarial validation technique, we managed the optimal train-test split of galaxies from training samples to test our convolutional neural network realistically. We found optimal image transformations, which helped increase the generalization ability of classifiers. Also, we have estimated the morphological parameters of galaxies with using the k-nearest neighbors method, applied to the `latent' features of galaxies, recovered from its images. Our method shows the state-of-art performance of morphological classification, with >94% accuracy for all classes, except cigar-shaped galaxies (~88%).

Lithium in stars

Ya.V.Pavlenko

Main Astronomical Observatory of the National Academy of Sciences of Ukraine, Kyiv, Ukraine

New and old results and problems of the lithium abundance determination in the atmospheres of stars of different spectral classes and evolution status are discussed. We know that lithium is an astrophysical tool to follow processes evolution of stars and brown dwarfs. On the second-hand lithium and its isotopic ratio if of cosmological importance. The lithium abundance determination procedure details differ for the stars of early and late spectral classes. Development of observational facilities and theoretical procedure provides new possibilities for the progress in lithium studies. Recently we obtained new information about the notable amount of lithium formed in the Recurrent Novae systems. De facto, it is a new source of galactical lithium. Nevertheless, only self-consistent understanding of the importance of lithium abundance determination results can provide new knowledge about present state and evolution of our Galaxy and other galaxies.

Non-existence of spherical singularities in static spherically symmetric configurations with N nonlinear scalar fields

V.I. Zhdanov[1], A.S. Stashko[2]

[1]Astronomical Observatory, Taras Shevchenko National University of Kyiv, Kyiv, Ukraine
[2]Faculty of Physics, Taras Shevchenko National University of Kyiv, Kyiv, Ukraine

The occurrence of singularities is a typical phenomenon in case of nonlinear equations. For example, in the case of a spherically symmetric configuration in flat space with the nonlinear scalar field (SF) escribed by the monomial potential, the spherical singularities can occur for nonzero values of radial variable $r>0$. On the contrary, the situation changes within the general relativistic treatment. We show that in the general relativity the gravitational field suppresses the occurrence of the spherical singularities under some generic conditions. Our consideration deals with asymptotically flat space-

times around static spherically symmetric configurations in the presence of N nonlinear SFs, which are minimally coupled to gravity. Constraints are imposed on the SF potentials, which guarantee a monotonicity of the fields as functions of r; also the potentials are assumed to be exponentially bounded. We give a direct proof that solutions of the joint system of Einstein-SF equations satisfying the conditions of asymptotic flatness are regular for all values of r, except for naked singularities in the center r=0 in the Schwarzschild (curvature) coordinates. Asymptotic relations for SF and a metric near the center are derived, which appear to be remarkably similar to the Fisher solution for free SF. These relations determine two main types of the corresponding geodesic structure when photons can be captured by the singularity or not. To illustrate, the case of one SF with monomial potential is analyzed in detail numerically. See our paper Phys. Rev. D 101, 064064 (2020) more details.

Магнітне поле в залишку наднової 1987A

В. Бешлей, О. Петрук

Інститут прикладних проблем механіки і математики ім. Я. С. Підстригача НАН України, Львів, Україна

Залишок наднової ЗН1987А, що утворився внаслідок спалаху у Великій Магелановій Хмарі є наймолодшим залишком наднової, структура якого може бути розділена сучасними засобами спостережень. Вибух зорі відбувся в середовищі з суттєво неоднорідною структурою, що ускладнює його моделювання. Числове магнітогідродинамічне моделювання цього залишку проведено в роботі [1]. Ці розрахунки використовують класичну модель довколазоряного магнітного поля Паркса.

Ми побудували карти розподілу параметрів Стокса для цієї моделі та порівняли її з нещодавно опублікованою спостережуваною картою поляризації цього ЗН [2]. Виявилося, що промодельовані карти не цілком відповідають спостережуваним, отже, в модель давколазоряного магнітного поля слід внести певні зміни. Оскільки тривимірні МГД розрахунки є надзвичайно ресурсоємними, ми розробили метод, що дозволяє побудувати розподіл магнітного поля всередині залишка з певної моделі початкового зовнішнього поля, використовуючи лише гідродинамічного параметри моделювання. Такий метод дозволяє швидко побудувати карти поляризації залишку для різних моделей міжзоряного поля та порівняти їх зі

спостережуваними даними.

1. S. Orlando et. al., A&A, 622, A73 (2019)
2. G. Zanardo et. al., ApJL, 861, L9 (2018)

Електромагнітні хвилі в полі Керра не поширюються вздовж ізотропних геодезійних: точний результат

В.О.Пелих, Ю.В.Тайстра

Інститут прикладних проблем механіки і математики ім. Я.С.Підстригача НАН України, Львів, Україна

Ми застосовуємо вихідний в сенсі Чандрасекара (один із двох алгебраїчно-спеціальних) розв'язок рівнянь Максвелла у просторі-часі Керра та отримуємо точні вирази хвильових векторів право- та лівополяризованих хвиль і доводимо, що з умови ізотропності як умови рівності нулеві інваріантів поля не випливає ізотропність хвильових векторів, а також, що інтегральна конгруенція хвильового векторного поля не є ізотропною геодезійною. Перший висновок було отримано у роботі [1] лише при певних наближеннях. Із нього авторами було зроблено висновок, що електромагнітні хвилі не завжди поширюються вздовж ізотропних. Ми пояснюємо, що причиною таких неузгодженостей є те, що розв’язки рівнянь Максвелла у полі Керра не є плоско-фронтовими (plane-fronted).

Із точного розв’язку ми отримуємо умову існування супервипромінювання, яка є точною скрізь поза горизонтом подій, тоді як умова Старобінського та Пресса-Тюкольського отримана наближено лише біля горизонту.

Ми отримуємо вираз для поверхні постійної фази, який задає невідому до цього геометричну фігуру, названу нами сфероїдним гелікоїдом. Його форма відрізняється у випадках наявності чи відсутності супервипромінювання.

1. F.Asenjo, S.Hojman. Do electromagnetic waves always propagate along null geodesics? Class. and Quant. Gravity, **34**, Number 20, 205011 (2017).

АСТРОМЕТРІЯ І МАЛІ ТІЛА СОНЯЧНОЇ СИСТЕМИ

ASTROMETRY AND SMALL BODIES OF THE SOLAR SYSTEM

Clues to cometary circular polarization from studying magnetic field in the vicinity of the nucleus of comet 67P/Churyumov-Gerasimenko

V.K. Rosenbush[1,2], L.O. Kolokolova[3], N.N. Kiselev[2,4], O.V. Ivanova[1,2,5], V.L. Afanasiev[6]

[1]Taras Shevchenko National University of Kyiv
[2]Main Astronomical Observatory of NAS of Ukraine
[3]University of Maryland
[4]Crimean Astrophysical Observatory
[5]Astronomical Institute of the Slovak Academy of Sciences, Tatranská Lomnica, Slovak Republic
[6]Special Astrophysical Observatory of the Russian Academy of Sciences

The more characteristics of the scattered light we study the more information about scattering medium we can accumulate and, thus, define characteristics of the scatterers more accurately. Circular polarization of the scattered light is one of those tools that allow narrowing down the range of possible properties of cometary dust particles and, thus, better define their composition, size, and structure.

Until the mid 1980s, measurements of circular polarization in comets were sporadic and had errors comparable to the measured polarization. For the first time, Dollfus and Suchail (1987) reliably measured non-zero circular polarization in comet 1P/Halley. The observed circular polarization was highly variable over the coma and showed temporal variations. Since that time, successful observations of cometary circular polarization were carried out repeatedly, and a big set of observational data has been accumulated, including spatially resolved maps of circular polarization.

Recently, imaging data on circular polarization have been obtained for number of comets using the 6-m BTA telescope (SAO RAS). However, despite of accumulation of significant amount of data, mechanisms of its formation in the cometary environment was a mystery as regular mechanisms (multiple scattering in optically thick medium, domination of particles or materials of a specific mirror asymmetry, including homochirality, and alignment of non-spherical particles) could not explain the observations. Particle alignment always was considered as the most feasible mechanism, although the cause of the particle alignment was not clear. Alignment in a magnetic field could be the most plausible mechanism to explain comet circular polarization. However, comets do not have their own magnetic field and in situ measurements of comet Halley showed (see Richter et al. 2011 and references therein) that the interplanetary magnetic

field could not penetrate into the coma closer than 4000–5000 km from the nucleus where it is stopped by bow shock produced by cometary ions. Thus, magnetic fields can possibly explain dust alignment only for nucleocentric distances larger than 4000 km. However, circular polarization was observed in comets at distances even less than 1000 km. New theoretical studies of interaction of the cometary coma with the solar magnetic field (Koenders et al. 2015) and, especially, Rosetta observations of the diamagnetic cavity at comet 67P/Churyumov-Gerasimenko, showed that the solar magnetic field can penetrate as close to the nucleus as some dozens kilometers (Goetz et al. 2016). This allows us to suggest alignment in the solar magnetic field as a reason for observed circular polarization. Based on the data obtained for comet 67P, we estimate the time necessary for the alignment of cometary particles in the solar magnetic field. The obtained estimates are consistent with the observations of the cometary circular polarization.

References:

Dollfus A. & Suchail J.L. 1987. Polarimetry of grains in the coma of P/Halley. I - Observations. Astron. Astrophys. 187, 669–688.

Goetz C., Koenders, C., Richter I. et al. 2016. First detection of a diamagnetic cavity at comet 67P/Churyumov-Gerasimenko, Astron. Astrophys. 588, id.A24, 6 pp.

Koenders C., Glassmeier K.-H., Richter I. et al. 2015. Dynamical features and spatial structures of the plasma interaction region of 67P/Churyumov–Gerasimenko and the solar wind. Planet. Space Sci. 105, 101–116.

Richter I., Koenders C., Glassmeier K.H. et al. 2011. Deep Space 1 at comet 19P/Borrelly: Magnetic field and plasma observations, Planet. Space Sci. 59, 691–698.

Morphology of the coma of comet C/2011KP36 (Spacewatch) on November 25, 2016

V. Kleshchonok[1], V. Rosenbush[1], O. Ivanova[1,2,3], I. Lukyanyk[1]

[1]Taras Shevchenko National University of Kyiv
[2]Main Astronomical Observatory of NAS of Ukraine
[3]Astronomical Institute of the Slovak Academy of Sciences

Comet 2011KP36 was observed on November 25, 2016. The multi-mode focal reducer SCORPIO-2 with the Sloan g-sdss (λ465/65 nm) and r-sdss (λ620/60 nm) broadband filters in the prime focus of the 6-m telescope BTA of the SAO RAS was used for observations. We revealed two strong

jet-like structures in solar and antisolar directions of the coma, labelled as J1 and J2, and two faint, short and narrow jet features in a direction perpendicular to the Sun–comet direction, marked as J3 and J4. The position angles (PA) are 261°,103°, 188°, and 8° for the J1, J2, J3, and J4 respectively. We used a simple geometrical model for analysis of the jet structures in comet 2011KP36. We received orientation of rotational axis of the nucleus (RA=280±15±, Dec=-60±10°), and latitudes of active regions which produce jets: -75±10° (J1), 75±10°(J2), -75±10°(J3 and J4). Also we determined a characteristic scale which is the product of the rotation period and the velocity of material outflow. For the date of observations, it is 13300 ±1200 km. We find a wave structure at the remote part of the J4 jet which explained by precession of the nucleus. Interpretation of the structure gives the angular radius of precession (6±0.6°) and the characteristic length of the precession which is equal to the product of the dust velocity and the precession ″period (30000±1500 km).

Spectroscopy of comet 46P/Wirtanen at 2008 and 2019 apparitions

V. Ponomarenko[1], P. Korsun[2], K. Churyumov[1], A. Sergeev[3], I. Sokolov[3]

[1]Taras Shevchenko National University of Kyiv
[2]Main Astronomical Observatory of the National Academy of Sciences of Ukraine
[3]IC AMER Terskol Observatory

Comet 46P/Wirtanen belongs to the small family of “hyperactive” comets whose activity level is higher than expected. The orbit of the comet is very suitable for the spacecraft rendezvous. It was the original target of Rosetta mission and possibly will be the target of one future mission as well.

We obtained the optical spectra of comet 46P/Wirtanen in January 2008 and in January 2019. The spectroscopic observations of comet 46P/Wirtanen were carried out with the 2-m Zeiss telescope of Pik Terskol Observatory (MPC code B18) operated by the International Center for Astronomical, Medical and Ecological Research of the NAS of Ukraine. The spectra with the average resolution $\lambda/\Delta\lambda \approx 1300$ were obtained. In the inner coma, the identification of the spectral emission lines and bands of molecules CN, C_2, C_3, NH_2 has been carried out. The distributions of

general and reflected energy in spectra have been built. The spectrophotometric gradient on the basis of the reflected energy is found. Some physical parameters of neutral gaseous and dust cometary atmospheres were calculated with the help of Haser model. The results that were obtained in 2008 and 2019 have been analyzed and compared with the data of other observations.

Photometrical and spectral observations of splitting comet C/2019 Y4 (ATLAS) on April 14 and 16, 2020

I. Luk'yanyk[1], O. Ivanova[1,2,3], A. Moiseev[4]

[1]Astronomical Observatory of Taras Shevchenko National University of Kyiv
[2]Astronomical Institute of the Slovak Academy of Sciences
[3] Main Astronomical Observatory of the National Academy of Sciences of Ukraine
[4]Special Astrophysical Observatory of the Russian Academy of Sciences

C/2019 Y4 (ATLAS) discovered by the ATLAS survey on December 28, 2019. This is a comet with a near-parabolic orbit. First observations showed that ATLAS is moving in the same orbit as the Big Comet of 1843. In this regard, the researchers suggested that it could be a fragment of that comet. But around March 22, 2020, the comet started disintegrating. Such fragmentation events are very common for Kreutz Sungrazers. We carried out the comprehensive observations of the comet at the 6-m BTA telescope of the Special Astrophysical Observatory (Russia) with the multimode focal reducer SCORPIO-2. Long-slit spectra in the visible region and photometric images with the medium-band SED500 (λ5019/246 Å) filter and the continuum narrowband filters Cont_4430 (λ4430/36 Å), Cont_6840 (λ6840/83 Å) were obtained on April 14 and 16, 2020 before perihelion passage, when heliocentric and geocentric distances of the comet were 1.2 au and 0.99 au, respectively. The emissions CN 0–0, 0–1 ($B^2\Sigma^+ - X^2\,\Sigma^+$), C_3 ($A^1\Pi_u - X^1\Sigma_g^+$), C_2 and others were identified. The gas production rates of CN, C_2, C_3 and NH_2 molecules were estimated using the Haser model. A detailed analysis of coma morphology and of colour and spectral gradient maps was made.

On the existence of long-period comet's families of giant planets

R. Guliyev, A. Guliyev.

Shamakhy Astrophysical Observatory of Azerbaijan National Academy of Sciences

We analyzes the minimum orbit intersection distances (MOID) for a sample of long-period comets (1360) and giant planets of the Solar System. Our calculations revealed a significant number of LPCs that may have had close encounters with planets: Jupiter (268), Saturn (176), Uranus (81) and Neptune (75). They include 107 cases when a comet is suitable for two or more planets. In addition, we carried out the analysis of the Tisserand criterion for cometary orbits, which showed that more than 10% of comets of the Jupiter group have values ($2 < T < 3$). Such values are also presented in slightly smaller scale for other planet groups. The statistical results and conclusions obtained in the work are also tested.

Activity of (6478) Gault during January 13 – March 28, 2019

O. Ivanova[1.2.3], Yu.Skorov[4], I. Luk'yanyk[3], D. Tomko[1], M. Husárik[1], Jü. Blum[4], O. Egorov[5], O.Voziakova[5]

[1]Astronomical Institute of the Slovak Academy of Sciences
[2] Main Astronomical Observatory of the National Academy of Sciences of Ukraine
[3] Astronomical Observatory of Taras Shevchenko National University of Kyiv
[4-] Technische Universität Braunschweig, Institute for Geophysics and Extraterrestrial Physics
[5-] Sternberg Astronomical Institute, Lomonosov Moscow State University

We present the results of photometric observations of active asteroid (6478) Gault performed at heliocentric distances from 2.46 to 2.30 au and geocentric distances from 1.79 to 1.42 au between January 15 and March 28, 2019. Observations were carried out at the 2.5-m telescope of SAI MSU (CMO) on January 15, 2019 and at the 1.3-m and 0.61-m telescopes (SPb) on February 6 and March 28, 2019, respectively. The direct images of the asteroid were obtained with the broad-band B, V and R filters. Comet-like structures were detected at all observation dates. Colour maps were built and colour variations along the tail for the observation made on January 15,

2019 were analyzed. The $Af\rho$ was calculated for the R filter, The evaluated value varies from 47 to 32 cm for the period from January to the end of March, 2019. The rotational period of the body is estimated from the light curve by different methods and is about 1.79 hr. Possible mechanisms of triggering Gault's activity are discussed.

Comparative analysis of the asteroid absolute magnitudes in the different datasets

V.G. Shevchenko[1,2]

[1]Department of Astronomy and Space Informatics, V.N. Karazin Kharkiv National University, [2]Institute of Astronomy, V.N. Karazin Kharkiv National University

At present, the main database of asteroid absolute magnitudes is the Minor Planet Center (MPC). The MPC receives asteroid magnitudes from many observatories in different spectral bands of different photometric systems, but calculates absolute magnitudes for *V* band of the Johnson photometric system using the *HG*-function. A comparison of the MPC absolute magnitudes with the dataset of high-quality absolute magnitudes in *HG*-system obtained by P. Pravec et al. (2012) revealed systematical differences between these datasets. K. Muinonen et al. (2010) recommended the new functions (three-parameter HG_1G_2-function and two-parameter HG_{12}-function for sparse photometric data) for calculating the asteroid absolute magnitudes. These functions were calibrated according to precise phase dependences of brightness, and the average parameters for main asteroid taxonomic classes were obtained. Using these average values, it allowed to calculate the absolute magnitudes of asteroids from the sparse observations obtained at the different phase angles. Recently, large-scale survey programs such as Pan-STARRS, Palomar Transient Factory (PTF), Zwicki Transient Factory (ZTF) and others have been performed, within which absolute magnitudes of asteroids have also been derived. These datasets are homogeneous, but they were obtained mostly in the different photometrical systems and then were transformed to the Johnson system. Comparison of absolute magnitudes of some these sets with the MPC dataset showed also systematical deviations. To check the quality of these datasets and identify systematic deviations, an independent set of high-quality data on absolute magnitudes is needed. Such set of the high-quality

absolute magnitudes using new functions was obtained at the Astronomical Institute of V.N. Karazin Kharkiv National University (Kharkiv dataset) from Kharkiv Asteroid Magnitude-phase Relations database (EAR-A-COMPIL-3-MAGPHASE-V1.0. NASA Planetary Data System).

In this work a comparative analysis of the asteroid absolute magnitudes between the Kharkiv dataset and the MPC, Pan-STARRS, and PTF datasets was performed. The analysis has shown that the absolute magnitude dataset obtained from the Pan-STARRS survey project is closest to Kharkiv dataset and can be the most suitable for the determination of diameters or albedos of asteroids.

Kharkiv photometric survey of near-Earth asteroids

Yu.N. Krugly[1], I.N. Belskaya[1], I.E. Molotov[2], R.Ya. Inasaridze[3,4], V.V. Rumyantsev[5], S.S. Mykhailova[1], V.G. Chiorny[1], T.A. Hromakina[1], O.I. Mikhalchenko[1], A.V. Sergeyev[1], V.G. Shevchenko[1], I.G. Slyusarev[1], V.R. Aivazyan[3,4], G. Kapanadze[3,4], O.I. Kvaratskhelia[3,4], A.O. Novichonok[2], Sh.A. Ehgamberdiev[6], O.A. Burkhonov[6], Z. Donchev[7], T. Bonev[7], I.V. Reva[8], A.V. Kusakin[8], A.V. Serebryanskiy[8], V.I. Kashuba[9], L.V. Elenin[2], A. Mokhnatkin[2], S.E. Schmalz[2], V.A. Voropaev[2], V.V. Kouprianov[10], A.R. Baransky[11]

[1]Institute of Astronomy of V.N Karazin Kharkiv National University, Kharkiv, Ukraine krugly@astron.kharkov.ua,
[2]Keldysh Institute of Applied Mathematics, RAS, Moscow, Russia,
[3]Kharadze Abastumani Astrophysical Observatory, Ilia State University, Georgia,
[4]Samtskhe-Javakheti State University, Georgia,
[5]Crimean Astrophysical Observatory, RAS, Nauchny, Crimea,
[6]Ulugh Beg Astronomical Institute, UAS, Tashkent, Uzbekistan,
[7]Institute of Astronomy, BAS, Sofia, Bulgaria,
[8]Fesenkov Astrophysical Institute, Almaty, Kazakhstan,
[9]Astonomical Observatory, Odesa National University, Ukraine,
[10]University of North Carolina, Chapel Hill, USA,
[11]Taras Shevchenko National University of Kyiv, Ukraine

We carry out regular photometric observations of near-Earth asteroids (NEA) to investigate their physical properties such as rotational parameters, surface characteristics, size, shape, and parameters of binary systems. The main our objects are newly discovered and potentially hazardous NEA, as well as targets of radar observations and space missions. Particular attention

is paid to recording the impact of YORP and BYORP effects on the asteroid dynamics.

The coordinated observations are carried out in the frame of ISON cooperation using telescopes located at observatories of Bulgaria, Georgia, Italy, Kazakhstan, Mexico, Ukraine and Uzbekistan. All telescopes are equipped with CCD cameras and sets of Johnson-Cousins filters BVRI. More than 50 asteroids per year are observed within the network.

We present results of photometry of 70 NEA made over 250 nights in 2019. These observations allowed us to determine new rotation periods for 18 NEAs, to examine rotation of 17 small NEAs with diameters smaller 300 m, to study binary nature of 4 NEAs, to explore 2 targets of space missions, to obtain new data needed for discovery and/or characterization YORP effect of 11 NEAs and BYORP effect for 4 binaries.

Search of areas with anomalous optical roughness on the Ceres and Vesta surfaces using Dawn FC images

I. Slyusarev[1,2], V. Kaydash[1,2], T. Hromakina[2], V. Rychagova[1], M. Stepaniuk[2], Yu. Mashtakova[1], I. Belskaya[1,2], Yu. Shkuratov[1,2], V. Shevchenko[1,2]

[1]Department of Astronomy and Space Informatics, V.N. Karazin Kharkiv National University
[2]Institute of Astronomy, V.N. Karazin Kharkiv National University, Kharkiv, Ukraine

The slope of the phase function f(α) of a regolith-like surface strongly depends on its albedo and texture. The contribution of albedo variations over the surface can be significantly suppressed when the phase ratio f(α1)/f(α2),i.e. the ratio of two images of the same region acquired at different phase angles is considered. The resulting phase-ratio image contains information mainly on the structural properties of the regolith. Reliability of this method has been proved by the detections of photometric anomalies related to changes in structure of lunar surface layer in the spacecraft landing sites (Kaydash, V., Shkuratov, Y., Videen, G., 2013). In order to obtain the distribution of the color- and phase-ratio images we used already calibrated, spatially combined, absolutized, photometrically normalized albedo images. Only after all this conversions it is possible to consider that the received images of color-ratio and steepness of the phase function distribution reflect real characteristics of the surface.

From July 2011 to September 2012 NASA Dawn spacecraft has been exploring asteroid (4) Vesta, and since March 2015 spacecraft orbiting around dwarf planet Ceres, the largest body in the Main asteroid belt (Russell C.T. and Raymond C.A. 2012). The onboard Framing Camera was equipped with a clear filter and seven color filters in the wavelength range from 0.4 to 1.0 μm (Sierks H. et al., 2011). During the mission to Vesta and Ceres a large volume of data at different illuminat.

CCD-photometry of selected asteroids

O. I. Mikhalchenko[1, 2], V. G. Shevchenko[1, 2], V. G. Chiorny[1], I. G. Slyusarev[1, 2]

[1]Department of Astronomy and Space Informatics, V. N. Karazin Kharkiv National University, [2]Institute of Astronomy, V. N. Karazin Kharkiv National University

The data obtained using photometric observations of asteroids make it possible to determine the position and orientation of the asteroid in space, to restore the shape of the asteroid, the speed and sense of its rotation, to draw preliminary conclusions about the physicochemical composition of its surface, etc. Knowing additionally the cross-sectional area of the asteroid (from stellar occultations, direct imaging using large telescopes) and the time of its determination, it is possible to restore the dimensions of the asteroid, as well as evaluate the so-called geometric albedo of its surface. Further combining photometric data with those obtained by other methods (polarimetric, infrared, spectral observations, etc.) and their analysis gives a more complete understanding of the nature of both individual asteroids and entire populations of such objects.

CCD-photometry of asteroids 95, 118, 152, 163, 212, 238, 241, 306, 404, 489, 568, 578, 757 (Main Belt), 87, 168, 420 (Cybeles), and 1583 (Jovian Trojan) was performed in 2016-2019 as part of the research program for the determination of high-accuracy geometric albedos of asteroids of different sizes and compositional types. Observations were carried out in the BVR-bands of the Johnson-Cousins system using 0.7-m telescope at Chuguev observational station of the Institute of Astronomy of V. N. Karazin Kharkiv National University. All objects were selected so that the aspect data at the time of observation were as close as possible to those at which the occultation diameters were obtained.

The report will present the results of photometric observations of selected asteroids (light curves, rotation periods, phase curves, etc.),

reestimations of their geometric albedos, and a comparison of our results with previous ones.

Influence of the light pressure forces on the dynamics of asteroids

O. Golubov

V. N. Karazin Kharkiv National University
Institute of Astronomy of V. N. Karazin Kharkiv National University

In the last few decades, the light pressure forces and torques were demonstrated to be a significant factor of evolution of small asteroids.

The force produced by the non-isotropic emission of thermal light by an asteroid (the Yarkovsky effect) can push the asteroid along its orbit, causing secular changes of the orbit over Myr time spans. This phenomenon is important for spreading of asteroid families, for transportation of asteroids to the near-Earth region via the Kirkwood gaps, and for exact prediction of asteroid orbits.

Similarly, the non-compensated torque of light pressure forces acting upon an asteroid can change the asteroid's rotation rate and the orientation of its orbital axis. This effect can slow the asteroid down and cause its tumbling, or spin it up and cause its disintegration by centrifugal forces.

Both the Yarkovsky effect and YORP have already been observationally confirmed for multiple asteroids.

In my talk, I will summarize the state of the art in the understanding of the Yarkovsky and YORP effects and their influence on the evolution of asteroids. A special attention will be paid to my recent results, such as the tangential component of the YORP effect, possibility of YORP equilibria during asteroids' evolution, and dynamics of binary asteroid systems.

Asteroid pairs: method validation and new candidates

I.I.Kyrylenko, Y. M. Krugly, O. A. Golubov

Institute of Astronomy Kharkiv National University, Kharkiv, Ukraine
ihor.kyrylenko@karazin.ua

It is well known that a lot of asteroids are included in families or pairs. Asteroid pairs are created by two different processes. First way is the other asteroid zooming and colliding, causing disruption into a pair, or by a mechanism called the YORP effect, which is essentially solar light pressure

which can slowly speed up the rotation of an asteroid, later causing the breakup of it by centrifugal forces. As a result, two separate asteroids with small initial relative distances and velocities are created. Over time their orbit drifts apart due to perturbations from planets, and the task emerges to identify such a pair and to uncover its dynamical history.

To identify such asteroids as a potential pair hierarchical clustering method is used, which consists of calculating the distance between asteroids in a phase space of osculating orbital elements. To confirm or invalidate those potential pairs we use the backtrack integration technique. For backtrack integration, we adopted Rebound package that is available as a library for Python and C programming languages. Using this package, we model dynamics of asteroids to the past to find possible moments of the parent body disruption into a pair. To mitigate uncertainties in the asteroids' orbital elements, we reproduce possible system states simulating a large number of asteroids represented by clones with varying orbital parameters (positions, velocities, masses).

As an outcome we obtained a pipeline, which allows us to process asteroids pairs' data starting from their orbital elements and ending with their age determination via simulations. During our survey we rediscovered some of already known pairs. To prove the working efficiency of our pipeline we took 20 of that pairs with already determined disruption ages and recalculated them. The results show a good agreement, that states that our pipeline can be used to reliably discover pairs and obtain their age. Using this, we surveyed the inner main asteroid belt and got five hundred pair candidates. In this talk we present our pipeline and 10 new pairs as a preliminary result.

Active asteroids: discovery and characterization

S.Mykhailova

Institute of Astronomy of V.N. Karazin Kharkiv National University

Since the 19th century two classes of the Solar system small bodies were distinguished based on their orbital properties and appearance, i.e. comets and asteroids. Comets are icy bodies at highly eccentric orbits showing coma and tail as the result of outgassing. Asteroids are small celestial solid bodies with no activity. However, this opinion existed until the discovery of a cometary tail for the asteroid (7968) Elst–Pizarro in 1996, which later obtained second designation as a comet 133P/Elst- Pizarro. This discovery gave start to the studying of a newly recognized class of small Solar system

bodies, which is called ‘active asteroids’. The main feature of active asteroids is comet-like activity due to mass lost. At present, there are more than 30 discovered active asteroids from different parts of Solar system. Nature of their activity is still not well known. Several possible mechanisms of mass-loss were proposed, such as sublimation, impacts, rotational fission or thermal effects. Recently, dust ejections were detected for very small 300 m asteroid (101955) Bennu during the space mission OSIRIS-REx. In a fundamental sense, the study of active asteroids can answer questions about the origin and evolution of the Solar system in whole. In the particular case, we are interesting to know physical properties of these bodies. We will present a review of available data on active asteroids as well as the results of our photometric observations of active near-Earth asteroids.

Near-Earth asteroids of cometary origin associated with the Virginid complex

G.I. Kokhirova, P.B. Babadzhanov, U.H. Khamroev, A.I. Zhonmuhammadi, I.V.Kulaev

Institute of Astrophysics, National Academy of Sciences of Tajikistan

The Virginid meteoroid streams produce a series of meteor showers active annually during February-May. A certain parent comet is not found but a related association of some showers with near-Earth asteroids was previously established and a cometary origin of these asteroids was suggested. We performed a new search for NEAs belonging to the Virginid asteroid-meteoroid complex. On the base of calculation of orbital evolution of a sample of NEAs and determination of theoretical features of related showers a search for observable active showers close to theoretically predicted ones was carried out. As a result, the predicted showers of 31 NEAs were identified with the showers of the Virginid complex. Revealed association points to a cometary nature of NEAs that are moving within the stream and may be considered as extinct fragments of a larger comet-progenitor of the Virginid asteroid-meteoroid complex.

Observations of the active asteroid 3552 Don Quixote at the Sanglokh Astronomical Observatory

G.I. Kokhirova[1], O.V. Ivanova[2,3,4], F. Dzh. Rakhmatullaeva[1]

[1]Institute of Astrophysics of the Academy of Sciences of the Republic of Tajikistan
[2]Astronomical Institute of the Slovak Academy of Sciences
[3]Main astronomical observatory of the National Academy of Sciences of Ukraine
[4]Astronomical Observatory named after T. Shevchenko
Kiev National University

The results of the multi-color optical observations of asteroid (3552) Don Quixote, performed at the Sanglokh observatory in July 2018 are presented. The apparent and absolute brightness of the asteroid in the VRI filters was determined. Analysis of the asteroid light curves showed a significant change in brightness - from 11.5 to 13.1 absolute magnitudes during the observation period. Such a significant change in brightness indicates an asteroid outburst; therefore, we have registered its activity, confirming the comet origin of the object.

Results of the observation of the dual object 2008GO98 (362P) in 2017

G.I.Kokhirova[1], O.V.Ivanova[2,3,4], F.Dzh.Rakhmatullaeva[1], A. Baransky[3], A.M. Buriev[1], U.Kh.Khamroev[1]

[1]Institute of Astrophysics of the Academy of Sciences of the Republic of Tajikistan
[2]Astronomical Institute of the Slovak Academy of Sciences
[3]Main astronomical observatory of the National Academy of Sciences of Ukraine
[4]Astronomical Observatory named after T. Shevchenko
Kiev National University

We present the results of optical observations of the dual object 2008 GO98 (362P) which were performed at the Sanglokh Observatory of the Institute of Astrophysics, National Academy of Sciences of Tajikistan and at the Astronomical Observatory, Taras Shevchenko National University of Kyiv in July-September 2017. The asteroid showed a sign of comet activity as a dust coma and tail during monitoring, the presence of which was

confirmed by the results of study of the images morphology. The apparent and absolute magnitudes of the asteroid in the R band were determined, their gradual decrease from 13.97 to 14.53 absolute magnitudes during the observation period indicate a ceasing of activity by the end of monitoring. The estimate of the asteroid effective diameter from our observations of ~7 km is consistent with the available data. The obtained new data proposed a cometary nature of the object. The coordinates of the asteroid were determined, the sufficient accuracy of astrometric measurements made it possible to calculate the orbit, the elements of which are consistent with the available orbital data. Asteroid activity did not affect a stability of the orbit.

Походження та динамічний час життя Кентаврів

А. М. Казанцев, Л.В. Казанцева

Астрономічна обсерваторія Київського національного університету імені Тараса Шевченка

Кентаврами називають малі тіла Сонячної системи, що рухаються в між орбітами Юпітера та Нептуна. Зазвичай вважається, що ці тіла перейшли на свої сучасні орбіти із зон за межами орбіти Нептуна і навіть з міжзоряного простору.

Виконані нами чисельні розрахунки показали принципову можливість переходу в популяцію Кентаврів тіл з поясу астероїдів, зокрема із зони сумірності 2 : 1 з Юпітером. В сумірностях ексцентриситети орбіт можуть досягати значень, достатніх для зближень тіл з планетами. Після таких зближень астероїди можуть переходити в інші зони Сонячної системи, зокрема і за межі орбіти Юпітера. Крім головного поясу астероїдів джерелом поповнення Кентаврів можуть бути й тіла групи Гільди, орбіти яких перебувають в сумірності 4 : 3 з Юпітером.

Обчислена еволюція орбіт всіх реальних Кентаврів з розмірами понад 1 км, відібраних з каталогу Міжнародного центру малих планет, на інтервали часу до 200,000 р. в минуле і в майбутнє. Оцінено точність чисельних розрахунків еволюції такого типу орбіт. Виявлено тіло, яке безсумнівно перейшло в популяцію Кентаврів 495 р. тому. До такого переходу велика піввісь його орбіти становила понад 70 а.о. Це перший випадок точного визначення моменту й зони переходу тіла в Кентаври.

Проаналізовано існуючу методику оцінки динамічного часу існування Кентаврів за чисельною еволюцією орбіт-клонів та показано

труднощі таких оцінок для тіл, що можуть зближуватись з Юпітером чи Сатурном. В деяких випадках динамічний час існування окремого тіла серед Кентаврів за методикою орбіт-клонів може перевищувати реальний час на два порядки і більше.

Малі тіла Сонячної системи з оцифрованих фотографічних спостережень в Балдоне: результати та попередній аналіз.

О.М. Їжакевич[1], С.В. Шатохіна[1], І. Еглітіс[2], Ю.І. Процюк[3], В.М. Андрук[1]

[1]Головна астрономічна обсерваторія
[2]Baldone Observatory, Institute of Astronomy, University of Latvi
[3]НДІ "Миколаївська астрономічна обсерваторія"

Довготривалі програми великих фотографічних оглядів зоряного неба, започатковані в минулому столітті, мали за основну мету отримати численні каталоги координат і зоряних величин зірок, поступово залучаючи до таких визначень більш слабкі об'єкти. Але реалізація цих програм повністю стала реальною тільки за можливості оцифрування фотографічних спостережень. Це суттєво зменшило витрати на обробку і максимально збільшило кількість отриманої з великою точністю інформації про всі зафіксовані на фотоемульсії об'єкти.

В процесі обробки сканів платівок і після створення позиційних зоряних каталогів ми вирішили ідентифікували зображення і координати інших незоряних об'єктів Всесвіту, як астероїди, комети, деякі планети Сонячної системи. В даній роботі аналізовані результати цифрової обробки спостережень зоряних скупчень в UBVR смугах, які були виконані в 1967-1993 роках за допомогою 1.2-м телескопа Шмідта Балдонівської обсерваторії Латвійського університету. На основі аналізу біля 300 U-платівок, понад 2000 V-плівок та декількох B- та R-платівок було складено каталог більш ніж 1700 положень і величин астероїдів і комет в інтервалі від 9^m до 18^m. Для виявлення неоднозначних ототожнень зображень координати всіх ідентифікованих об'єктів були порівняні з координатами зірок каталогу Gaia DR2. У випадках покриття на небесній сфері зображень астероїдів і зірок, близьких за координатами і зоряними величинами, положення астероїдів вважались неоднозначно визначеними і були виключені з складу каталогу. Кількість таких випадків зазвичай більша для слабких астероїдів.

Серед об'єктів складеного каталогу є астероїди, які представляють особливий інтерес, комети 31P та C/1969 T1. Оброблені пластинки з зображеннями деяких астероїдів Головного поясу, чиї положення зафіксовані на 20-25 років раніше до їх офіційного відкриття. Отримано велику кількість положень і величин слабких астероїдів до 17.5 зоряної величини, які були відкриті на початку 21 століття. Для деяких з них ранні спостереження або зовсім відсутні в світових базах даних, або їх замало у часовий інтервал, попередній до офіційного відкриття астероїда. Інформацію про це можна отримати тільки з старих фотографічних спостережень. Такі дані положень астероїдів та їх аналіз може бути корисним не тільки для сучасних розрахунків ефемерид, але і для вивчення еволюції орбіт астероїдів.

За результатами O-C порівнянь з ефемеридами виконано попередній аналіз позиційної точності всіх положень астероїдів. Отримані значні відмінності в позиційній точності для положень астероїдів в різних спектральних смугах, які були підтверджені і для зірок за результатами порівнянь координат, отриманих на U-, B-, V-, R-платівках, і відповідних координат зірок Gaia DR2 каталогу. Зазначені похибки визначення координат можуть бути наслідками особливостей фотографічного матеріалу (гнучкі V-плівки, плоскі U-, B-, R-платівки) та нерівномірними викривленнями поверхні плівки під час сканування.

Цифрова обробка серії фотографічних спостережень астероїдів 1924-1925 рр.

Л.В. Казанцева [1], С.В. Шатохіна[2]

[1]Астрономічна обсерваторія Київського національного університету імені Тараса Шевченка
[2]Головна астрономічна обсерваторія Національної Академії Наук України

Космічна місія Gaia вже дозволила отримати високоточні положення та фотометричні значення для понад 14 тисяч астероїдів. Нові дані дозволяють покращити знання про їхні маси, альбедо та орбіти. Це в свою чергу дає можливість більш детально вивчати динаміку руху окремих астероїдів та їхніх сімейств, відслідковуючи можливі збурення на тривалих проміжках часу. Для цієї задачі важливо мати довгі та щільні ряди наземних спостережень. В нагоді стають фотографічні спостереження, оцифрування і обробка яких

виконана в нових системах відліку, забезпечених реперними точками. Особливо цінними є спостереження, якнайбільше віддалені за часом від епохи Gaia.

Склотека Київської університетської обсерваторії в числі інших містить серію програмних спостережень астероїдів періоду з 18.08.1924 по 16.04.1925.

Негативи 9x12 см були отримані І.І. Путіліним з подвійним астрографом Анрі-Репсольда ДАІШ (фотографічний об'єктив D=381 мм, F=6400 мм). На знімках експоновані 26 малих планет і комета Шайна, причому на більшості платівок одночасно сфотографовано декілька астероїдів. Таким чином, для кожного з них отримано 2-4 положення.

На теперішній час обробка оцифрованих спостережень виконується з використанням комплексу програм PyPlate міжнародного проекту Archives of Photographic PLates for Astronomical USE. Результатом роботи є отримані астрометричні положення та зоряні величини астероїдів відносно зір каталогу Gaia. Точність координат і зоряних величин за попередніми оцінками є високою, а отримані положення цілком придатні для включення до бази даних MPC, тим більше, що саме в ці роки спостереження згаданих астероїдів в MPC відсутні.

High-speed spectrophotometry of meteors

S.M.Pokhvala, B.E.Zhilyaev

Main Astronomical Observatory of NAS of Ukraine

This work is devoted to spectrophotometry of meteors. Spectrophotometry methods allow determining the chemical composition, temperature, and density of meteor plasma. Photometry of the meteor track indicates brightness variations, as well as fluctuations in the trajectory transverse to the direction of motion. Spectroscopic analysis of a meteor of about - 4 visual magnitude is presented on the basis of a spectrogram with absolute line intensities. The stony composition of a fireball was found. Photometry of the meteor made it possible to determine the oscillation frequency estimated at 36 Hz, as well as the transverse oscillations of the trajectory. It is shown that the meteor moves along a spiral trajectory. The radius of the spiral at an altitude of about 27 km reaches 90 meters.

Оценка физических характеристик аномально высоких метеоров по наблюдениям в Киеве

П.Н Козак

Киевский университет имени Тараса Шевченко, Астрономическая обсерватория

Данная работа является продолжением исследований аномальных метеоров, в данном случае метеоров с аномально большими высотами регистрации, превышающими условную границу 130 км. Приводятся вычисленные ранее кинематические характеристики, включая параметры траектории и элементы орбиты, семи метеоров: одного Персеида 1993 года, одного спорадического метеора 2001 года, и пяти Леонид 2002 года, зарегистрированных во время предсказанного метеорного шторма. Высоты появления упомянутых метеоров лежат в диапазоне 135–145 км, их геоцентрические скорости лежат в диапазоне 63–72 км/с. Начальные массы составили приблизительно 0.03–0.06 г соответственно. Также приводятся кривые блеска спорадического метеора, и метеоров потока Леониды. Обсуждаются особенности ассиметричного изображения комы спорадического метеора, которая является уникальной, и была зарегистрирована впервые. Также рассматриваются особенности кривых блеска всех пяти Леонид ввиду их идентичности, и особенностей асимметрии в кривых блеска сразу после достижения максимума излучения.

Были оценены скорости потери массы метеороидов: для спорадического метеора данная величина составила 0.14 г/с в максимуме, и 0.20 г/с – для Леонид. При помощи классических уравнений нагревания и абляции, вызванной интенсивным испарением, было показано, что спорадический метеороид представлял из себя каменное тело с плотностью, вероятно, около 2 г/см^3, хотя данное значение сильно зависит от выбранной температуры испарения, и может варьироваться в диапазоне 1–3.5 г/см^3. Моделируемые кривые блеска хорошо описывают максимум блеска метеора, а также конечную часть его кривой блеска. Для расчета начальной высоты появления в модели была принята гипотеза частично изотермичного тела с некоторой фронтальной областью, прогретой до температуры плавления, и далее испарения. Было показано, что физика излучения метеоров с высотой появления 136–135 км может быть связана со сдувание поверхностной расплавленной

пленки космической частицы, а излучения ниже 124 км – с интенсивным испарение тела. Для некоторых метеоров потока Леониды с высотой детектирования 145–140 км возможно допустить начало излучения связанным с процессом обмена энергией атмосферных молекул и атомов с «холодной» поверхностью метеороида. Другим возможным объяснением может быть допущение о низкой температуре плавления метеороидов потока Леониды, до 1500–1700 К – это обеспечивает начало излучения на высотах 145–135 км также из-за плавления поверхностной пленки.

The first results of video-spectral basic observations of meteors in Kharkiv

O. Golubaev [1], A. Mozgova[2], Ye. Koniaieva[3]

[1]Institute of Astronomy, V.N. Karazin KhNU, Kharkiv, Ukraine
[2]Astronomical Observatory of Taras Shevchenko KNU
[3]Faculty of Physics, V.N. Karazin KhNU

An automated video-spectral meteor patrol (AVSMP) of the Research Institute of Astronomy of V.N. Karazin Kharkiv National University was used to observe meteor phenomena and obtain their spectra. Meteor patrol developed and constructed in 2018 and it is located at the Chuhuiv observation station. The spectral camera provides meteor spectra in the wavelength range 350 - 1000 nm with an inverse linear dispersion of the order of 1.5 nm \ pixel. The temporal resolution of observations in meteor spectra changes is 20 ms. The maximum magnitude for the observation complex (for a camera without a diffraction grating) is + 5.4^m. For the spectral camera, the maximum magnitude is + 4.0^m. In 2019, the meteor patrol was supplemented by a camera, which was located at the Institute of Astronomy in Kharkiv and it is used for basic observations of meteor phenomena. During 2019, the basic and spectral observations of Perseids, Leonids, Alpha-Monocerotids, Taurids meteor showers were carried out.

During August - December 2019, 581 video fragments with recorded meteor phenomena (non-spectral observations) and 181 video fragments with recorded meteor spectra were received by a meteor patrol at the Chuhuiv observation station. 250 video fragments of meteor phenomena (non-spectral observations) were received by the camera in Kharkiv.

The necessary software has been developed for the processing of video-spectral meteor observations. The observation data obtained during the basic and spectral observations of meteors is processed.

Система наведения телескопа системы Шмидта наблюдательной станции Крыжановка.

Ю.М. Горбанёв, С.Р. Кимаковский

НИИ “Астрономическая обсерватория”
Одесского национального университета имени И.И. Мечникова

Телескоп системы Шмидта с июня 2003 года был задействован в комплексе телевизионного метеорного патруля на станции Крыжановка. Параметры телескопа: главное зеркало: диаметр 271.25 мм, радиус кривизны 880 мм, параксиальное фокусное расстояние 440 мм, светосила 2.24; коррекционная пластина: диаметр 223.9 мм, световой диаметр в оправе 219.2 мм. Телескоп разработан и создан в оптической и механической мастерской станции Маяки. В качестве гидирующей установки применялся промышленный параллактический штатив АПШ-4, для которого был создан шаговый привод. В качестве приемника использовалась телевизионная камера WATEC LCL 902K, в такой комплектации телескоп использовался до августа 2015 года. В результате регулярных патрульных наблюдений метеоров база данных пополнилась 2345 видеозаписями зафиксированных метеорных явлений с временным разрешением 20 мс и координатным разрешением в 1 угловую секунду и проницающей до 12 звездной величины.

В результате выхода из строя в 2015 году телевизионной камеры телескоп был подвергнут модернизации в виде реставрации трубы, нанесения нового покрытия для зеркала, установки нового привода и нового приемника излучения VIDEOSCAN-415-2001.

При работе в режиме телевизионного метеорного патруля патрулирование окрестностей радиантов метеорных потоков не требовало большой точности и скорости наведения телескопа. После модернизации телескопа объектами наблюдений стали кометы и астероиды. Возникла потребность в быстром и надежном наведении телескопа на наблюдаемые объекты.

Установка приводов для осей прямого восхождения и склонения штативов АПШ требует больших затрат и не гарантирует большую точность наведения.

Поэтому мы попытались выполнить поставленную задачу другим способом, а именно использовать современные методы отождествления звездных изображений.

Для этого была создана программа Navigator, задача которой облегчить наведение для наблюдателя. Описан процесс анализа графических файлов получаемых при помощи камеры VIDEOSCAN-415-2001. Процесс отождествления осуществлен при помощи локального пакета программ Astrometry.net, который представляет собой Linux пакет программ, запуск которых на операционных системах семейства Windows возможен благодаря эмулятору Linux - Cygwin.

Разработанная система позволяет отождествлять наблюдаемый участок звездного неба и вычислить экваториальные координаты центра снимка за время не более пяти секунд. Программа вычисляет разности между координатами объекта и текущим положением, что позволяет наблюдателю проводить коррекцию по вычисленным поправкам для прямого восхождения и склонения.

Предполагается дальнейшая модернизация телескопа Шмидта.

New mobile complex for observation of occultation

V.V. Kleshchonok[1], V.L.Karbovsky[2], M.V. Lashko[2], M.I. Buromsky[1]

[1]Taras Shevchenko National University of Kyiv, Kyiv
[2]Main Astronomical Observatory of NAS of Ukraine

The method of occultation by stars of solar celestial objects allows obtaining valuable information about the geometric dimensions, surface brightness distribution, detection of structural features with such a resolution that is unattainable for ground-based telescopes. The mobile astronomical complex was developed and manufactured for monitoring observations of star occultations by celestial objects on the basis of the Main Astronomical Observatory of the NAS of Ukraine for increasing the number and possibility of simultaneous observations from several points. The mobile complex consists of a telescope (D = 153 mm, F = 1200 mm) with an automatic guidance system Sky-Watcher EQ-5; light filter unit with 3 BGR filters; Apogee Alta U47 CCD cameras (1024x1024, 13x13μ pixels); control computer; GPS receiver; power supply of electronic units of the complex, DC/AC 12V / 220V converter. It is easily transported by car and uses a car battery to power during observations. Test observations were carried out with the mobile complex, which showed its efficiency. The following system parameters were obtained: image scale - 2.2″/px, field of

view - 37.5 arcminutes, star image size 2.3″-2.8″. Objects with a maximum magnitude 16.8 mag are possible registering for 100 seconds of exposure without a filter.

Gravity capture of a small asteroid by the Earth-Moon system

Nozdrachev T. A.[1], Kochergin A. V.[1,2], Zubko E. S.[3]

[1]Far Eastern Federal University, School of Natural Sciences;
nozdrachev.ta@mail.ru
[2]Institute of Applied Astronomy of RAS, 10 Kutuzova Emd., Saint-Petersburg 191187, Russia
[3]Humanitas College, Kyung Hee University, 1732 Deogyeong-daero, Yongin-si, Gyeonggi-do 17104, Republic of Korea
Scientific adviser – Zubko E. S.[3]

1. Introduction

In the past billions of years of the existence of the solar system, small fragments of asteroids and cometary nuclei could be captured in stable near-earth orbits. The discovery of such small natural satellites was not possible in the past due to the low efficiency of the then existing astronomical technology. Significant progress over the past twenty years, achieved in improving astronomical telescopes and detectors, could make it possible in principle to detect fragments of asteroids and cometary nuclei. However, near-Earth space is already littered with space debris by inoperative artificial Earth satellites (AES) and their debris. For example, the number of space debris objects larger than 10 cm today already exceeds 30,000, and this number continues to grow continuously, making it difficult to find fragments of asteroids and cometary nuclei. In this short article, using numerical modeling methods, we study the conditions necessary for the capture of a small body by the Earth's gravity and, thus, answer the fundamental question - where in the near-Earth space is the appearance of small satellites of natural origin most likely?

2. Model

We simulate the motion of a small body weighing 1000 kg (diameter ~ 1m) in the gravitational fields of the Earth, the Sun, and the Moon. At the initial moment of time t_0, the location of all four bodies with the corresponding initial velocities is set. For simplicity, we associate the

origin with the sun and set it motionless. It is worth noting, however, that we show the results in *Fig. 1* and *Fig. 2* in the coordinate system associated with the Earth. Using the law of gravity, it is possible to calculate the acceleration of the Earth, the Moon and the small body. These accelerations are assumed to be constant over the time interval Δt. Using the known initial coordinates, velocities and accelerations of all three bodies, we simulate the motion from time moment t_0 to $(t_0 + \Delta t)$. At the final moment of time, the velocities and accelerations of all three bodies are updated for their new locations, and the whole procedure is repeated for the next time interval Δt. Thus, it is possible to obtain the trajectory of a small body in the Earth-Moon system. We put $\Delta t = 1$ s. It is important to note that we also investigated smaller Δt, however, this did not change the resulting trajectories of the small body.

3. Capture conditions and simulation results

Studies show that representatives of all four groups of near-Earth asteroids, the so-called *Amur, Atir, Apollon,* and *Aton,* can potentially be captured into near-Earth orbit (see, for example, [1]). Our simulation shows that the main role, in this case, is played by the moon. In some geometric configurations, the Moon is able to noticeably slow down a small object approaching the Earth with a relative speed of up to 1500 m / s. Moreover, the attraction of the moon is also able to change the direction of the velocity vector of a small body and, thus, transfer it to a geocentric orbit. This can happen, in particular, when a small body approaches the Moon to distances of less than 40 thousand km. In such proximity, the gravitational impact of the moon markedly exceeds the Earth.

As a result, the orbit of the captured satellite will either cross the lunar or close to it. This is an important feature that makes the geocentric orbit of a captured small body unstable. For this reason, the captured small body is likely to be thrown back from the geocentric orbit over the next three years. In rare cases (< 1%), a captured body can spend in a geocentric orbit for up to 10 years. It is important to note, however, that the return of the small body to the heliocentric orbit is not the only possible scenario. There is also a high probability, according to our estimates, ~ 30%, that a small body will collide with the Moon or the Earth.

4. Types of geocentric orbits of captured bodies

The orbits of captured asteroids can be divided into two types. The first includes orbits whose perigee is beyond the orbit of the moon, i.e., over 384,000 km, while the second type of orbits implies perigee lying inside the lunar orbit.

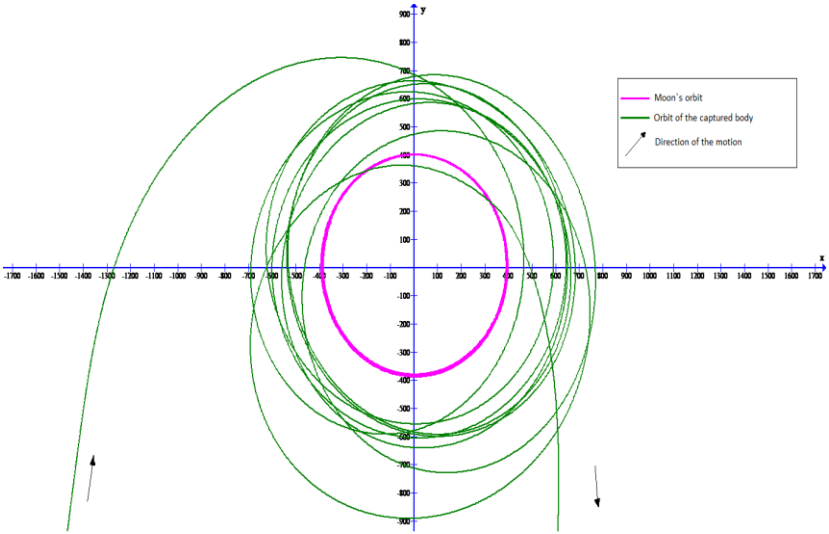

Fig. 1. An example of a geocentric unstable orbit of a captured small body. The earth is in the center of coordinates, the pink circle corresponds to the orbit of the moon, and the distance is given in thousands of kilometers

The first type of orbits, an example is shown in Fig. 1 is extremely unstable for several reasons. Indeed, at large distances the gravitational attraction of the Earth may be weaker than the lunar one. In this case, in case of approaching the moon, the satellite can be dispersed, which will increase the apogee of its orbit. However, at the farthest point in the orbit, a small body can turn out to be again captured by the gravity of the Sun and thus go into a heliocentric orbit. The investigation of the asteroid orbit 2006RH 120 [see 2], showed that it had left the geocentric orbit this way.

Fig. 2 shows an example of the transition of a small body from an orbit of the first type to an orbit of the second type, with a major semi-axis of 225 thousand km and an eccentricity of 0.56. Such transitions occur

when the Moon approaches a body that is already captured in a geocentric orbit, at a distance of less than 25 thousand km. In Fig. 2, the case of approaching up to 18 thousand km is shown. Two points in the orbits of the small body and the moon show their locations at the time of closest approach.

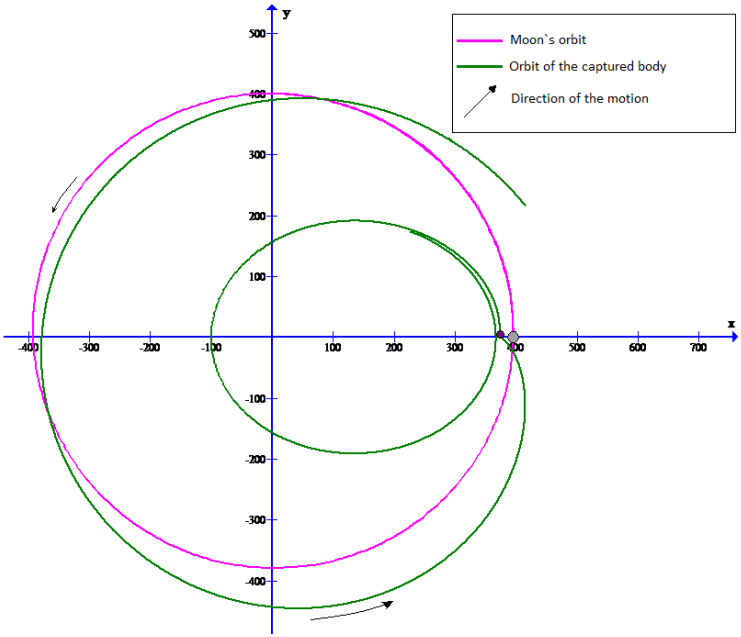

Fig. 2. Demonstration of the transition of an asteroid from an orbit of the first type to a lower one

5. Conclusions

Our simulation showed that in order for a small body to be captured in a geocentric orbit, the perihelion of the original orbit should be in the range from 0.8 a. u. to 1.017 a. u., and aphelion from 0.983 a. u. to 1.2 a. u. Moreover, the eccentricity of the initial heliocentric orbit should not exceed a value of 0.1. These conditions provide a small relative velocity of approach of a small body to the Earth and, thus, the possibility of transition to a geocentric orbit. However, the geocentric orbit of the captured body will be unstable. In this case, two scenarios are possible,

either the return of the body to the heliocentric orbit, or a collision with the Earth or the Moon. However, the return of the small body to the heliocentric orbit implies the possibility of its re-capture by the Earth in the future.

References

[1] – Zausaev. A. F., Pushcarev A. N. On the probability of asteroids colliding witch the Earth // Solar System. Res. 1994. V. 27. P. 465-468.

[2] - Kwiatkowski, T., Kryszczyńska, A., Polińska, M., Buckley, D.A.H., O'Donoghue, D., Charles, P.A., Crause, L., Crawford, S., Hashimoto, Y., Kniazev, A., Loaring, N., Romero Colmenero, E., Sefako, R., Still, M., Väisänen, P., 2009. Photometry of 2006 *RH*120: an asteroid temporary captured into a geocentric orbit. Astron. Astrophys. 495, 967–974.

Simulation of coma 67P/Churyumov-Gerasimenko with hierarchical dust particles

V.Reshetnyk[1,2], Yu. Skorov[3], O.Ivanova[2,4]

[1]National Taras Schevchenko University of Kyiv, Ukraine

[2]Main astronomical observatory of National academy of sciences of Ukraine

[3]IGEP TU, Braunschweig, Germany

[4]Astronomical Institute of Slovak Academy of Science

Each comet has a unique coma shape. Its size and structure obviously depend on many parameters. In comas, various phenomenon can be observed: jets, shells, etc. Some active structures are stable but other are rapidly changing. Ground-based observations of comet 67P/Churyumov-Gerasimenko showed the existence of typical structures that persisted for a long time. Some of them were observed at several approaches to the Sun. The direct observations from the Rosetta spacecraft possible large-scale structures near the nucleus of the comet did not show. Most likely, the reason of that was a significant difference in spatial scales between ground-based and in-situ observations. We have developed the program for simulating of the dust particles motion in the coma. The main task of our work is a simulation of the 67P/Churyumov-Gerasimenko coma brightness distribution. As initial conditions we used the information about the shape of the cometary nucleus and orientation of the rotation axis. We also used

the hierarchical dust particles in our simulation. Preliminary maps of the dust distribution and coma brightness were obtained. Preliminary results show that taking into account of the complex shape of the nucleus already allows to obtain jet-like structures in a coma. We are going to investigate influence of other parameters on our coma shape model.

Final results of astrometric and photometric observations of six trans-Neptunian objects at the Kyiv comet station

A. Baransky[1], O. Lukina[1], S. Borysenko[2]

[1] Astronomical Observatory of Taras Shevchenko National University of Kyiv, Observatorna Str. 3, 04053, Kyiv, Ukraine
[2] Main astronomical observatory, National Academy of Sciences, Akad. Zabolothoho, Str., 27, 03127, Kyiv, Ukraine
abaransky@ukr.net

In this work we focused on observations, analysis and review of six trans-Neptunian objects (TNOs) whose apparent magnitudes lie below 20^m. We present the results of astrometric and photometric observations of Pluto (134340), Haumea (136108), Makemake (136472), Eris (136199), Orcus (90482), and Varuna (20000) obtained at the Kyiv comet station (Code MPC 585) in 2017 – 2019. For observations we used the 0.7 m (f/4) reflector AZT-8 with FLI PL4710 CCD camera and filters of Johnson – Cousins photometric system. From our images we measured the objects' astrometric positions, calculated apparent magnitudes in *BV RI* (mostly *R*) bands using aperture photometry method, and found colour indices and absolute magnitudes in several bands. Using the known values of effective diameters, we calculated *R*-band geometric albedo, and using (in some cases deriving) Bond albedo, we approximated surface temperatures of the six TNOs. Analysing our calculations, results from other ground-based and space observations and findings of New Horizons mission, we continue discussion about possible surface properties of six the brightest TNOs and perspectives in their explorations.

For astrometric measurements Astrometrica 4 software was used with Gaia DR2 and UCAC 4 star catalogs. The orbits of TNOs and residuals (O–C) for both coordinates (RA and Decl.) were determined using Find Orb (version Mar. 17, 2019) software, combining our own observations with other observations from the MPC database over the last 2 – 4 years. We sent

observations to the Minor Planet Center database with the maximum O–C residual of less than 0.5″. In total, 157 precise astrometric observations of 6 TNOs, obtained during 7 observation nights, are published in the MPC database and the Minor Planet Supplement. The (O–C) RA residual varies from -0.254 to 0.289, ±σ ″ RA – from 0.058 to 0.487. The (O-C) Decl. residual varies from -0.042 to 0.325, ±σ ″ Decl. – from 0.040 to 0.383.

Final results of physical parameters calculation include absolute magnitudes in R filter (Pluto -1.10±0.01, Haumea 0.24±0.02, Makemake -0.27±0.02, Eris -1.34±0.03, Orcus 1.58±0.05, Varuna 3.40±0.10), geometric albedo in R filter (Pluto 0.51, Haumea 0.55, Makemake 0.78, Eris 0.83, Orcus 0.33, Varuna 0.13), and estimated surface temperatures, K (Pluto 35, Haumea 35, Makemake 31, Eris 23, Orcus 39, Varuna 41).

The results of our astrometrical and photometrical observations are in good agreement with others, obtained by ground based observations and correlate with the results of New Horizons space mission, Spitzer, Herschel and Hubble Space Telescopes observations.

This work is the continuation and completion of the contribution "Astrometry and photometry observations of transneptunian objects (Pluto, Eris, Haumea) at Kyiv comet station" presented at the Astronomy and Space Physics in the Kyiv University conference in 2019.

Photometric observations of the cataclysmic variable star V1432 Aquila at the Kyiv comet station

A. Baransky, N. Kaplina

Astronomical Observatory of Taras Shevchenko National University of Kyiv, Observatorna Str. 3, 04053, Kyiv, Ukraine

Observations cataclysmic variable star of the Polar class - V1432 Aql, allows to study the evolution of such objects and the accretion processes in a strong magnetic field. For observations we used the 0.7 m (f/4) reflector AZT-8 with FLI PL4710 CCD with R filter. Phorometric measurements were made using MuniWin software. The reference stars were taken from APASS star catalogs. The difference in the amplitude of the magnitude change and the phase light curve were analysed comparing with the article of Ivan Andronov and Alexei Baklanov (2007) "Thread Radius and Synchronization of the white dwarf in the unique magnetic cataclysmic variable V1432 Aql". The photometric results were published in the AAVSO database.

ФІЗИКА СОНЦЯ ТА СОНЯЧНА АКТИВНІСТЬ

SOLAR PHYSICS AND SOLAR ACTIVITY

Analysis of H-alpha observations of the M6.4 circular-ribbon solar flare

S. Chornogor, N. Kondrashova

Main Astronomical Observatory, National Academy of Sciences of Ukraine, Kyiv, Ukraine

We analyze the 2000 July 19 solar flare that occurred in the active region NOAA 9087. The H-alpha images from the Meudon spectroheliograph have been used to study morphology and evolution of the flare. The active region had a complex multipolar magnetic field configuration. According to Solar Geophysical Data (SGD) the 3N/M6.4 class solar flare occurred at 06:37 UT, peaked at 07:23 UT and lasted 2.5 hours. A set of H-alpha images shows a continuously changing state of the chromosphere during the flare. The energy was released successively in different places. The kernels appeared along the magnetic inversion line consistently and were located at the boundaries of the chromospheric network.

The flare studied began with the appearance of two bright kernels near the large positive-polarity sunspot. A few minutes later bright kernels appeared in the center of the active region near magnetic inversion line. Hard X-ray (HXR) coronal source in the 14-23 and 23-33 keV energy bands was located in this place above magnetic inversion line. Then a tunnel of bright H-alpha loops appeared southwest of these kernels. In the first flare site in the footpoint of the post-flare loop arcade the ejection occurred. New kernel appeared in the southern part of the flare. Flare ribbons of the circular shape were formed. It is known that circular flares occur when spine-fan type magnetic topology containing null points take place. Flare ribbons are the locations of intersections of the fan quasi-separatrix layer with the lower atmosphere. In the main flare phase, the H-alpha images show the reconnecting loops in the eastern part of the active region that are clearly visible in the EIT 195 A observations. Arcade of post-reconnection EUV loops connected the main flare ribbon to the location of these loops in the late phase one and a half hours after the flare maximum. Additional heating may be required for the explanation of the long flare decay phase.

QUASI-ANNUAL VARIATIONS IN THE TOTAL AREA OF SPOT GROUPS IN 12-24 CYCLES OF SOLAR ACTIVITY

V.M. Efimenko

Astronomical Observatory of the Taras Shevchenko National University of Kyiv, Kyiv, Ukraine
efim@observ.univ.kiev.ua

Periodicity in the indexes of solar activity was studied by many authors. The main ones, such as the eleven-year cycle of solar activity, Hale's double cycle (about 44 years old) are considered to be sufficiently studied. At the same time there is evidence of the existence of other cycles of solar activity, which require additional study.

The search of short-term fluctuations in the index of the total area of groups of sunspots on the basis of the Greenwich catalog of solar activity and its expansion NOAA-USEF for 1879-2016 is carried out. To search for short-term fluctuations in the changes in the total area of groups of spots, the Fourier rapid conversion program was used to analyze the deviations from the trend of smoothed monthly values for each cycle of solar activity. The main purpose of the work was to find the existence of periods in these deviations. It is found that there are two modes of short-term fluctuations of 8-10 months and 14-16 months.

The features of quasi-annual changes in activity in the 23rd cycle of solar activity are investigated. For this, an analysis was made of the groups of spots that appeared on the solar disk at the moments of each increase in activity. It was found that in 6 out of 11 cases, increased activity is caused by the appearance of large groups of spots on the Sun.

Forward modelling of particle acceleration and transport in an individual solar flare

M. Gordovskyy[1], P. Browning[1], G. Vekstein[1], S. Inoue[2], K. Kusano[2], E. Kontar[3]

[1]University of Manchester, UK
[2]University of Nagoya, UK
[3]University of Glasgow, UK

The aim of this study is model maps of hard X-ray emission produced by energetic electrons in individual solar flares and compare them with

observations. The ultimate goal is to test the viability of the combined MHD/test-particle approach for forward data-driven modelling of active events in the solar corona and their impact on the heliosphere.

We use MHD models of individual solar flares developed using non-linear force-free reconstructions of the coronal magnetic field. Based on the evolving three-dimensional structure of the magnetic and electric fields in the corona, we calculate trajectories of a large number of electrons and protons using the relativistic guiding centre approach. Using the obtained particle trajectories, we deduce spatial and energy distribution of energetic electrons in the corona and calculate bremsstrahlung hard X-ray emission using the 'thin target' approximation.

Our approach predicts some key characteristics of energetic particles in the considered flare, including size and location of the acceleration region, energetic particle trajectories and energy spectra. Most importantly, the hard X-ray bremsstrahlung intensity maps predicted by the model are in a good agreement with those observed by RHESSI: our model successfully predicts the location of the brightest footpoint sources. Therefore, the adopted approach can be used for observationally-driven modelling of individual solar flares, including manifestations of energetic particles in the corona, as well as inner heliosphere.

Cleaning solar LOFAR images using a known radio source observations

M. Gordovskyy[1], E. Kontar[2], P. Browning[1]

[1]University of Manchester, UK
[2]University of Glasgow, UK

In this study we explore a simple method for CLEANing solar radio intensity maps using observations of a known point radio source. A set of spherical geometry equations is derived to predict the point-spread function (PSF) of an instrument for an arbitrary location in the sky, taking into account the effect of ionospheric refraction. The developed method is particularly useful for solar observations, making it possible to clean solar radio images using a limited pool of bright radio sources, such as Tau A, Cyg A etc. We test the method by applying it to Tau A observations and to three solar type III and type IV events observed by LOFAR.

Study of magnetism cyclicity of the Sun in the framework of the macroscopic magnetohydrodynamics theory

V. N. Krivodubskij

Astronomical Observatory of Taras Shevchenko National University of Kyiv
e-mail: krivod2@ukr.net, krivod1@observ.univ.kiev.ua

Since the mid-70s of the last century, a new direction in theoretical studies of the evolution of the global magnetism of the Sun in the framework of macroscopic MHD has been launched at the Astronomical Observatory of Kiev National University. The report presents the results of a study of the processes of generation and reconstruction of a large-scale (global) magnetic field based on the $\alpha\Omega$-dynamo model, taking into account new turbulent effects discovered in the theory of macroscopic MHD.

It was established that a sharp radial gradient of turbulent velocity in the lower half of the solar convective zone (SCZ) leads to a change in the sign of the azimuthal component of the helicity parameter α, resulting in the formation of a relatively thin layer of negative α-effect near the bottom of the SCZ. It was found that this layer of negative α-effect, together with the positive radial gradient of the angular velocity, detected in helioseismological experiments, makes it possible to explain the direction of migration of dynamo-waves on the solar surface. The magnetic saturation of the α-effect (alpha-quenching) in the deep layers of the SCZ was calculated. An explanation of the protracted duration of the 23rd solar cycle of about 13 years is proposed. For this, we used the observed data on a significant increase in the annual module of the magnetic fields of sunspots. The calculated north-south asymmetry of the structure of the global magnetic field provides an opportunity to explain the phenomenon of the seeming magnetic "monopole", which is observed during reversal of polar magnetism. It was found that the values of turbulent electrical conductivity and turbulent magnetic permeability of the solar plasma are significantly less than the corresponding gas-kinetic parameters. Therefore, the turbulent dissipation of solar magnetic fields is enhanced by 4-9 orders of magnitude compared with classical ohmic dissipation. Macroscopic turbulent diamagnetism of solar plasma was investigated. It has been found that in the lower part of the SCZ, turbulent diamagnetism acts against magnetic buoyancy, thus fulfilling the role of "negative magnetic buoyancy". As a result of the balance of the effects of magnetic buoyancy and turbulent

diamagnetism, a layer of blocked magnetic field of magnitude ≈ 3000 G is formed in the depths of the SCZ. The turbulent advection of a magnetic field in an inhomogeneous plasma density of the SCZ was studied. It was found that in the lower half of the SCZ of the equatorial domain, turbulent advection is directed upwards. As a result of the combined action of magnetic buoyancy and turbulent advection, deep strong toroidal fields are carried to the surface of the Sun in the latitudinal "royal zone" of sunspots. The role of horizontal turbulent diamagnetism in ensuring the long-term stability of sunspots was noted. To explain the observed phenomenon of double maxima of the solar spot cycle, a scenario was developed containing the generation of a magnetic field in the tachocline at the bottom of the SCZ and its subsequent removal from the depth layers to the surface in the latitudinal "royal zone". The role of the radial omega-effect in the radiant zone in explaining the observed asymmetry in the amplitude of two neighbouring 11-years sunspot cycles was noted.

Generation of the radial magnetic field of the Sun by global hydrodynamic flows

A.A. Loginov[1], V.N. Krivodubskij[2], O.K. Cheremnykh[1]

[1]Space Research Institute, National Academy of Sciences of Ukraine and State Space Agency of Ukraine
[2]Astronomical Observatory, Taras Shevchenko National University of Kyiv
[1]e-mail: lesha.loginov@gmail.com, [2]e-mail: krivod2@ukr.net

A concept of the emergence of global hydrodynamic flows of matter and the generation of global magnetic fields in the solar convective zone is proposed. The unstable profile of differential rotation plays a crucial role in it: all hydrodynamic flows on the Sun (poloidal circulation, torsion oscillations, and spatiotemporal variations of the poloidal flow) are generated due to the loss of stability of differential rotation. None of the models known to us, wherein torsion oscillations and variations of the meridional circulation are typically calculated separately and are thus considered to be independent flows, reproduce this result. The calculations within our model suggest, on the contrary, that the indicated flows are actually toroidal and poloidal components of a single, 3-dimensional global flow. The decisive role of torsion oscillations in the generation of the radial alternating magnetic field is highlighted in the present study. It is demonstrated by numerical simulation that the time-varying radial magnetic field on the surface of the Sun reaches its maximum at the poles, where it

changes polarity with a period of ~22 years. This process may be identified with the observed effect of polarity reversal of the polar field within the Hale magnetic cycle. It is demonstrated that the lines of zero values (polarity reversal) of the surface radial magnetic field pass through the maxima of the velocity modulus of zonal flows (torsion oscillations). In addition, the lines of magnetic polarity reversal of the radial field and the maximum velocities of surface zonal flows drift from the poles to the equator. It is noted that the obtained results on the latitudinal evolution of surface zonal flows correlate with the behaviour of deep zonal flows determined by processing helioseismological data.

Unique mixed-polarity magnetic field structure in great X17.2/4B solar flare observed on photospheric and chromospheric levels

V.G. Lozitsky[1], N.I. Lozitska[1], A.A. Solov'ev[2], Ye.O. Kravchenko[3], E.A. Baranovsky[4],
V.P. Tarashchuk[4]

[1] Astronomical Observatory of the Taras Shevchenko National University of Kyiv, Kyiv, Ukraine
[2]Central Astronomical observatory at Pulkovo, S-Peterburg, Russia
[3] Physical Faculty of the Taras Shevchenko National University of Kyiv,
[4] Crimea Astrophysical Observatory, Nauchny 98409, Crimea
lozitsky_v@ukr.net, olozitsky@gmail.com, solov.a.a@mail.ru, eliza.schedrina@gmail.com, edward@craocrimea.ru, veratar4@gmail.com

In our report, we present new yet unpublished data on magnetic fields in an exceptionally powerful solar flare of 2003 October 28 of X17.2 / 4B class, which was observed with Echelle spectrograph of Astronomical Observatory of Taras Shevchenko National University of Kyiv. This flare originated in super-powerful active region NOAA 0486. By the peak magnitude of the X-ray flux, this flare takes the third position in ranking of all flares observed during era of regular measurements of this parameter of solar activity (i.e. since 1976). According to CORONAS, GOES, INTEGRAL, RHESSI, SOHO and TRACE data, the impulsive phase of the flare was from 11:06 to 11:16 UT and had a line-broadening temperature of a few hundred thousand degrees (Schrijver et al, 2006). From the data of High Energy Neutron Detector (HEND) onboard of the Mars Odyssey Mission it follows that the total energy of non-thermal electrons in the flash phase was from 2×10^{32} to 6×10^{33} erg (Nizamov et al, 2018). It is useful to

recall that this flare was studied earlier by many authors, e.g. Kiener et al (2006), Mandrini et al (2006), Kosovichev (2006) and Zharkova & Zharkov (2007), Lozitsky et al. (2018), etc.

The value of our observations lies in the fact that there were recorded the spectra of this flare in a very wide spectral range, which includes almost the entire visible region of the spectrum. Another advantage of our observations is that the spectra were obtained for such a place on the Sun, which practically coincided with the seismic source S2 / S3 according to Kosovichev (2006) and Zharkova and Zharkov (2007).

The inverse ratio of effective magnetic fields B_{eff} by by FeI 6301.5 and FeI 6302.5 lines was firstly recorded in the region of the seismic source of the flare (Fig. 1).

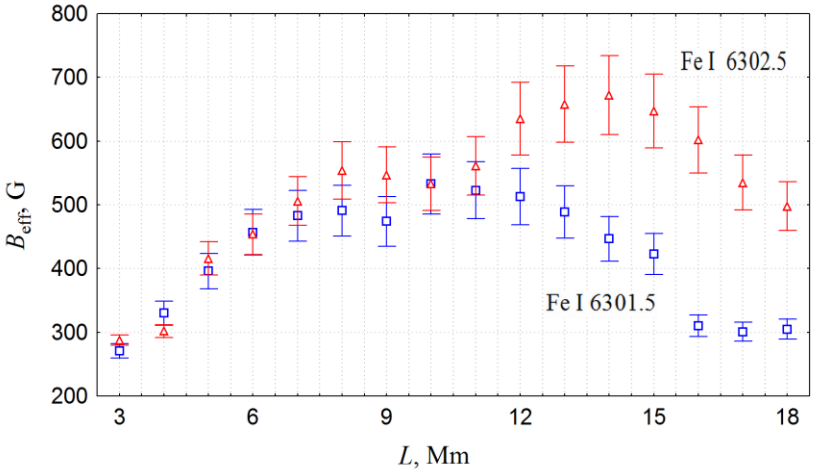

Fig. 1. Distribution along the direction of entrance slit of the Echelle spectrograph of effective magnetic field B_{eff} measured by FeI 6301.5 and FeI 6302.5 lines. One can see remarkable effect – inverse ratio between B_{eff} (6302.5) and B_{eff} (6301.5) for L=12-20 which corresponds to the place of the seismic source.

In frame of 'line-ratio' method (Stenflo, 1973; Wiehr, 1978), unequality B_{eff} (6302.5) ≠ B_{eff} (6301.5) indicates presence of spatially unresolved magnetic elements with magnetic fields of kG range. If magnetic polarities in ambient field and in spatially unresolved fluxtubes are the same, we should observe B_{eff} (6302.5) < B_{eff} (6301.5). The inverse ratio B_{eff} (6302.5) > B_{eff} (6301.5) is possible in two cases: (a) the magnetic polarity in

the small-scale flux tubes is opposite to the background field, and (b) the small-scale flux tubes give the emissive manifestations of the Zeeman effect; magnetic polarities in the flux tubes and in the background field are the same in this case (Lozitsky & Staude, 2009). Option (a) seems to be more likely. This means, that there was a moderately strong background field (~10^2 G) of S polarity, in which there were inclusions of strong fields of kG range and N polarity.

Evidence of very strong magnetic fields of opposite polarity was also found at the chromospheric level according to the data in the lines of the Balmer serie (Fig. 2). Despite the fact that in the photosphere under the flare the magnetic field was at the level of several hundred gauss (Fig. 1), fields of 1250 ± 200 G, 650 ± 150 G, 800 ± 300 G and 2150 ± 400 G were observed in the chromosphere by the Hα, Hβ, Hγ, Hδ lines, respectively. It was unexpected that the magnetic polarity only by the Hγ line was the same (S) as the polarity of the sunspot on the photosphere where seismic source was located. The remaining lines showed the magnetic polarity N, i.e. opposite to the polarity of the sunspot. Note, the theoretical model by Solov'ev (2020) predicts similar strong mixed-polarity fields.

From Figure 2 it follows the repeating features in the splitting of bisectors of chromospheric lines, which may indicate even stronger magnetic fields. This issue is planned to be studied in more detail in the future. Apparently, the intense energy release in the region of the seismic source of this flare was so mehow related to the close contact of the indicated magnetic fields of opposite polarity.

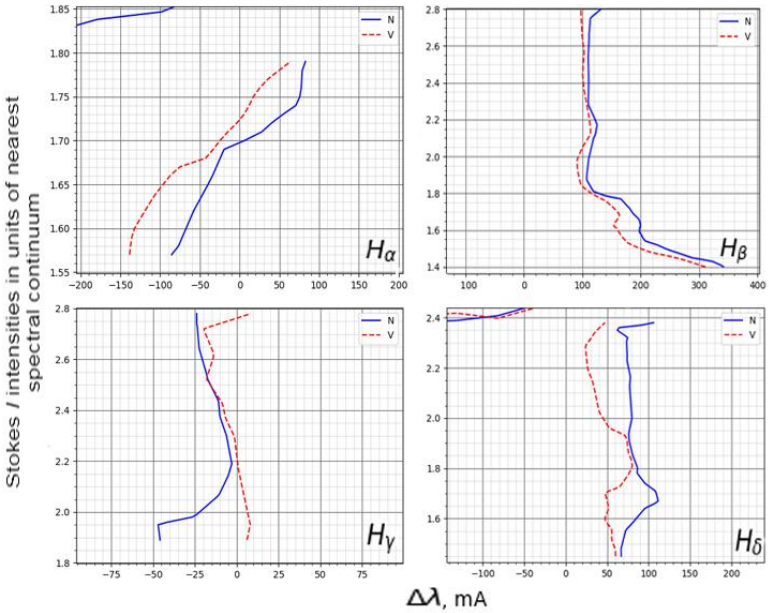

Fig. 2. Comparison of splitting of bisectors of I ± V profiles for the indicated four lines of the Balmer serie. Solid lines show bisectors for I + V profiles, and dashed lines show I − V profiles. A change in the relative displacement of these bisectors in the case of the Hγ line indicates an inversion of the polarity of the magnetic field with respect to the other three lines.

Acknowledgements. The authors are grateful to Yakovkin I.I. for providing computer program for analyzing of I ± V profiles of spectral lines. This study was funded by the Taras Shevchenko National University of Kyiv, projects Nos. 19БФ023-01 and 19БФ023-03, and by the Crimea Astrophysical Observatory, the project "Physical relationships of solar formations", grant РФФИ № 16-42-910467 р-аэ.

Note: Ye.O. Kravchenko and Yelyzaveta Shchedrina is the same person.

Comparative study of magnetic fields in a sunspot from observations in spectral lines with different Landé factors

V.G. Lozitsky [1], S.M. Osipov [2], A.A. Solov'ev[3], M.I. Stodilka[4]

[1] Astronomical Observatory of the Taras Shevchenko National University of Kyiv, Kyiv, Ukraine
[2] Main Astronomical Observatory of National Academy of Science, Kyiv, Ukraine
[3]Central Astronomical observatory at Pulkovo, S-Peterburg, Russia
[4] Astronomical Observatory of Ivan Franko National University of L'viv, L'viv, Ukraine
lozitsky_v@ukr.net, osipov@mao.kiev.ua, solov.a.a@mail.ru, m.stodilka@gmail.com

We analyze the spectral observations of a sunspot in six metal lines near Fe I 5434.5 Å, which have effective Lande g_{eff} factors from –0.014 to 2.14. The observations were made on August 25, 2015 on the ATsU-5 telescope of GAO NAS of Ukraine, using a circular polarization analyzer and spectra registration with the SBIG ST-8300 CCD camera. The tail sunspot in the active region of NOAA 2403 was observed; it was located at a distance $\rho/R = 0.415$ ($\mu = 0.91$) from the center of the disk. The diameter of the penumbra of this spot was about 45 Mm; the spot was irregular in shape, especially its umbra (Fig. 1).

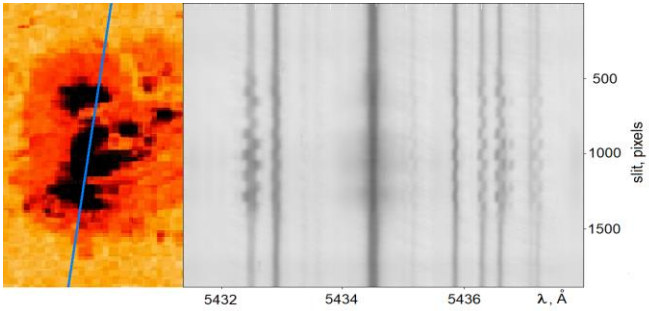

Fig. 1. The image of the studied spot in white light according to the SOHO data (left), as well as of the spectrum according to the observations on the ATsU-5, which is analyzed in this report (right). The strongest spectral line

approximately in the middle of this part of the spectrum is Fe I 5434.5 Å line (g_{eff} = –0.014).

The following line parameters were compared: observed splitting of the I ± V profiles, the width and depth of the Stokes I profiles. Magnetic field measurements were carried out by the method of 'centers of gravity' of I + V and I – V profiles. Difference between positions of these profiles in a spectrum was considered to be $2\Delta\lambda_H$, i.e. double Zeeman splitting. It is necessary to note that it is correct for pure longitudinal field only when angle γ between field line and line of sight is 0° or 180°. In other cases, measured splitting should be smaller than true one, and determined magnetic field strength is expected to be reduced in comparison with actual magnetic field value.

Significant differences of the observed magnetic field strengths B_{obs} were found in separate places of the spot and by lines with different g_{eff} values. For example, in the interval of entrance slit S =1220–1290 on Fig 1, the magnitude of B_{obs} by Mn I 5432.548 line (g_{eff} = 2.143) equals 1200 G, whereas by Fe I 5432.950 (g_{eff} = 0.666) – up to 2200 G. However, in other places of the sunspot, these differences are smaller, generally within the range of 300-500 G.

We found spectral evidences to the Zeeman effect also in line Fe I 5434.5 (g_{eff} = –0.014). For example, this is well seen in Fig. 2, in the abscissa intervals S = 670–720 and 820–830, where the "center of gravity" of the line deviates in opposite directions for different positions of the quarter-wave plate. If this phenomenon to interpret as a manifestation of the Zeeman effect, then the corresponding magnetic field should be at the level of $B_{obs} \approx$ 20 kG. It is important to note that the magnetic polarity of this superstrong field should be opposite to the background polarity in the sunspot umbra. Namely this case the theoretical model by Solov'ev (2020) predicts. Similar magnetic field values were assumed earlier in solar flares (Lozitsky, 1993, 1998, Lozitsky et al., 2019).

Stokes I profile (integral intensity) is important parameter for that case when magnetic field is very tangled, e.g. in form of spatially unresolved discrete structures of opposite magnetic polarity. Strong magnetic field should expand Stokes I profile in both cases, namely, if this field has the same (regular) polarity and if this field has mixed polarities.

Comparison of the widths and depths of the Stokes I profiles revealed two peculiar places approximately at the 'umbra – penumbra' border, where the Fe I 5434.5 Å line was expanded by ≈ 15–30%, whereas other lines with larger Lande factors did not have such a feature. One of the reasons for this expansion could be a sharp and local increase of turbulent velocities, but no

active processes such as solar flares or significant Doppler flows were observed at this location. Another reason for this expansion may be the presence of extremely strong and spatially unresolved magnetic fields of mixed magnetic polarity.

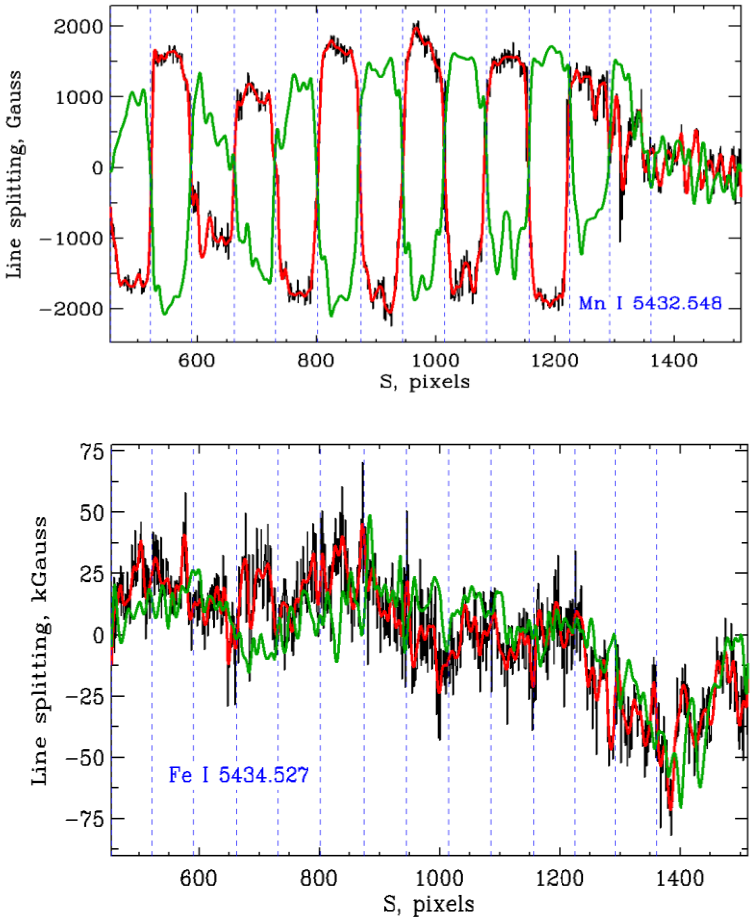

Fig. 2. Comparison of spectral effects in lines with very different Lande factors, g_{eff} = 2.143 (above) and g_{eff} = –0.014 (below). Red and green lines presents calibrated positions of 'center of gravity' of these lines along direction of entrance slit of spectrograph for two orientations of quarter-

wave plate, + 45° and – 45°. A sharp change in the position of first line during the transition to a different orientation of the quarter-wave plate indicates the Zeeman effect. Limits of bands of polarization mosaic by Skomorovsky (1974) are shown by vertical stroke lines.

Acknowledgements. This study was funded by the Taras Shevchenko National University of Kyiv, project No.19БФ023-03, by Main Astronomical Observatory of National Academy of Sciences of Ukraine, project No. 352B, by Russian RFBR project 18-02-00168, and by Ivan Franko National University of L'viv, project No. АО91-Ф.

Comparison of physical conditions in two phases of the solar flare on 19 July 2000 of M6.4/3N class

V.G. Lozitsky [1], M.I. Stodilka [2]

[1] Astronomical Observatory of the Taras Shevchenko National University of Kyiv, Kyiv, Ukraine
[2] Astronomical Observatory of Ivan Franko National University of L'viv, L'viv, Ukraine
lozitsky_v@ukr.net, m.stodilka@gmail.com

We compare the physical conditions in two phases of the solar flare of July 19, 2000 of M6.4 / 3N class, which occurred in the active region NOAA 9087. Echelle Zeeman spectrograms of this flare were obtained on a Horizontal Solar Telescope of the Astronomical Observatory of Taras Shevchenko National University of Kyiv. Physical conditions are studied in the same flare place in the picture plane, but in two different times, namely 7^h13^m and 7^h21^m, which correspond to the pre-peak phase and the flare maximum. Comparison of the effective magnetic field B_{eff} by FeI 6301.5 and FeI 6302.5 lines shows that they were almost the same for both times and both spectral lines (Table 1). At the peak of the flare, the magnetic field measured by the splitting of the emission peaks of the Fe II and Hβ lines turned out to be 300-500 G stronger than those for the above-mentioned FeI lines. On the other hand, magnetic field determined by D3 He I line was found to be close to zero. This may indicate a local magnetic field amplification in height range from temperature minimum zone to the lower chromosphere.

Table 1. Comparison of effective (averaged) magnetic fields measured in the flare
by different spectral lines

Spectral line	B_{eff}, G		Which sections of the line profiles were used for B_{eff} measurements	Altitude range in the atmosphere
	7^h13^m	7^h21^m		
Fe I 6301.5	900 ± 50	900 ± 50	Fraunhofer profiles	Middle photosphere
Fe I 6302.5	1050 ± 30	900 ± 50	Fraunhofer profiles	Middle photosphere
Fe II 4923.97	-	1250 ± 100	Emission peaks	Upper photosphere – temperature minimum zone
Fe II 5018.4	-	1300 ± 100	Emission peaks	Upper photosphere – temperature minimum zone
Hβ	1200 ± 100	1400 ± 100	Emission peaks	Lower-middle chromosphere
Hα	-	1000 ± 100	Emission peaks	Middle chromosphere
D3 He I	-	0 ± 150	Emission peaks	The transition zone between the chromosphere and the corona

A semi-empirical model of the photospheric layers of the flare was constructed on a base of observations of 'non-split' lines FeI 5123.7 and FeI 5434.5 lines which have close to zero Lande factors ($| g_{eff} | \approx 0.01$). For this purpose, the inverse problem for non-equilibrium radiative transfer was solved using Tikhonov stabilizers (Stodilka, 2003). This is one of the radical methods to clearly separate the contributions of the magnetic field and non-magnetic factors in profiles of spectral lines. Thanks to this approach number of free parameters in the interpretation decreases (because the magnetic field is excluded) and the conclusions about non-magnetic changes in the flare become more reliable. This approach was used by the authors in our previous work (Lozitsky and Stodilka, 2019), but only for one moment of the solar flare. In this study, we use this analysis approach

for the two moments of the flare, trying to establish the nature of evolutionary changes in it.

Our analysis shows that the kinetic temperature in the flare was increased by several hundred K (up to 500 K) in altitude range 50-400 km (Fig 1). The micro-turbulent velocity was increased before the maximum of the flare in the deep layers (altitudes from –150 to 100 km), while at bigger altitudes these velocities were close to each other (Fig 2). The obtained results indicate that in the pre-peak phase the altitude perturbations in the photosphere were greater than in the peak phase. The flare, thus, led to the smoothing of altitude inhomogeneities of physical conditions in the range of photospheric altitudes. A possible reason for this is the downward flow of matter and energy from the area of the main energy release of the flare localized in the chromosphere and corona.

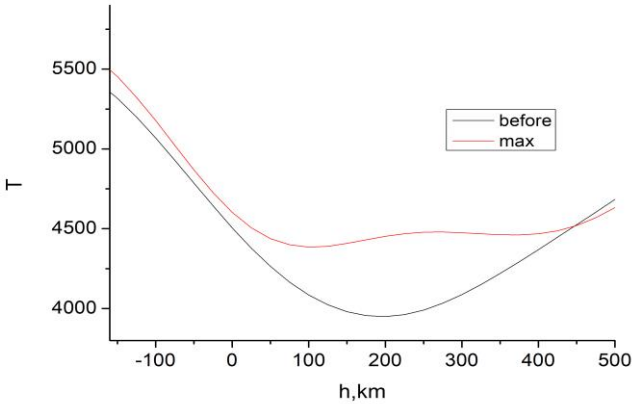

Fig. 1. The reproduced altitude dependences of the temperature T in the flare for two phases – pre-peak ("before") and the phase of the maximum ("max").

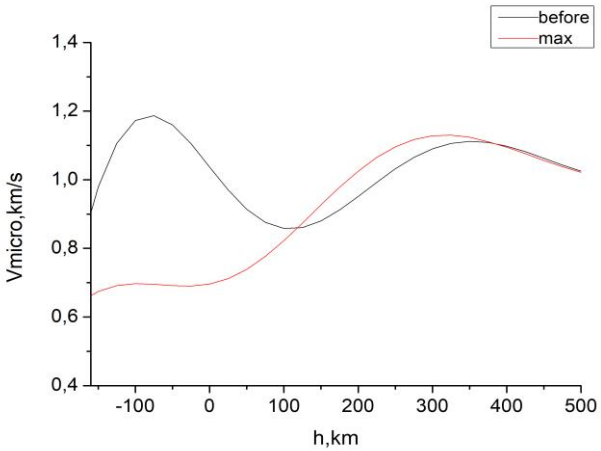

Fig. 2. The reproduced altitude dependences of the micro-turbulent velocity in the flare for two phases – pre-peak ("before") and the phase of the maximum ("max").

Acknowledgements. This study was funded by the Taras Shevchenko National University of Kyiv, project No.19БФ023-03, and by Ivan Franko National University of L'viv, project No. АО91-Ф.

Spectral study of active region site with Ellerman bomb and ejections. Chromosphere

M.N. Pasechnik

Main Astronomical Observatory, NAS of Ukraine, 27, Zabolotnoho Str., 03143 Kyiv, Ukraine

The emergence of a new magnetic flux in a developing active region is often accompanied by such small-scale events in the solar atmosphere as Ellerman bombs and Hα- ejections (surges). A lot of EBs appeared under the so-called Arch Filament Sistems. To understand the nature of these phenomena, it is important to study in detail the formation and development of individual Ellerman bombs, as well as their relationship with different types of chromospheric ejections.

We presents the results of the analysis of spectral observations in the Hα

line of a site of the active region of NOAA 11024, on which the Ellerman bomb and various types of chromospheric ejections developed. Spectral data with high spatial and temporal resolution were obtained on the THEMIS Franch-Italian solar telescope (Tenerife, Spain) on July 4, 2009. During observations from $9^h52^m35^s$ to $10^h11^m26^s$, 400 spectra with a time interval of ~ 3 seconds were obtained. From them, we used 36 spectra of the best quality. Stokes I profiles were obtained, with an interval corresponding to 160 km on the surface of the Sun. The Hα line profiles obtained for different periods of the Ellerman bomb development were very diverse, generally they consisted of several components and were asymmetric with an excess of emission in the short-wavelength wing, as in most EBs.

The features of changes in the intensity of the Hα line in the spectra of AR site obtained during observations were studied. The temporal variations of intensity in the Hα line wings at several distances from the line center (±0.1 and ±0.16 nm) and in its center were studied. It was found that EB appeared in an area of increased brightness and that during its development there was both the gradual and pulsed release of energy. The time curves of the EB brightness show that during our observations several times there was a sharp increase in the Hα line wings intensity, which indicates that magnetic reconnections took place at this time. The maximum increase in intensity in the short-wave by 73% and long-wave by 35% wings compared to the profile for the AO area without active formations, occurred at the distance of about 0.15 and 0.16 nm from the line core center, respectively.

The line-of-sight velocities (Vlos) of chromospheric matter in the studied AR area at the level where the Hα line core is formed, were determined. It was found that Vlos in the area without active formations varied from -2 to 2 km/s. The chromospheric ejections, in most cases, consisted of several components of different brightness and moving at different velocities. At some time points, side by side there could been two oppositely directed streams of matter, for example, a downward flow with Vlos of 11 km/s and an upward flow with Vlos of -17 km/s. During an ejection that occurred over the EB area, there was a vortex movement, as evidenced by the inclined dark streaks in the spectra. During the development of this ejection, the brightness of EB increased. In the reverse ejection, the chromospheric matter initially moved upwards with velocity of -94 km/s. On the spectrum the ejection was visible in the blue wing of the Hα line. After a while, the ejection appeared in the same place, but in the red wing - apparently the chromospheric matter reached the top of the magnetic loop and began to descend on the same trajectory, with Vlos reached 74 km/s. In a loop ejection, the chromospheric matter moved both up and down simultaneously. The velocity of movement up one side of the

loop reached -22 km/s, and the maximum velocity down the other side of the loop reached 14 km/s. At some time periods, the ejections had a fine structure - they consisted of several chromospheric matter jets.

Our results allow us to confirm the relationship between EB and chromospheric ejections, and also help in the construction of theoretical models of these active formations.

Spectropolarimetric study of stellar magnetic fields

S.I. Plachinda[1,2], V.V. Butkovskaya[1,2]

[1]Main Astronomical Observatory of NAS of Ukraine, Kyiv, Ukraine
[2]Crimean Astrophysical Observatory, Nauchny, Crimea

The research on stellar magnetism in Crimea was founded by A. B. Severny, V. E. Stepanov, and D. N. Rachkovsky. Since 1980, regular studies of the magnetic fields of stars of different spectral classes and luminosity types – hot stars, classical magnetic chemically peculiar stars, pulsating stars, stars with convective envelopes – have been conducting in the Crimean Astrophysical Observatory. Historically, preference is given to long-term observational programs that allow one to study the magnetic field behavior at different time intervals (hours, days, years).

Due to the rapid discovery of new exoplanets, the search for life in other planetary systems has become an actual task. The origin and evolution of life on the planet is possible with a sufficiently low activity of the host star. The level of activity of a star depends on dynamo processes in its interior, therefore long-term direct measurements of the magnetic fields of stars of late spectral classes, as the most suitable candidates for the habitability of their planetary systems, are one of the priority tasks.

A method for measuring magnetic fields by the centers of gravity of single spectral lines has been developed at the CrAO. It allows not only to estimate the magnitude and variability of global magnetic fields of stars, but also to reveal such manifestations of stellar activity, as, for example, the emergence of magnetic flux tubes on the surface of a star.

We offer a brief review of the development of the instrumental base and the methods for measuring stellar magnetic fields and present selected results of the study of the magnetic fields of various objects, first obtained in CrAO.

Polarized Radiation Diagnostics for Exploring the Magnetism of the Outer Solar Atmosphere

N.G. Shchukina[1,2,3]

[1]Main Astronomical Observatory of NAS of Ukraine, Kyiv, Ukraine
[2]Taras Shevchenko National University of Kyiv, Kyiv, Ukraine
[3]Instituto de Astrofsica de Canaris, La Laguna, Spain

The scientific goal of the talk is to review the scientific project "Polarized Radiation Diagnostics for Exploring the Magnetism of the Outer Solar Atmosphere" (abbreviation POLMAG). The research group POLMAG* has been created in January 2018 within the framework of the Advanced Grant (AdG) that the European Research Council (ERC) under the European Union's Horizon 2020 research and innovation programme awarded to Prof. Javier Trujillo Bueno (Instituto de Astrofisica de Canarias, Spain).

POLMAG aims at a true breakthrough in the development and application of polarized radiation diagnostic methods for exploring the magnetic fields of the chromosphere, transition region and corona of the Sun via the interpretation of the Stokes profiles produced by optically polarized atoms and the Hanle and Zeeman effects in ultraviolet (UV), visible and near-infrared spectral lines. To this end, POLMAG will combine and expand expertise on atomic physics, on the quantum theory of radiation, on high-precision spectropolarimetry and data analysis techniques, on advanced methods in numerical radiative transfer, and on the confrontation of spectropolarimetric observations with spectral synthesis in increasingly realistic three-dimensional (3D) numerical models of the solar atmosphere.

Confinement of strong magnetic field in sunspots

A.A. Solov'ev

Central Astronomical observatory at Pulkovo, S-Peterburg, Russia

Problem of strong and superstrong magnetic fields observed in solar atmosphere, in particular in the umbra of sunspots, is one the more important and intriguing question in solar physics. In particular, an interesting case was observed when magnetic field of ~90 kG had opposite polarity in comparison with surrounding field of the sunspot penumbra (see, e.g., Lozitsky V.G., Baranovsky E.A., Lozitska N.I., Tarashchuk V.P.

Mixed-polarity magnetic fields in the area of a seismic source associated with a large proton flare // Journal of Physical Studies. – 2019. – Vol. 23, No.4. - 4903 (7 p.). DOI: https://doi.org/10.30970/jps.23.4903

Here, a new approach to the problem is proposed. The idea of this approach is that we consider a axisymmetric vertical magnetic flux tube with a very strong potential internal field, which is kept from lateral expansion due to the pressure of an external uniform field, which is much weaker (two to three orders of magnitude) than the field in the center of the configuration (Fig. .1). The paper presents numerical calculations of the magnetic structure, as well as the pressure and plasma density in this kind of equilibrium magnetoplasma configuration, based on the results of the magnetohydrostatics theory described in papers (Solov'ev A.A. & Kirichek E.A. Magnetohydrostatics of a vertical flux tube in the solar atmosphere: Coronal loops, a model of a ring flare filament//**Astronomy Letters**, vol.**41**, no.5, pp. 211-224. (2015) DOI: 10.1134/S1063773715050072; Murawski K., Solov'ev A., Musielak Z.E., Srivastava A.K., Kraskiewicz J. // Torsional Alfven waves in solar magnetic flux tubes of axial Symmetry. **Astronomy and Astrophysics.** Vol. **577**, A126 (11), 2015. DOI: http://dx.doi.org/10.1051/0004-6361/201424545).

It should be emphasized that the direction of the external field is opposite to the direction of the field in the central part of the configuration.

The work is supported by RFBR (project 18-02-00168)

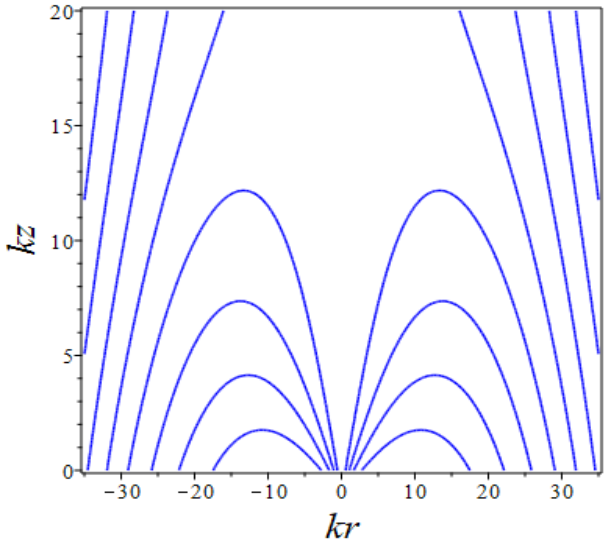

Fig.1 shows the magnetic structure of axisymmetric magnetic flux tube bounded in equilibrium by a relatively weak external field.

Strong magnetic field in a twisted coronal flux tube

A.A. Solov'ev

Central Astronomical observatory at Pulkovo, S-Peterburg, Russia

Flare energy release in coronal filament involves the concentration of a sufficiently strong magnetic field in a relatively small volume. But then the problem arises of keeping this field in equilibrium at times significantly longer than Alfvén time. The gas pressure in the solar corona is too small for this, therefore, the retention of a strong field should occur due to the pressure of the external magnetic field, which is much weaker than the magnetic field in the center of the flare configuration. It is such a magnetic configuration that is presented in this paper. Its basis is an axisymmetric magnetic flux tube, in the upper part of which there is a current magnetic structure with a large supply of free magnetic energy (geometry of magnetic field lines in this upper part of configuration is presented in Fig 1). The main problem that arises in modeling such a magnetic structure is to avoid

the appearance of negative values of pressure and gas density at any point in this configuration. A theoretical calculation based on the theory presented in (Solov'ev A.A. & Kirichek E.A. Magnetohydrostatics of a vertical flux tube in the solar atmosphere: Coronal loops, a model of a ring flare filament//**Astronomy Letters**, vol.**41**, no.5, pp. 211-224. (2015) showed that in such a system, at a level of several Mm above the photosphere, it is possible to store magnetic energy of 10 to the power of 32 ergs with an external magnetic field strength of only 50 Gauss, which is quite a bit for the field of an active region. The flash energy release in this model is due to the fact that, at high magnetic field intensities, the density of charge carriers in the current channel drops to a critical level at which plasma instabilities are excited.

The work is supported by RFBR (project 18-02-00168)

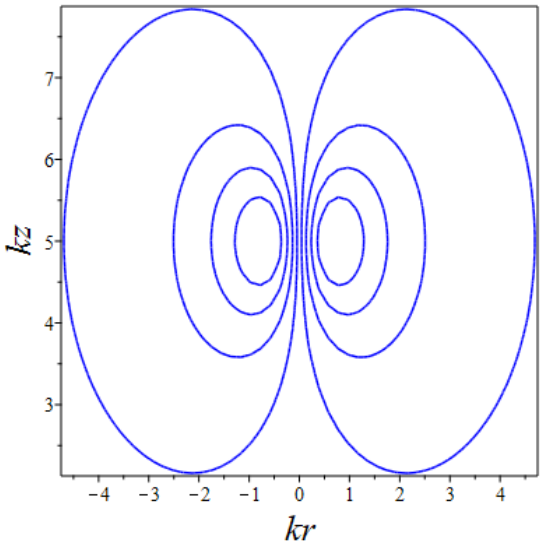

Fig.1. The vertical cut of the twisted part of the flare flux tube.

SOLAR FACULAE: MICROTURBULENCE AS AN INDICATOR OF INCLINED MAGNETIC FIELDS

M. I. Stodilka[1], R. I. Kostyk[2]

[1] Astronomical Observatory of Ivan Franko National University, Lviv, Ukraine
[2] Main Astronomical Observatory of National Academy of Sciences of Ukraine, Kyiv, Ukraine
m.stodilka@gmail.com, kostik@mao.kiev.ua

According to the observations of the solar facula in the BaII λ 4554.03 A line, a 3D model of the facula area was obtained by solving the inverse nonequilibrium radiative transfer problem. The fine structure of the field of unresolved velocities (microturbulence) was studied.

In the layers of the upper photosphere, new turbulent structures are formed, they are localized mainly between ascending and descending flows with the formation of ring-shaped structures of increased turbulence around these flows.

We proposed a mechanism of the magnetic anisotropy of microturbulent velocity (small-scale eddy-like plasma movements occur predominantly in planes perpendicular to the magnetic field), which makes it possible to explain the height dependence of the field of unresolved velocities.

Anisotropy of microturbulence starts to appear in the lower photospheric layers outside ascending and descending flows, while inside these flows it takes place in higher layers. An increase of microturbulence in the layers of the upper photosphere and lower chromosphere in the areas between the plasma flows indicates the presence of oblique magnetic fields, which, along with the blurring of its spatial structure, indicates the existence of a magnetic canopy region.

Microturbulence can be used as an additional tool for the diagnosis of oblique magnetic fields.

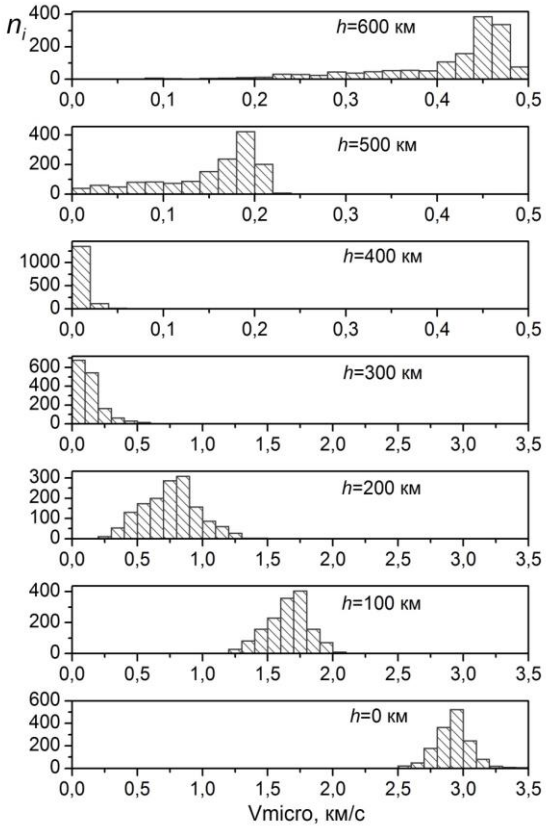

Fig. 1. Received distributions of Vmicro at different heights of the solar photosphere. New structures are seen to exist in the higher photosphere layers.

Numerical simulation of thermal sub-THz emission on the basis of RADYN code

Yu.T. Tsap[1], A.S. Morgachev[2], V.V. Smirnova[1], G.G. Motorina[3]

[1]Crimean Astrophysical Observatory, Nauchnyi, Crimea
[2]Lobachevsky State University of Nizhny Novgorod
[3]Astronomical Institute ASCR, Ondřejov
yur@craocrimea.ru

The time evolution of the thermal sub-THz bremsstrahlung emission for models of the flare transition region and chromospher on the basis of the RADYN code (https://www.fchroma.org) describing the hydrodynamic and radiative response of the solar atmosphere to the heating by the electron beam is investigated. It has been found that during the entire duration of sub-THz bust the positive spectral slope (spectral flux density increases with frequency) of radio emission is formed from 93 to 400 GHz. The peaks of sub-THz emission can be ahead and behind of the electron ejection peaks. The time profiles of sub-THz emission owing to the gas-dynamical phenomena in the flare atmosphere may be quite complex and also have a pulsating character.

Coronal loops and optical emission from flaring stars

Yu.T. Tsap[1], A.V. Stepanov[2], Y.G. Kopylova[2], Z.S. Akhtemov[1], V.M. Malashchuk[1]

[1]Crimean Astrophysical Observatory, Nauchnyi, Crimea
[2]Pulkovo Observatory, Saint-Petersburg
yur@craocrimea.ru

The possibility of a significant contribution to the white-light continuum emission from large scale coronal loops of solar type stars and M dwarfs is considered. It has been shown that that the existence of high density ($> 10^{12}$ cm^{-3}) coronal loops contradicts to the standard model of solar and stellar flares. As a result, the optical flare emission can’not be determined by free-free and free-bound processes within loops. The contribution from the lower atmosphere which is heated beneath the loops due to irradiation of soft X-ray emission should be also negligible. The possible alternative scenarios have been discussed.

On the dependence of the magnetic field of coronal holes on their areas

Yu.T. Tsap, Z.S. Akhtemov, V.M., V.I. Haneychuk

Crimean Astrophysical Observatory, Nauchnyi, Crimea

The evolution of the averaged longitudinal magnetic field and area of the low latitude coronal hole during its passage through the central meridian near an equator from February to October 2012 is considered. The CHIMERA code [2] posted on the website https://solarmonitor.org, as distinguished from the earlier work [1], is used. It has been shown that contours of corona holes strongly depends on the selected method of their determination. The correlation between the magnetic field of the coronal hole and its area was not revealed. The consequences of results are discussed in the light of the coronal-sunspot analogy proposed by Obridko and Nagovitsyn [3].

1. Heinemann S.G., Hofmeister S.J., A.M.Veronig, Temmer M. Three-phase evolution of a coronal hole. II. The magnetic field //Astrophys. J., 863. 29. 2018.
2. Garton T.M., Gallagher P.T., Murray S.A. Automated coronal hole identification via multi-thermal intensity segmentation // J. Space Weather & Space Climate, 8. A02. 2018.
3. Обридко В.Н., Наговицын Ю.А. Солнечная активность, цикличность и методы прогноза // Санкт-Петербург: Изд-во ВВМ, 2018, 466 с.

Simultaneous observations of K Ca II, Hδ and He I 4471.5 Å lines in a limb solar flare

I.I. Yakovkin, V.G. Lozitsky, N.I. Lozitska

Astronomical Observatory of the Taras Shevchenko National University of Kyiv,
yakovkinii@gmail.com, lozitsky_v@ukr.net, olozitsky@gmail.com

We present the study of the limb solar flare of 17 July 1981 according to the observations carried out with the Echelle spectrograph of the horizontal

solar telescope of the Astronomical Observatory of Taras Shevchenko National University of Kiev. We analysed the $I \pm V$ profiles of the K Ca II 3933.7 Å, Hδ 4101.7 Å and He I 4471.5 Å lines for 8^h17^m UT, close to the flash phase. The lines had very wide emission profiles with wing lengths of 5–8 Å. In the violet wings of these lines the narrow emission peaks with widths of only 0.25–0.35 Å were present (Fig. 1). Our observations of such narrow emission components in limb solar flares at altitudes of 10–14 Mm above the level of photosphere are the first direct data of this kind.

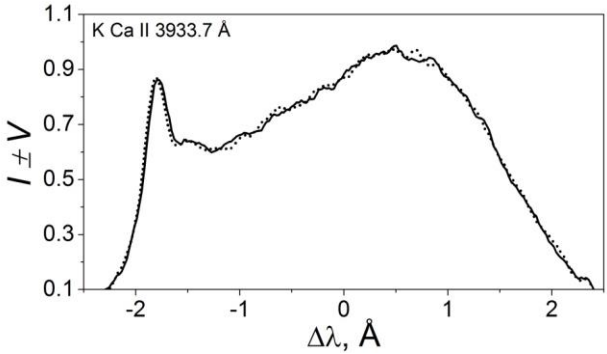

Fig. 1. The $I \pm V$ profiles of the K Ca II line in the photometric section No. 2. A narrow component in the 'violet' wing of the flare emission (at $\Delta\lambda \approx -1.8$ Å) is clearly visible.

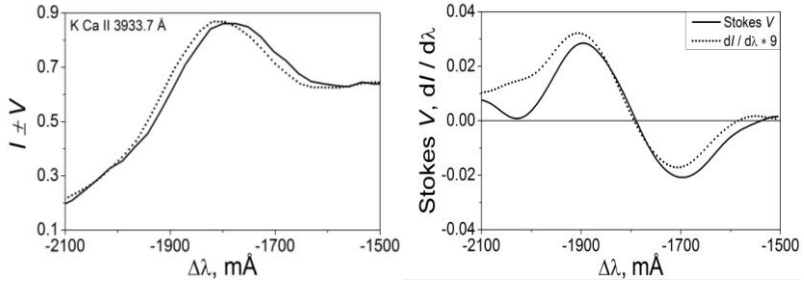

Fig. 2. Magnetic field measurement in the K Ca II line by the splitting of narrow emission peaks (on the left) and by the amplitude of the Stokes V parameter (on the right).

Under assumption that all three spectral lines are formed in the same volume of the flare, we found that the temperature in the flare was in the

range of 5000–17000 K and the turbulent velocity – in the range of 11–13 km/s. The magnetic field was measured by two different methods, namely by the splitting of narrow emission peaks and by the amplitude of the Stokes *V* parameter (Fig. 2), was found to be 1300–2100 G. The values of the local magnetic fields in the flare may be even larger since the obtained results represent a longitudinal component of the magnetic field, with the assumption that the filling factor equals unity.

Acknowledgements. This study was funded by the Taras Shevchenko National University of Kyiv, projects Nos. 19БФ023-01 and 19БФ023-03.

A program on processing the solar spectra scans

I.I. Yakovkin

Astronomical Observatory of the Taras Shevchenko National University of Kyiv
yakovkinii@gmail.com

We present a program on processing the solar spectra scans. It serves as a convenient tool for obtaining the spectral line profiles from the scans of spectrograms. The program is set to perform the following primary actions:

1. Convert optical densities of the spectrogram into spectral line intensities for the selected photometric section using the characteristic curves of the scanner and the photo-emulsion.
2. Calculate the correct wavelengths knowing the dispersion value for the line under processing.
3. Make additional adjustments including noise subtraction and smoothing.

The program provides user-friendly interface, displaying the processed line, the specified photometric section and the corresponding spectral profile preview (Fig. 1). The output is saved in a common *.dat file format. The program is suitable for scans obtained by both reflection and transmission scanning techniques and is readily-configured for use with the Epson Perfection V 550 scanner.

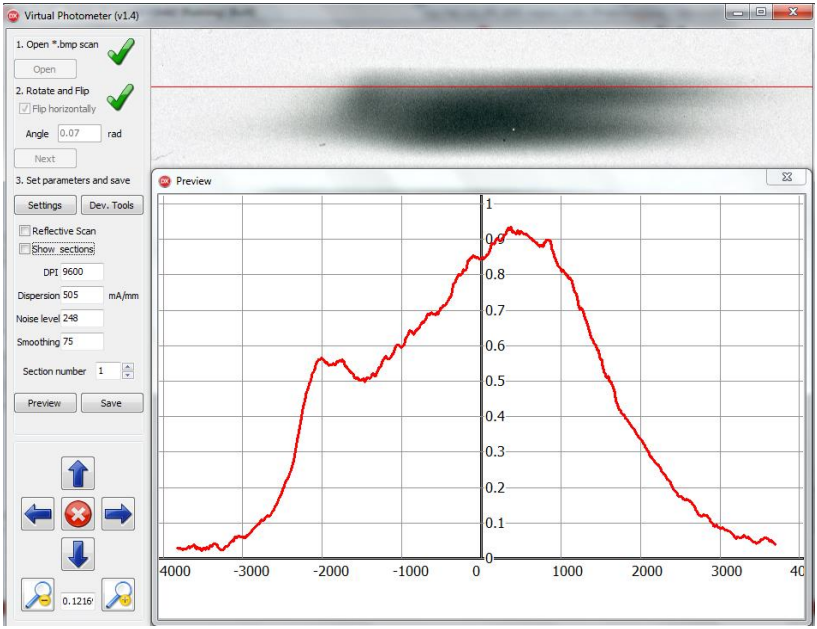

Fig. 1. Screenshot of the program. The processed scan is shown on the top of the screen, the preview of the selected section is in the center and the control panel is on the left.

The program is written in Delphi and has been extensively tested by comparing its output to the data obtained by the MF-4 microdensitometer for multiple lines and photometric sections. The spectral line profiles obtained by the two techniques are found to be well consistent and therefore the program is a reliable tool for processing the spectral data.

Acknowledgements. This study was funded by the Taras Shevchenko National University of Kyiv, project No. 19БФ023-03.

Optical and technical solutions for digital recording of the solar spectrum in various diffraction orders of the Echelle spectrograph

S.V. Kaminsky, V.G. Lozitsky

Astronomical Observatory of the Taras Shevchenko National University of Kyiv

The Echelle spectrograph of the Horizontal Solar Telescope of the Astronomical Observatory of Taras Shevchenko National University of Kiev allows observe simultaneously the spectrum of almost entire visible region of the Sun (4000-6600 Å) with a spectral resolution of 30 mÅ in the green region. In order to fix such a wide spectral region at the same time, large photographic plates of sizes 24×24 and 18x14 cm were used, mainly WP1 and WP3 ORWO. The advantage of spectrograms on such large photographic plates is their documentality as well as a large content, i.e. huge and valuable information about thousands of spectral lines in previous solar cycles, starting from the 19th (1954-1964).

Unfortunately, at present such large photographic plates are so far unrealistic to replace with equivalent CCD matrices. It is necessary to use CCD matrices of a much smaller size, the working area of which is about 2% of the area of photographic plates. In this regard, the experiment on the use of a digital camera for quickly recording the spectra of active formations on the Sun is of interest. Such registration may be relevant for observing the spectra of solar flares, especially their explosive phase, when the flare spectrum changes very rapidly with time. As a receiver, it is proposed to use a digital camera "Canon 5D" with or without a standard lens, which has a sensitive matrix size 36x24mm with high resolution. To obtain a high-quality image of the spectra, it is necessary to develop and manufacture a mount adapted to the focal plane of the spectrograph, which will provide the ability to select the desired part of the spectrum and the stability of the digital camera during exposure. There was made a study of the possibility of using this digital camera in the optical circuit of the Eschelle spectrograph, preliminary modeling and technical calculations.

Machine learning classification of solar activity based on Mg II h & k resonance lines

M. Tsizh

Ivan Franko National University of Lviv
Abto software
maksym.tsizh@lnu.edu.ua

Although large volumes of solar data exist, the vast majority of these data remain unlabeled and are therefore out of reach for modern supervised machine learning methods. Having a way to automatically classify spectra into categories related to the degree of solar activity is highly desirable and will assist and speed up future research efforts in solar physics. To achieve this goal, we used a labeling scheme from a pre-existing vector quantization technique in conjunction with several machine learning algorithms to categorize Mg II spectra measured by NASA's small explorer satellite IRIS into their correct groups. Our training data set is a human-annotated list of 85 IRIS observations containing 29097 frames in total or equivalently 9 million Mg II spectra. The annotated types of Solar activity are: active region, pre-flare activity, Solar flare, Sunspot and quiet Sun. We used the nearest neighbors algorithm to reduce the complexity of data before training our classifiers. It appears, that XGBoost method is the best and yields over 95% prediction rate when applied to this problem, outrunning other ML methods like convolution neural network, k nearest neighbors, naive Bayes classifier and support vector machine.

Сонячна активність і землетруси

І. Васильєва

Головна астрономічна обсерваторія НАН України

Землетруси – найжахливіша з природних катастроф. Можливість передбачати землетруси і, тим самим, зменшувати можливі збитки від них, є актуальним завданням на сьогоднішній день. Сонце - основне джерело променевої енергії для Землі. Про вплив сонячного випромінювання і заряджених частинок на Землю і її атмосферу шпроко відомо, і можна очікувати, що існує деякий вплив і на геофізичні процеси, такі як землетруси. Ми спробували виявити зв'язок між сонячною циклічністю і виникненням землетрусів. Як

механізм запуску землетрусів в результаті сонячних впливів розглядалися різні прояви сонячної активності. Дуже часто висновки про зв'язок землетрусів і будь-яких проявів сонячної активності робиться на основі одного-двох подій з тієї чи іншої сторони. Ми намагалися розглянути якомога більшу кількість землетрусів (розглянуто 830301 подій) та порівняти результати з результатами, отриманими в умовах обмеженої вибірки. Як випливає з наших досліджень, необхідно залучати якомога повніші дані при аналізі можливих зв'язків між сонячною активністю і землетрусами. Але, чим більше даних ми аналізуємо, тим слабшим здається цей зв'язок.

За результатами наших досліджень, на даний момент не існує статистично значущих залежностей між сонячно-земними змінними і виникненням землетрусів. І хоча не можна остаточно відкинути гіпотезу про сонячний механізмі запуску землетрусів, поки він явно не проявляється. Що стосується довгострокових і, особливо, короткочасних прогнозів землетрусів, то нам здається, що робити їх на основі даних про сонячну активність невиправдано.

Квазідворічні сонячні коливання. Вейвлет-аналіз.

І. Васильєва

Головна астрономічна обсерваторія НАН України

Добре відомий 11-річний ,період, т.зв. цикл Швабе є домінуючим в циклічної солнечнпй активності. Цей цикл був виявлений ще в 19 столітті за допомогою простого аналізу числа сонячних плям, і в подальшому підтверджений в інших проявах сонячної активності. Але існують інші періоди в сонячної мінливості. Деякі з цих періодів довші, ніж цикл Швабе (наприклад, цикл Глейсберга з типовим часом близько 80-100 років), а інші коротші. Короткострокові квазіперіоди складають 16-32 дня, 40-50 днів, 60-80 днів, 90-108 днів, 120-130 днів, 140-150 днів, 245-250 днів, 350-370 днів, 1.3 року. В даний час найбільш обговорюваним квазіперіодичним циклом в середньостроковому діапазоні є квазідворічний цикл (QBO). В поняття QBO входить досить широкий діапазон періодів - від 0.6 до 4 років. Раніше було прийнято описувати активність сонячних плям як мультигармонійний процес з декількома основними гармоніками. Проте, було показано, що результат такого спрощеного підходу залежить від обраного еталонного часового інтервалу і не може

адекватно описати довгостроковий розвиток сонячної активності. Нами, за допомогою вейвлет-аналізу, було підтверджено існування періодів сонячної змінності тривалістю 0.97 та 1.06 роки. Ці періоди були виявлені при аналізі кількості сонячних плям, випромінення Сонця на довжині хвилі 10.7 см та магнітного поля Сонця. Виявлені нами періоди не є сталими. Їхній зв'язок із фазами 11-річного циклу досліджується.

ДОСЛІДЖЕННЯ АТМОСФЕРИ ТА ІОНОСФЕРИ

ATMOSPHERE AND IONOSPHERE RESEARCH

Spatio-temporal distribution of atmospheric pollutions over Belarus in 2018 according to model simulation

N. Miatselskaya

Institute of Physics of the NAS of Belarus, Minsk, Belarus
nata.miat@gmail.com

The chemical transport model GEOS-Chem is used in the present work to estimate the near-ground monthly mean concentration of CO, NO_2, O_3, and SO_2 over Belarus in 2018. The GEOS-Chem is a global three-dimensional chemical transport model which is developed and used by research groups worldwide with general management by the team based at Harvard University and Dalhousie University. The GEOS-Chem model provides spatial and temporal distribution of atmospheric species concentrations. In this work, the v12-01 version is used with full-chemistry mechanism. The simulation is performed at 2° latitude by 2.5° longitude horizontal resolution for the first vertical layer (up to ~100 m).

The results of simulation show the highest concentration of CO and NO_2 over the urban area around Minsk in the central part of Belarus. The SO_2 contamination prevails in the southern part of the country with high anthropogenic loads. CO, NO_2, and SO_2 contamination is higher in the cold period. This can be associated with the heating season. The concentration of O_3 is higher in summer that can be explained by higher temperature and longer daylight hours.

This work is partly supported by Belarusian Republican Foundation for Fundamental Research.

Physical effects of the Kamchatka meteoroid

L. F. Chernogor

V. N. Karazin Kharkiv National University, Kharkiv, Ukraine
leonid.f.chernogor@univer.kharkov.ua

This study aims at estimating main physical effects associated with the passage through the atmosphere and airburst of the Kamchatka meteoroid (Russia) on December 18, 2018. The initial kinetic energy of the meteoroid was equal to approximately 173 kt TNT. About 18 % or 130 TJ of the initial kinetic energy of the celestial body was transformed into the flare. The meteoroid was found to be stony with the matter density of 3.3 t/m^3. The

celestial body moved along the trajectory inclined at angle of approximately 79° to the horizon. The initial mass of the body was equal to about 1410 t, its initial speed 32 km/s, and the initial diameter 9.4 m. The altitude of the Kamchatka meteoroid explosion was about 25.6 km. Comprehensive modeling of the processes launched by the meteoroid passage through all geospheres has been performed. Mechanical, optical, gas-dynamic effects, thermodynamic and plasma effects, as well as the effects of the plume and turbulence, magnetic, electric, electromagnetic, ionospheric, and seismic effects, the effects of acoustic and gravity waves associated with the passage of the Kamchatka meteoroid have been estimated. The main release of energy (10^{14} J) is shown to occur at approximately 25 – 27 km altitude where the rate of mass loss attains approximately 1.6 – 1.7 kt/s and the deceleration about 20 km/s^2. In the vicinity of the meteoroid explosion, the meteoroid speed decreased by about 10%, and its mass by approximately 10%. The main parameters of the shock wave have been estimated. The shock wave energy and power are equal to approximately 100 TJ and 8 TW. At the epicenter of the meteoroid explosion, the pressure at the shock reached ~ 1 kPa. The energy and optical radiation power were equal to 130 TJ and 20 – 30 TW, respectively. The relative disturbances in air pressure at ionospheric heights above the explosion epicenter attained tens or even hundreds of percent.

It is shown that the passage of the celestial body led to the formation of a gas-dust plume. The heated trail of the meteoroid cooled for several hours. Four stages of meteoroid trail cooling are considered in detail. The first of these persisted for ~0.01 s, and the temperature of the trail decreased by a factor of two due to emissions. During the second stage of order of ~1 s in duration, cooling due to the trail emissions and expansion took place, and the temperature of the trail decreased by ~15%. In the course of the third stage of order of ~3 s in duration, the products of the explosion and the heated gas, thermic, experienced an ~100 – 200 m/s^2 acceleration and attained an ~200 m/s speed of uplifting, and the temperature decreased by ~10 percent. The fourth stage persisted for ~100 s, during which the thermic absorbed the cool air at an intensive rate and gradually cooled off and decelerated. The maximum altitude of the uplifting of the thermic reached ~15 – 20 km. Contained in the thermic, the products of the explosion, specks of dust and aerosols, further took part in the following three processes: a slow precipitation to the surface of the Earth, turbulent mixing with the ambient air, and the transport by the predominant winds around the globe. The effect of turbulence in the trail has been shown to be well-pronounced, while the effect of magnetic turbulence has been shown to be

weakly displayed. The following basic parameters of the plasma in the trail have been estimated: the height dependences of the electron densities per unit length and per unit volume, their relaxation times, the particle collision frequencies, the plasma conductivities, and the electron temperature relaxation time. At the initial moment, the linear and volume electron densities in the trail have been shown to be equal to about $2\times10^{23} – 4\times10^{24}$ m^{-1} and $(1 – 4)\times10^{21}$ m^{-3}, respectively, and the plasma conductivity to be equal to ~ 10^3 $\Omega^{-1}\cdot m^{-1}$. The role of the dusty plasma component is discussed.

The magnetic effect of turbulence has been shown to be insignificant. The magnetic effect of the ionospheric currents and the current in the wake of the meteoroid could be substantial (~1 nT). Under the action of an external electric field, a transient current pulse with the current up to ~10^4 – 10^5 A could occur. The electrostatic effect could be accompanied by the accumulation of an electric charge of ~ 10 mC producing the electric field intensity of ~ 0.1 – 10 MV/m. The flow of the electric current in the wake of the meteoroid could result in the generation of an electromagnetic pulse in the ~ 40 – 80 kHz band with the electric field intensity of ~10 – 100 V/m. The electromagnetic effect of infrasound has been determined to be significant (~1 – 10 V/m and ~1 – 10 nT). The absorption of the shock wave at ionospheric dynamo region altitudes (~100 – 150 km) could generate secondary atmospheric gravity waves with the ~0.1 – 1 relative amplitude. The passage of the meteoroid acted to produce a plasma wake not only in the lower but also in the upper atmosphere in the range no less than 1,000 km. The possibility of appearing of the electrophonic effect, the generation of the ion and magnetic sound by infrasound, as well as the generation of gradient-drift and drift-dissipative instabilities are discussed. A conclusion is drawn that magnetic, electric, and electromagnetic effects dealt with in this report appreciably fill up gaps in the theory of physical effects produced by meteoroids in the Earth–atmosphere–ionosphere–magnetosphere system. The magnitudes of magnetic, electric, electromagnetic, ionospheric, and acoustic effects were significant. The magnitude of the earthquake caused by the meteoroid explosion did not exceeded 2.5. The mean rate of the fall of celestial bodies similar to the Kamchatka meteoroid is equal to 0.034 yr^{-1} or one fall during 30 yr.

Infrasonic effects of the Kamchatka meteoroid

L. F. Chernogor[1], O. I. Liashchuk[2], M. B. Shevelev[1]

[1]V. N. Karazin Kharkiv National University, Kharkiv, Ukraine
[2]Main Center of the Special Monitoring
leonid.f.chernogor@univer.kharkov.ua

The purpose of this report is to present the observations of the infrasonic signals associated with the fall and explosion of the meteoroid of 173-kt TNT equivalent initial kinetic energy, on 18 December 2018. The matter of the study is the infrasonic signals generated by the fall and explosion of the high-speed, 32 km/s, high-energy, 173 kt TNT, massive, 1410 t, and large, 9.4 m, celestial body commonly termed the Kamchatka meteoroid, on December 18, 2018. The total luminosity energy is estimated to be 130 J and the maximum luminosity altitude 25.6 km at (56.9°N, 172.4°E). The subject of the study is the parameters of the infrasonic signals launched by the Kamchatka meteoroid.

As input data, the temporal dependences of pressure in the infrasonic signal recorded by the network of the I53US, I30JP, I59US, I46RU, I57US, and SAIS2 infrasonic stations included into the International Monitoring System set up by the Comprehensive Nuclear-Test-Ban Treaty Organization have been used. The measurements taken on a relative scale were converted into quantities in absolute units. Then the temporal dependences of infrasonic wave pressure were subjected to band-pass filtering in the 1 – 40-s period range. After that, the system spectral analysis of the temporal dependences, which have already been filtered, has been performed by applying the mutually complementary integral transforms: the short-time Fourier transform, the Fourier transform in a sliding window with a width adjusted to be equal to a fixed number of harmonic periods, and the wavelet transform employing the Morlet wavelet as a basis function.

The infrasonic signal amplitude has been shown to decrease quite rapidly with distance from the meteoroid explosion to the station taking measurements. The time delay of the infrasonic signal has been observed to increase with distance from the point where the celestial body exploded to the point where the signal was recorded. The signal celerity depends on both the distance and the pass orientation, and it varies over the 269 – 308-m/s range. The duration of the infrasonic signal virtually does not depend on the distance between an infrasonic station and the celestial body terminal point. The infrasonic signal spectra are ultra-wide, and they contain harmonic periods from ~ 5 s to ~ 40 s. At the same time, the maximum

power falls on the 12 – 15-s and 28 – 33-s period ranges.

The infrasonic effect from the Kamchatka meteoroid was observed on a global scale. The basic parameters of the infrasonic signal generated by the Kamchatka meteoroid have been studied.

On the 16-year period of winter temperature in the Antarctic Peninsula region

O.M. Evtushevsky[1], A.V. Grytsai[1], V. O. Kravchenko[1] and G.P. Milinevsky[1,2,3]

[1]Taras Shevchenko National University of Kyiv, Kyiv, Ukraine
[2]International Center of Future Science, Jilin University, Changchun, China
[3]National Antarctic Scientific Centre MON of Ukraine, Kyiv, Ukraine
o.m.evtush@gmail.com

Decadal periodicity in the Antarctic Peninsula (AP) winter temperature with the 16-year period has been firstly described in (Kravchenko et al., 2011). Based on The Scientific Committee on Antarctic Research Reference Antarctic Data for Environmental Research (SCAR READER) from the early 1950s to 2009, the winter temperature time series were analyzed using Fourier and wavelet analyses. The three to eight year periods related to the El Niño–Southern Oscillation and Antarctic Circumpolar Wave signals were clearly separated from a decadal oscillation with a period of around 16 years. However, a source of the 16 year oscillation has not been identified in the cited work. We have prolonged the time series to 2017 and show that this oscillation is associated with the Southern Hemisphere (SH) mid-latitude zonal wave 3, which is typical for the SH circulation and is usually combined with the Southern Annular Mode pattern. Our results show that the 16-year oscillation is closely correlated with the surface pressure anomalies to the east of southern South America, and, therefore, is enhanced near the northern tip of the AP. This periodicity is clearly visible from the Esperanza winter temperature and is much less regular toward the southern AP (e.g., in the Vernadsky station data). The decadal oscillation has a positive phase at Esperanza and negative phase at Vernadsky during the last decade that contributes to the warming and cooling tendencies, respectively. This is consistent with the different climate change tendencies observed on the northern and southern AP in the recent decades. In view of the obvious differentiated contributions of the decadal periodicity to the

temperature variations along the AP, a more detailed additional study of this component in regional climate variability is needed.

The work was partly supported by Taras Shevchenko National University of Kyiv, project 19BF051-08, by the International Center of Future Science, Jilin University and by National Antarctic Scientific Center MON of Ukraine.

Kravchenko, V.O., Evtushevsky, O.M., Grytsai, A.V. and Milinevsky, G.P. Decadal variability of winter temperatures in the Antarctic Peninsula region. Antarctic Science, 23, 614–622, 2011.

Statistical characteristics of infrasonic signals generated by the Lipetsk meteoroid

L. F. Chernogor, M. B. Shevelev

V. N. Karazin Kharkiv National University, Kharkiv, Ukraine
leonid.f.chernogor@univer.kharkov.ua

The purpose of this report is to construct basic scatter diagrams and plot the corresponding regression functions for the parameters of the infrasonic signals launched by the Lipetsk meteoroid (the Russian Federation). The celestial body that entered the Earth's atmosphere at 01:16:20 UT on June 21, 2018 had the following initial parameters: speed 14.4 km/s, mass about 113 t, scale size about 4 m, and kinetic energy about 2.8 kt TNT. The celestial body moved along the trajectory inclined at an angle of 79° to the horizon, and 10.4% or 1.22 TJ of the initial kinetic energy transformed into the outburst at the terminal flare point at an altitude of 27 km at (52.8°N, 38.1°E).

The infrasonic signals generated by the celestial body were observed on a global scale, and they were recorded by the International Monitoring System (IMS) set up by Comprehensive Nuclear-Test-Ban Treaty Organization. Techniques of mathematical statistics have been invoked for data processing.

The list of the basic results of the study includes the following. The infrasonic signal exhibits a linear dependence of the infrasonic signal time delay on the great-circle distance from the meteoroid explosion epicenter, and the signal celerity averaged over all propagation paths is estimated to be approximately 304 – 305 m/s. The infrasonic signal celerity first shows a rapid enough decrease with distance, but farther it exhibits fluctuations about the 302 m/s value over the 4.5 – 8.66-Mm distances range. The duration of the infrasonic signal shows a linear decrease with distance, and the signal duration dispersion is insignificant in the 5 – 8 Mm distance range. The mean periods of

the infrasonic signal, independent of distance and averaged over various regression functions, are estimated to be 6.28±0.98 s and 6.14±0.76 s. The mean of the initial kinetic energy estimated using the oscillation period of the infrasonic signal is 2.26 – 2.43 kt TNT, which differs insignificantly from the NASA estimates, 2.8 kt TNT. The approximation for the dependence of celerity vs. sine of the back-azimuth angle of arrival shows that the corrected value of the celerity is about 300 m/s, and the mean of the troposphere-stratosphere wind is approximately 25 – 31 m/s. Analysis of the scatter diagrams has shown that a steady statistical link exists between the true and observed back-azimuth angles of infrasound sources. It is noted that the level of fluctuations in the azimuth tends to increase with distance.

The scatter diagrams that describe the main parameters of infrasonic signal dependences on range and azimuth have been plotted, and the respective regression dependences have been proposed.

Ten years of ozone measurements at Kyiv-Goloseyev station

G.P. Milinevsky[1,2], A.V. Grytsai[1], O.M. Evtushevsky[1], N.O. Eremenko[3], V.O. Danylevsky[1], V.O. Kravchenko[1], I.G. Mischishina[1], O.I. Ivaniha[1], Z.I. Grytsai[1], Yu. Yu. Yukhymchuk[4], M.G. Sosonkin[3]

[1]Taras Shevchenko National University of Kyiv, Kyiv, Ukraine
[2]International Center of Future Science, Jilin University, Changchun, China
[3]Main Astronomical Observatory, National Academy of Sciences of Ukraine, Kyiv, Ukraine
[4]Institute of Physics, National Academy of Sciences of Ukraine, Kyiv, Ukraine
genmilinevsky@gmail.com

Dobson spectrophotometer No. 040 was transferred to Ukraine in the spring 2010. At Kyiv-Goloseyev station, the first total ozone measurements were realized on 13 May 2010. Systematical observations have been carried out during the last decade mainly by researchers from Taras Shevchenko National University of Kyiv and Main Astronomical Observatory. In addition to total ozone measurements, Umkehr method was used to determine vertical ozone profiles over Kyiv-Goloseyev.

The Dobson measurements are realized in the near ultraviolet by double-pair method including standard AD and CD pairs. Total ozone calculation is possible not only from Direct Sun (DS) observations but also from zenith

ones (Zenith Blue and Zenith Cloud types). Respectively, the instrument can act under different weather conditions except intensive precipitation. Our observations indicate better quality of DSAD and ZBAD relative to other types of observations. Distinctive pattern is typical near the winter solstice with high solar zenith angles when the CD measurements are more reliable.

Decadal total ozone data exhibit seasonal cycle with a maximum in March–April and a minimum in October that is usual in the middle latitudes of the Northern Hemisphere. Maximal values reach 400–450 Dobson Units (DU) with rare jumps even above 500 DU. Minimal total ozone content is equal to near 250 DU during mid-autumn. Summer total ozone measurements show very low level of variations. Altitudinal maximum of partial ozone content exists at the heights near 20 km that is supported by Umkehr observations.

Results of Kyiv-Goloseyev station are permanently delivered to the World Ozone and Ultraviolet radiation Data Center (WOUDC) in Toronto, Canada. Our comparisons of the Dobson 040 ozone series with satellite measurements are among the evidences of the good quality of the Kyiv-Goloseyev observations. Discrepancies between the ground-based data and satellite overpasses are typically in range of several per cent. The Dobson 040 instrument remains only one similar instrument in Ukraine.

We thank all persons who were observers or assisted the measurements during last ten years and hope for the successful work of Kyiv-Goloseyev station in future.

The work was partly supported by Taras Shevchenko National University of Kyiv, project 19BF051-08, by the International Center of Future Science, Jilin University and by National Antarctic Scientific Center MON of Ukraine.

Global-scale quasi-periodic variations in the geomagnetic field during the greatest geospace storm of September 7 – 9, 2017

L. F. Chernogor, M. B. Shevelev

V.N. Karazin Kharkiv National University, Kharkiv, Ukraine
leonid.f.chernogor@univer.kharkov.ua

Despite the Solar Cycle 24 minimum in the vicinity, September in 2017 was characterized by high solar activity, when forty class C solar flare events, fifteen class M events, and four class X solar flare events occurred. Huge coronal mass ejection events and strong geospace storms, according to

L. F. Chernogor's conception sets of magnetic, ionospheric, and atmospheric storms, as well as electric field disturbances, have been reported.

The purpose of this report is to present the results of analysis of global-scale quasi-periodic variations in the geomagnetic field during the unique geospace storm that occurred on September 7 – 9, 2017.

To analyze the time variations, the data acquired with 0.1-nT resolution and at the 1-min sampling interval from the Intermagnet magnetometer network (including Tamanrasset (22.79°N, 5.53°E), Duronia (41.35°N, 14.466°E), Lonjsko Polje (45.408°N, 16.659°E), Belsk (51.84°N, 20.79°E), Uppsala (59.903°N, 17.353°E), Abisko (68.358°N, 18.823°E) observatories) have been used. The local time variations in the horizontal field components that occurred on September 7 – 9, 2017 have been analyzed. Band-pass filtering and the system spectral analysis have been performed within the period range of 2 – 120 minutes per cycle, when the mutually complementary the short-time Fourier transform, the Fourier transform in a sliding window with a width adjusted to be equal to a fixed number of harmonic periods, and the wavelet transform employing the Morlet wavelet as a basis function were used simultaneously. The latitudinal dependence of quasi-periodic disturbances in the horizontal components of the geomagnetic field during the unique geospace storm and on a reference day has been studied. The amplitude, spectral content, and the duration of the disturbances have been determined.

The geospace storm has been shown to be accompanied by both aperiodic and quasi-periodic disturbances in the geomagnetic field. The quasi-periodic variations occur in the 35 – 55- and 70 – 110-min period range. The quasi-periodicity strengthens as the geographic latitude of the magnetic observatory decreases. When the geographic latitude increases from ~20° to ~70°, the amplitude of the disturbances increases from 20 to 1500 nT. On September 8 – 9, 2017, the duration of the oscillation trains averages from a few hours to ~16 hours.

The main global-scale features of the severe magnetic storm in Solar Cycle 24 have been studied. The dependence on magnetic latitude of the main parameters of aperiodic and quasi-periodic disturbances in the geomagnetic field has been determined.

Sentinel-5P data usage for the monitoring of accidental elevated pollution episodes in Ukraine

M.V. Savenets[1], I.V. Dvoretska[1]

[1]Ukrainian Hydrometeorological Institute, Kyiv, Ukraine
savenetsm@gmail.com

Sustainable development has become the major direction for future economic growth with significant role of air quality monitoring as the indicator of planning and strategy success. Accurate estimates of air quality changes cannot be done only by using ground-based measurements due to its spatial coverage. Many elevated pollution episodes in Ukraine appeared in the regions without any in-situ measurements therefore were not properly taking into consideration. The overwhelming majority of them originated during unwise industrial and agricultural activity and was detected only by satellite measurements. Until the accidental elevated pollution episodes are underestimated, any actions for air quality improvement will tend to fail. Sentinel-5P launch revolutionize the ability for pollutants' measurements in the atmosphere, providing new possibilities for precise air quality monitoring. The study presents analyses of accidental elevated pollution episodes in Ukraine detected by Sentinel-5P in 2018 – 2020 and discussed the details for proper data usage.

The most frequent accidental elevated pollution episodes in Ukraine caused by huge short-term industrial point emissions. The highest nitrogen dioxide (NO_2), carbon monoxide (CO) and sulfur dioxide (SO_2) content observed over power plants and distributed on more than 200 km. During the most unfavorable weather conditions NO_2 total column in plumes over gas-running power plants exceeded $2 \cdot 10^{-4}$ mol/m^2 which is 4-5 times higher than background content in Ukraine. Over coal-running plant CO and SO_2 total columns exceeded $4 \cdot 10^{-2}$ mol/m^2 and $4 \cdot 10^{-3}$ mol/m^2 respectively. Despite being among the most polluted areas, some of the cities, e.g. Zmiiv, Ladyzhyn, Burshtyn, Kurakhove, Novyi Svit, etc., even do not have any ground-based indicative measurements.

Another type of huge accidental pollutants' emissions are wildfires and open burning on agricultural lands. Some of the fires in ecosystems in 2019 and 2020 caused air quality worsening over the biggest part of Ukraine. Despite industrial emissions and wildfire events, Sentinel-5P data allowed providing the monitoring of air quality along the coastline during tourist season. Overall, from May to September 2019 the atmospheric air over the Ukrainian shoreline is 2-3 times more polluted than over adjacent inland

territories. In April 2020 using absorbing aerosol index the dust storm were detected one hour before it reached Kyiv. Combination of Sentinel-5P data with HYSPLIT modelling gives the opportunity to detect the dust storm speed movement, probable territory of dust origin, and atmospheric humidity changes of particular air masses.

Depends on the monitoring purpose, Sentinel-5P data need additional processing: filtering, latitude vs. longitude binning, and spatial/temporal averaging. It was found that most industrial point emissions and wildfires events are better visible after averaging, whereas maximal values (after filtering with quality assurance index) are more appropriate for other accidental elevated pollution episodes.

Solar flare of September 2017 magnetic effect

Y. Luo, L. F. Chernogor, K. P. Garmash, M. Yu. Holub, S. G. Leus, V. T. Rozumenko

V. N. Karazin Kharkiv National University, Kharkiv, Ukraine
leonid.f.chernogor@univer.kharkov.ua

September in the year 2017 was characterized by a significant solar activity. During this period, forty class C solar flare events, fifteen class M events, and four class X solar flare events occurred. The most powerful solar flares were observed to occur in the AR2673 active region at 09:10 UT (a class X2.2 event) and 12:02 UT (a class X9.3 event) on 6 September 2017, as well as at 16:47 UT (a class X8.2 event) on 10 September 2017. The class X9.3 and X8.2 solar flares were the most powerful during Solar Cycle 24. The coronal mass ejections and geospace storms followed the solar flares. The solar flares gave rise to sharp increases in the ionospheric electron density lasting for periods of no less than 15 – 20 min. An increase in vertical TEC by 8 – 10 TEC units and by 15 – 16 TEC units was detected for 11 X9.3 solar flares at middle and low latitudes, respectively, on the dayside.

The purpose of this report is to present results of an analysis of temporal geomagnetic field fluctuations during and after the solar flares.

Variations in the *H* and *D* horizontal magnetic field components acquired with 0.1 pT – 0.1-nT resolution within the 1 – 1000-s period range at the 0.5-s sampling interval from the fluxgate magnetometer at the V. N. Karazin Kharkiv National University Magnetic Observatory (49°40′N, 36°50′E) have been used in the study. Band-pass filtering and the system spectral analysis have been performed in the 1 – 10-s, 10 – 100-s, and 100 – 1000-s period ranges. The system spectral analysis consist of the mutually complementary

short-time Fourier transform, the Fourier transform in a sliding window with a width adjusted to be equal to a fixed number of harmonic periods (the so-called adaptive Fourier transform), and the wavelet transform employing the Morlet wavelet as a basic function.

The geomagnetic effect caused by the class X9.3 solar flare event is described in what follows. Aperiodic and quasi-periodic variations in the *H* and *D* magnetic field components took place. In about 8 min after the solar flare onset, the fluctuations in the level of the geomagnetic field showed an increase from 1 – 2 nT to 5 – 8 nT, which lasted for no less than 15 min. In particular, the level of both components first showed a sharp, 1-min duration, decrease in both components by a factor of 7 – 8 times, which followed by a sharp increase by a factor of 5 times above background. Then, the level of fluctuations was observed to exhibit mainly a positive increase, by a factor of 2 – 3 times above background. The spectrum at first exhibited predominantly ~1 – 3-min period oscillations, and then components with ~10 – 17-min periods showed maximum amplitudes, which attained no less than 2 nT.

(1) The class X solar flares launched significant aperiodic and quasi-periodic variations in the horizontal geomagnetic field components, as measured at V. N. Karazin Kharkiv National University Magnetic Observatory. (2) The excursion of the aperiodic variations towards negative values attained a factor of 7 – 8 times, while towards positive values a factor of ~5 times as compared to the background. The aperiodic disturbances were observed to show a temporal duration of no less than 15 min. (3) The quasi-periodic variations had maximum amplitude, up to 2 nT, in the 10 – 17-min period range. (4) The geomagnetic effect was caused by the disturbances in the electron density at the dynamo region heights with the subsequent impact on the current system.

Cases of aerosol pollution over Nicosia during 2019, Cyprus

Yu. Yukhymchuk[1], Ph. Goloub[2], G. Milinevsky[1,3,4]

[1]Main Astronomical Observatory of National Academy of Sciences of Ukraine, Kyiv, Ukraine
[2]Laboratory of Atmospheric Physics University of Lille, Lille, France
[3]Taras Shevchenko National University of Kyiv, Kyiv, Ukraine
[4]College of Physics, International Center of Future Science, Jilin University, Changchun, China
juliyuhim@gmail.com

Cyprus is known as a hot spot for climate change studying. It is located

in one of the most polluted areas in the world and has affected influence from different parts of the world (Asia, Europe, Africa, etc). For aerosols observations of the atmosphere over Nicosia during 2019 were used next methods: AERONET (Aerosol Robotic NETwork), MODIS (Moderate Resolution Imaging Spectroradiometer) and HYSPLIT (The Hybrid Single Particle Lagrangian Integrated Trajectory Model). For details research during the mentioned period were chosen 2 cases of strong air pollution events and analyzed next aerosol characteristics: aerosol optical thickness (AOT), Angstrom exponent, single scattering albedo, refractive index (imaginary and real parts) and size distribution. Potential sources of aerosol pollution events defined due to obtained aerosol parameters, satellite images, and backward trajectories of air mass moving.

For the event that took place on 25 April 2019 with detected AOT values around 0.8 the main aerosols sources were a mix of dust from North Africa and marine aerosol. On 5th August (AOT was around 0.7) the dominant pollution was mix anthropogenic (industrial/urban) aerosols from Europe, secondary organic aerosols (SOA), and also dust and marine aerosols.

Total electron content disturbances for Maidanak GPS station data on May 2, 2020

H.E. Eshquvatov[1,2], O.T Asatov[2]

[1]Ulugh Beg Astronomical Institute, Uzbekistan
[2]Tashkent Chemical Technological Institute, Tashkent, Uzbekistan
eshquvatov86@mail.ru

We have analyzed variations Total electron content for Maidnak GPS station on May 2, 2020. One of the most important characteristics of the Earth's ionosphere is the total electron content (TEC), however, to date, over the territory of Central Asia its global monitoring was not performed. Analytical models give a good estimate of this parameter provided quiet geomagnetic conditions, but in the case of a perturbed ionosphere TEC assessment becomes less accurate. Radio-raying of the atmosphere by means of signals of satellite navigation systems and a network of ground based stations are readily available and low-cost way to monitor the F-layer of the ionosphere in real time. Each GPS satellite emits two high-stable signal at the frequencies f1 = 1575.42 MHz and f2 = 1227.60 MHz. The

signals are refracted due to electron density gradients, and since the ionosphere is a dispersive medium, the ray paths of the f1 and f2 signals will be slightly different. The obtained phase and pseudo-range measurements contain information about the TEC along the ray paths. On the basis of this technique, it is created software to analyze GPS data in the Receiver Independent Exchange (RINEX) format, provided an international network of the International GNSS Service (IGS).

Effect of solar wind plasma near-earth with reference to geomagnetic storms during 2008 to 2018

Sh. Singh, A. P. Mishra

Department of Applied Sciences, Chandigarh Engineering College,
Landran, Mohali, Punjab India 140307
shamrathore@yahoo.com

In the present study, we have analyzed large geomagnetic storms during 2008 to 2018, a set of seven large geomagnetic storms which were associated with disturbance storms time (Dst) decreases of less than -100nT to decreases of less than -200nT. The relationship between solar parameters, such as solar wind speed (V), average interplanetary magnetic field (B), international sunspot number (R), proton temperature (K) and geomagnetic indices (Ap), (Kp) is studied in the present report. The result shows positive correlation between Ap, Kp indices and solar wind parameters. However a very high correlation is found between the product of VB and geomagnetic indices Ap, Kp.

Comparison of MERRA-2 and CMIP6 ozone data for South Hemisphere during spring

O. Ivaniga[1], G. Milinevsky[1,2,3], A. R. Klekociuk[4,5]

[1]Taras Shevchenko National University of Kyiv, Kyiv, 01601, Ukraine
[2]International Center of Future Science, Jilin University, Changchun, 130012, China
[3]National Antarctic Scientific Center, Kyiv, 01601, Ukraine
[4]Antarctica and the Global System, Australian Antarctic Division, Kingston, 7050, Australia
[5]Antarctic Climate and Ecosystems Cooperative Research Centre, Hobart, 7000, Australia
ivaoksi94@gmail.com

Monthly mean data from the MERRA-2 reanalysis and CMIP6 model have been examined for austral spring months (September, October, November) over the 1980–2014 period. Analysis was made for 2D (total ozone column) and 3D (ozone partial pressure) climatological mean (1980-2014) values for the zonal band (0º – 90º S) at pressure levels (1000–0.1 hPa) for each month of the chosen period. The monthly, latitude, longitude and altitude analysis have been provide. It is shown that the largest longitudinal variation in ozone field , so called zonal asymmetry, is observed in spring, especially in October, with dominant wave-1 structure with zonal minimum over 0º – 90º W, and maximum over 120º – 180º E longitudinal sectors. The area with high ozone content is located at the 40º – 80º S zonal band and gradually shifts to the south from September to November. The most noticeable differences between the model and reanalysis are observed in the periods when the largest ozone variations exist. In the longitudinal distribution wave-1 pattern dominates with a shift of longitude ozone minimum. From September to October the shift is eastward, and from October to November westward by MERRA-2 data but only eastward by CMIP6 data. CMIP6 underestimates amplitude of ozone zonal asymmetry in October by 42.1% and overestimates in August by 43.7%, and in December by 166.6%. In latitudinal distribution there is also a difference – mean longitude maximums in zonal mean ozone distribution are observed over 62° S, in October – 66° S, and in November – 68° S for MERRA-2 and over 64° S, 65° S and 66° S respectively for CMIP6. Therefore, poleward shift of ozone latitude maximum in the model is slower. The highest difference in altitude ozone distribution is observed

during October in the stratosphere between ozone zonal minimum and maximum points and reaches approximately 68 % (44%) of the zonal average value at 65° S (65.4° S) by MERRA-2 (CMIP6) data. MERRA-2 profiles unlike CMIP6 one show higher location of altitudinal maximum over the zonal minimum and lower over the zonal maximum with mean between them zonal mean. All three CMIP6 profiles have the same height of altitude maximum.

The work was partly supported by Taras Shevchenko National University of Kyiv, project 19BF051-08 08 and the PACT Project of SCAR Action group.

Magnetic and ionospheric effects of the 5 – 6 August 2019 geospace storm

Y. Zheng[1], Q. Guo[2], L. F. Chernogor[3], K. P. Garmash[3], V. T. Rozumenko[3]

[1]Qingdao University, Qingdao, People's Republic of China
[2]Harbin Engineering University, Harbin, People's Republic of China
[3]V. N. Karazin Kharkiv National University, Kharkiv, Ukraine
leonid.f.chernogor@univer.kharkov.ua

In accordance with the conception by L. F. Chernogor, geospace storms are comprised of synergistically interacting magnetic storms, ionospheric storms, atmospheric storms, and the storms in an electric field of magnetospheric, ionospheric, or atmospheric origins. Geospace storms are very diverse, and different storms exhibit different behaviors. Therefore, studying the effects of each new storm becomes an urgent task for us. Such studies reveal both the general laws and individual characteristics of storm processes.

The purpose of this report is to present the general information about the geospace storm and the results of analysis of magnetic and ionospheric storm features.

In order to analyze the magnetic environment, we used the measurements of magnetic field fluctuations within the period range of 1 s to 1,000 s, performed at the V. N. Karazin Kharkiv National University Magnetometer Observatory, and variations of the three components of the geomagnetic field carried out at the IRA NASU Low-frequency Observatory. To analyze ionospheric environment, we used multi-frequency multiple-path measurements made at the Harbin Engineering University (China), as well as ionosonde data.

An increase in the main parameters of the solar wind on August 5, 2019

led to the geospace storm, which was observed mainly on August 5 and 6, 2019. The storm's main phase lasted from 06:00 a.m. to 08:30 a.m. on August 5, 2019, and the recovery phase persisted for no less than 4 days. The magnetic storm was observed to show significant variations in all components of the geomagnetic field and to exhibit an increase in the oscillation level of geomagnetic field by an order of magnitude in the period range from 400 s to 950 s. During the ionospheric storm, significant disturbances occurred in the *F* region of the ionosphere, while ionospheric *E*-region remained almost unperturbed. The ionospheric storm severely affected the Doppler spectra of radio waves in the 5 – 10 MHz frequency range, which were significantly broadened, and the Doppler frequency shift exhibited quasi-periodic variations with 20–40-min periods and 120–240-min temporal durations. The quasi-periodic variations of the Doppler shift of frequency were due to quasi-periodic variations in the electron density with relative amplitude of perturbations in the 3% to 16% range. Over one of the propagation paths, the amplitude of the Doppler frequency shift attained 0.7 Hz, which could be caused by perturbations in the electron density with amplitude of 80 – 90%. At the same time, the signal amplitudes over most of the propagation paths were little affected by the ionospheric storm.

The main manifestations of the magnetic and ionospheric disturbances in radio waves during the 5 to 6 August 2019 geospace storm have been studied in detail.

View from GNSS - modelled ionosphere on troposphere. Case study of some severe weather events in the Missouri part of "Tornado Alley"

Y.M. Zanimonskiy[1], G. Nickel[2], M. Figursky[2]

[1] Radio Astronomical Institute of the National Academy of Sciences of Ukraine, Kharkiv, Ukraine
[2] Gdańsk Polytechnic University, Gdańsk, Poland
zanimonskiy@rian.kharkov.ua

Despite the presence of huge arrays of meteorological information, it is advisable to use additional sources to understand severe weather conditions. One of them may be the ionosphere, which responds to tropospheric events as a sensitive environment, with the capture of information by radio means, in particular GNSS (Hung et al., 1979; Nishioka et al., 2013).

This study simulates the spatio-temporal dynamics of the total electron content (TEC) of the ionosphere during several tornadoes over the United States. According to the GNSS (Global Navigation Satellite Systems) receivers of the CORS (Continuously Operated Reference Stations) network, maps of variations of TEC with a resolution of 30 s in time and 0.2° in latitude and longitude were calculated based on the method described in (Nykiel et al., 2017).

The most common meteorological phenomena of tornadoes occur in the area of the so-called "Tornado Alley". This area stretches from the south to the north of the United States from Texas to North Dakota. The state of Missouri looks like a kind of alley where there are almost no serial events - several tornadoes in one day. For single events, it is easier to interpret the ionospheric response, which manifests itself in an increase in the random scattering of TEC in a limited region.

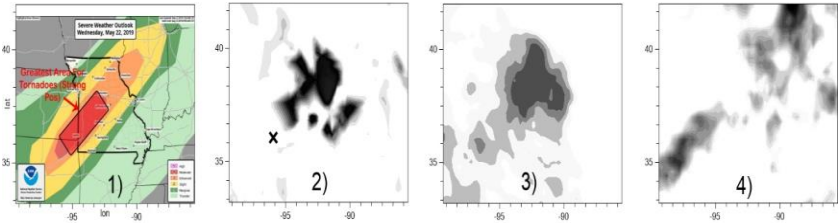

Examples of maps: 1) - tornado forecast in Missouri from the site http://www.missourichase.com/; 2) - dispersion of TEC - during the tornado August 6, 2017; 06h 10m. UTC; 3) - dispersion of TEC for three days, 4 - 6 08 2017; 4) - dispersion of TEC for the day 13 03 2013. The cross shows coordinates of the tornado.

Analysis of numerous sets of maps, similar to those shown in the figure, provides grounds for confirming the conclusion in (Nishioka et al., 2013) that the ionosphere responds not to the tornado in the surface layer, but to the powerful tropospheric processes that form the tornado and beyond. Ionospheric disturbances, which are registered by GNSS methods, visualize stable zones of occurrence of conditions for the appearance of a tornado, even if the tornado has not formed.

Hung R.J., et al. Coupling of ionosphere and troposphere during the occurrence of isolated tornadoes on November 20, 1973. J. Geophys. Res., 84, A4,1261-1268, 1979.

Nishioka M., et al. Concentric waves and short-period oscillations observed in the ionosphere after the 2013 Moore EF5 tornado. Geophys.

Res. Lett., 40, 5581–5586, 2013.

Nykiel G., et al. Efficient Usage of Dense GNSS Networks in Central Europe for the Visualization and Investigation of Ionospheric TEC Variations. Sensors, 17, 10, 2298, 2017, doi: 10.3390/s17102298.

On the possibility of Earth atmosphere multimode aerosol component parameters recovering from the spectral polarimetric measurements data

O.S. Ovsak, O.V. Morozhenko

Main Astronomical Observatory NAS of Ukraine, Kyiv, Ukraine
ovsak@mao.kiev.ua

The optical and microphysical characteristics of Earth's atmosphere aerosols are usually determined using the photometric measurements obtained by solar photometers and lidars. However, such devices used individually do not allow a sufficiently large number of essential aerosol parameters to be determined. Joint simultaneous use of these devices can significantly increase the number of defined aerosol parameters, but it requires the preparation and special arrangement of observation sites, and also complicates the processing of measurement data. At the same time a number of works demonstrate the possibility of confidently determining the characteristics of aerosol component in the upper parts of other Solar system planets atmospheres via the both the photometric and the polarimetric measurements data. This indicates a high potential of analysis methods for the photopolarimetric measurements data and states on the possibility of their application to restore the aerosol component characteristics in the Earth's atmosphere.

Based on the previous papers results we have proposed a reconstructing method for microphysical parameters of main aerosol modes in the Earth atmosphere from measurements of spectral phase dependences the degree of linear polarization (DoLP) of the sky. The highlight of the method is the ways for determining a relative contribution of the molecular and the aerosol scattering and for detection the weight coefficients of main fractions (modes) in the atmospheric aerosol mixture. Also we have proposed the criteria for assessing the possibility presence of several aerosol fractions in the studied atmosphere. Note that technique in use allows one to determine the probable gas-aerosol medium parameters averaged over the atmospheric column with a height determined by the Sun zenith distance.

A set of special computer program codes to calculating the DoLP, the

volume scattering coefficient and the phase function for the unit volume of investigated atmosphere at physically acceptable range of aerosol parameter values has been created by us. We have justified the use of a model the polydisperse ensemble of homogeneous spherical non-absorbent aerosol particles. Final result is determining by comparison of sums of squared deviations between the calculated model and measured DoLP dependencies for all the phase angles. The processing results for measurements data of DoLP spectral phase dependences for the daytime and twilight sky showed the effectiveness of both the proposed analysis method and the developed set of program codes application in a wide wavelength range.

We have analyzed the spectral phase dependences of the sky DoLP at the zenith above the Main astronomical observatory site (Kyiv, Golosiiv) measured in 1962. A presence of two main aerosol fractions the coarse and the fine dispersing modes was been set. Here are the aerosol parameters determined by us for a normal-logarithmic particle size distribution function with dispersion value of $\sigma^2 \approx 0.1$: for the coarse-grained mode 1 with a weight coefficient $k_1=0.2$ the real part of the particles refractive index is $n_{r1} \approx 1.45$, the average geometric radius is $r_{01} \approx 6.7$ μm and for the fine-grained mode 2 there are $n_{r2} = 1.45$, $r_{02}=0.12$ μm. The mentioned aerosol parameters turned out to be close to the characteristics obtained by independent studies of the sky over the Main astronomical observatory site in 2015 on the simultaneous measurements using of solar photometer and lidar.

Ozone altitude profiles by Umkehr Dobson observations at Kyiv-Goloseyev in 2011–2017

Yu. Andrienko[1], G. Milinevsky[1,2,3], V. Danylevsky[1], V. Kravchenko[1]

[1]Taras Shevchenko National University of Kyiv, Kyiv, 01601, Ukraine
[2]National Antarctic Scientific Center, Kyiv, 01601, Ukraine
[3]International Center of Future Science, Jilin University, Changchun, 130012, China
andrienko.j@gmail.com

Since 2010, the regular ozone observations at Kyiv-Goloseyev station have been carried out using Dobson 040 spectrophotometer. These observations at different wavelengths provide data for calculating the total ozone column (TOC) and Umkehr vertical ozone distribution profiles. In this report the Umkehr observation data was processed for the period 2010–

2017. We have developed the software based on the processing package of the World Ozone and UV radiation Data Centre (WOUDC). Before applying the algorithm UMK04 of calculation of the distribution of ozone with altitude, the observed data were repeatedly tested for compliance with WOUDC standards. The ozone altitude profiles were plotted.

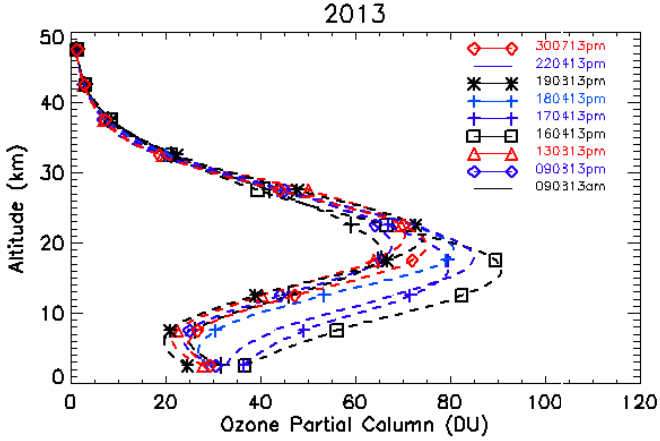

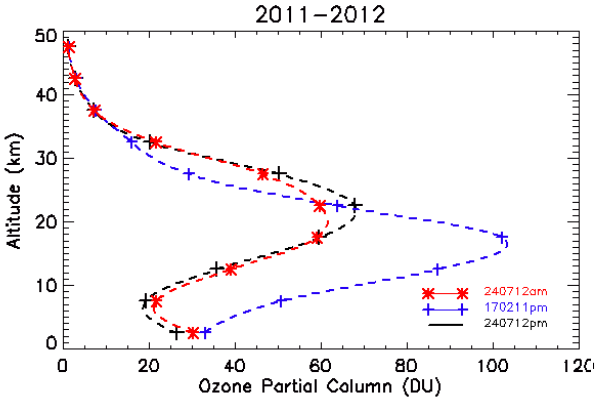

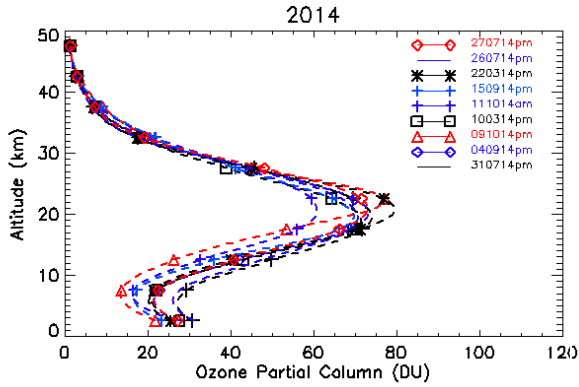

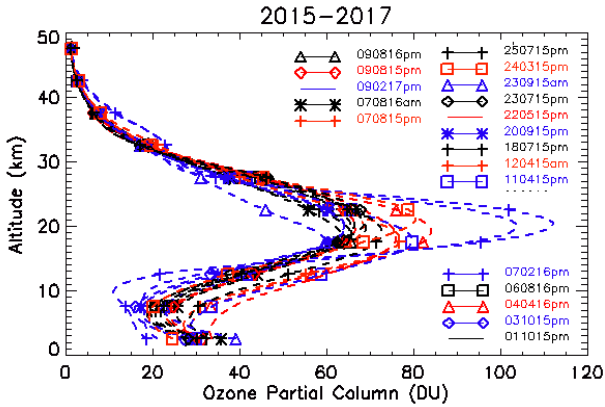

The general analysis of the obtained profiles indicates that the ozone distribution did not change sharply during the observed period. The maximum value of ozone partial column is in the range of 60–80 DU and corresponds to altitudes ~18–23 km.

Data processing software for the Umkehr ground-based observations at the Kyiv-Goloseyev station by Dobson spectrophotometer

Yu. Andrienko

Taras Shevchenko National University of Kyiv, Kyiv, 01601, Ukraine
andrienko.j@gmail.com

To build the altitude profiles of the atmosphere ozone distribution using Umkehr measurements, the software package has been developed using the World Ozone Data Center (WODC) processing package. Umkehr data obtained using the Dobson spectrophotometer requires significant pre-processing with the ability to control intermediate results because the standard WODC software packages requirements input format features. The special software was developed for pre-processing and analysis of the initial measurements, format data, ran the necessary standard procedures and construct the resulting ozone altitude profiles. Data files created during the processing can also be checked by the operator manually. The software allows performing data processing in a few days. With the help of the created software the observation data from 2010 to 2017 were processed. From the obtained altitude profiles it can be concluded that the maximum value of ozone concentration during the observation period is about 72 DU and variations of the maximum concentration in the profile are 15–20%.

Часова мінливість основних забруднюючих речовин в атмосферному повітрі міст України з низьким рівнем забруднення

Л. Надточій, М. Баштаннік, Т. Козленко, А. Уманець

Український гідрометеорологічний інститут, Київ, Україна
onoslyuda@uhmi.org.ua

Особливості забруднення атмосферного повітря в містах України з високим рівнем забруднення вивчені досить добре, з низьким – значно гірше, оскільки незначний вміст домішок в повітрі зазвичай не викликає хвилювань. Проте, згідно Директив ЄС, для створення планів управління якістю атмосферного повітря, необхідно в кожному місті проаналізувати стан забруднення повітря, сезонні та міжрічні зміни домішок, їх зв'язок з метеорологічними характеристиками і т.д.

Для дослідження використовувались дані середньомісячних концентрацій основних домішок (пил, SO_2, CO та NO_2) за період 2000

– 2014 рр. в містах України з низьким рівнем забруднення (Біла Церква, Бровари, Горішні Плавні, Житомир, Івано-Франківськ, Ізмаїл, Обухів, Олександрія, Полтава, Тернопіль, Українка, Харків, Чернігів). На основі цих даних проаналізовано сезонну мінливість забруднюючих речовин та встановлено закономірності її появи. Виявлено, що найкраще сезонні коливання прослідковуються для пилу.

Досліджено міжрічну мінливість забруднюючих речовин та виявлено її наявність для всіх домішок. Тренди забруднюючих речовин характеризуються різноспрямованістю (збільшення концентрацій чи зменшення) та добре узгоджуються із викидами (SO_2 – від стаціонарних джерел, NO_2 та CO – від пересувних). Отримано декілька груп міжрічних квазіперіодичних коливань, що узгоджуються із відомими природними коливаннями (2–3.7, 4–5.2, 6.2 роки). Амплітуди значущих коливань досягали змін до 50% від середніх багаторічних значень. Виявлено залежність міжрічних коливань забруднюючих речовин з метеорологічними характеристиками, що є ключовими для їх накопичення чи розсіювання в атмосфері.

Проведено класифікацію синоптичних умов за ступенем забруднення атмосферного повітря окремо для теплого та холодного періодів. Для розуміння отриманих результатів, в усіх досліджуваних містах, проаналізовано розташування постів спостережень щодо джерел емісії. Результати дослідження можуть бути використані при розташуванні нових об'єктів промисловості, створенні планів управління якістю повітря, тощо.

Penetration of electric field from the near-earth sources to the ionosphere under different configurations of the geomagnetic field

Yu.G. Rapoport[1,2], V.V. Grimalsky[3], S.S. Petrishchevskii[1], A.V. Grytsai[1], V.M. Ivchenko[1]

[1]Taras Shevchenko National University of Kyiv, Kyiv, Ukraine
[2]Space Research Institute, National Academy of Sciences of Ukraine and State Space Agency of Ukraine, Kyiv, Ukraine
[3]Autonomous University of State Morelos, Cuernavaca, Mexico
yuriy.rapoport@gmail.com

The problem of lithosphere–ionosphere coupling is important for searching the precursors of hazards like earthquakes, typhoons, etc. One of the channels of the coupling is the electromagnetic one, which results in the

penetration of the electromagnetic fields to the ionosphere and the magnetosphere from near-Earth sources. This work is devoted to the theoretical investigation of this channel of coupling under different configurations of the geomagnetic field lines. The 1st case is the penetration of the lines deeply into the magnetosphere, whereas the 2nd one is the return of these lines to the Earth's surface.

We have carried out a simulation of the electromagnetic field vertical propagation. The simulation is dynamic based on the equations for the locally horizontal components of the electric field. The proper boundary conditions are formulated.

The problem also considered in the quasi-electrostatic approach. In the 1st case the results of the dynamic simulations differ essentially from the quasi-electrostatic approach. Generally, the dynamic approach should be used to consider the problem of the ULF electric field penetration to the ionosphere. The results there do not depend on the position of the upper boundary. In the 2nd case, the results are practically the same within both approach. The correct consideration of this problem should be realized within the dynamic method, independently on the configurations of the geomagnetic field.

Small-scale fluctuations in plasma density of the lower ionosphere

Yu.V. Kyzyurov, P.P. Malovichko

Main Astronomical Observatory, NAS of Ukraine, Kyiv, Ukraine
kyzyurov@mao.kiev.ua

Neutral gas turbulence is an important source of fluctuations in plasma density of the lower ionosphere. We discuss small-scale plasma fluctuations resulted from turbulent mixing of the gas in the ionosphere and their dependence on the intensity of turbulence. The consideration was based on expression for the 3D spectrum of fluctuations induced by the turbulence in the ionosphere. The expression gave opportunity to obtain formulae for the 1D spectrum and for the rms level of fluctuations in the given wave-number range. Variability of the 1D spectra expected from rocket experiments was analysed for fluctuations in the altitude range 95-105 km under intensification of turbulent mixing (the rate of turbulent energy dissipation increased from 10 to 100 mW/kg). It was shown that the enhancement of turbulence results in the rise of the fluctuation level and in decrease in the slope of spectrum. The level of fluctuations with length-scales smaller 500 m near 95 km altitude increased from 2.7 to 2.8 % and near 105 km from

4.4 to 5.0%. If the fluctuation spectrum is approximated by a power law then the power index increased from –2.12 to –1.95 for h=95 km and from –1.97 to –1.82 for h=105 km. The obtained results are explained by decreasing of the dissipation length-scale from 14.4 to 8.1 m (h=95 km) and from 54.1 to 30.4 m (h=105 km) under the rise of the dissipation rate.

ІСТОРІЯ АСТРОНОМІЇ

HISTORY OF ASTRONOMY

Діяльність професора Б.Я. Букрєєва для розвитку астрономії

Л.С. Баштова

Державний політехнічний музей при «КПІ ім. Ігоря Сікорського»

Математику та її світ створювали багато вчених протягом дуже довгого часу. Кожне нове покоління включалося в творчість, зважаючи на властивий математиці спосіб пізнання світу, йшло далі, взявши за основу створене попередниками. З давніх-давен про славу математики, про її дивовижні результати, красу, логічність, стисліcть, бездоганну послідовність писали великі математики.

Г. Галілей (1564—1642) назвав Всесвіт найвеличнішою книгою природи, яка написана мовою математики. А. Ейнштейн наголошував, що математика справді-таки поезія, поезія думки, «поезія логіки ідей». Нині створюють математичні моделі які за допомогою обчислювальної техніки відтворюють та прогнозують певні явища в навколишньому світі, зокрема й в астрономії.

Професор Б. Я. Букреєв (1859–1962) служив математиці до свого 100-літнього ювілею. Він говорив — «Математика — богиня наук, біля її ніг — усі науки і в першу чергу фізика.» Вчений засновник школи київських геометрів. 25 років своєї діяльності присвятив Київському політехнічному інституту і, майже до останнього подиху, викладав в Київському університеті; залишився в історії математики як фахівець в галузі теорії спеціальних класів фуксових функцій, теорії поверхонь і геометрії, продовжувач учення Лобачевского.

Основні його роботи присвячені також математичному аналізу й алгебрі. Символічно, що він став одним з перших, хто дав інтерв'ю на радіо у зв'язку з польотом першої людини планети Земля в космос. На той момент йому був 101 рік.

Всі його дослідження сприяли розвитку астрономії та вивченню космосу, створенню географічних карт. Вчений розробляв та викладав спеціальні прикладні математичні курси для астрономічних розрахунків. Він виховав багато поколінь астрономів в стінах Київського університету, Української Академії Наук, Інституті математики (в Києві), які відточували свою майстерність завдяки інструментам Астрономічної обсерваторії Київського університету (засн. 1845 р.). Професор Б.Я. Букрєєв був засновником математичних кабінетів вишів та керівником наукових семінарів, ще наприкінці XIX, початку XX ст., був активним діячем київського Математичного товариства та Гуртка любителів астрономії.

Він випускник фізико-математичного відділення, 1882 р., факультету природничих наук Київського університету Св. Володимира, згодом сам викладав у цьому виші різні математичні дисципліни: математичний аналіз, основи диференціального й інтегрального числення з вправами, диференціальну геометрію, варіаційне числення, теорію і практику математичних інструментів та ін. Він став подовжувачем передових ідей своїх талановитих вчителів з математики - В. П. Єрмакова, М. Є. Ващенко-Захарченка і П. Е. Ромера; з фізики — М. П. Авенаріуса і М. М. Шиллера; з механіки — у І. І. Рахманінова, з астрономії — у М. Ф. Хандрікова. У своєму закордонному відряджені вивчав теоретичну фізику у Гельмгольца, практичну фізику у Кундта, філософію у Целлера, теорію функцій у Фукса і Вейєрштрасса. Його студентська робота «Геометрическая теория движения неизменной плоской фигуры в своей плоскости» була удостоєна великої золотої медалі (1880 р.). Вже в 1884 р. вийшла в світ його перша наукова робота «Аналитические выражения однозначных функций», яка стосувалась теорії функцій.

Наприкінці 90-х рр. XIX ст. його наукові інтереси зосередились головним чином на диференціальній геометрії. Саме цій темі була присвячена його праця «Выражение элемента поверхности постоянной кривизны в симметрических координатах», а пізніше — в 1900 р., була видана його відома книга «Курс приложений дифференциального и интегрального исчисления к геометри — элементы теории поверхностей». В ній автор вперше застосував симетричні координати. В основу курсу теорії поверхонь він поклав вивчення двох диференціальних форм. Детально освітлені питання відображення поверхонь, зокрема конформні відображення, вигинання. Вони стали основою теорії побудови географічних карт. В подальшому його дослідження зосереджуються на геометрії Лобачевского.

На підставі викладання математичних курсів він розробив посібники «Вступ до теорії рядів» (1905), «Елементи теорії визначників» (1908, 1912). В 1928 р. Борис Якович написав курс «Диференційна геометрія», а в 1930 р. статтю «До теорії просторових кривих». В цьому ж році вийшов з друку підручник Б. Я. Букреєва «Вступ до варіаційного числення». В ньому вміщена велика кількість класичних та нових задач з різних галузей математики, астрономії, механіки та техніки. Математик вважав, що варіаційне числення займає центральне місце серед фізико-математичних наук.

Праці вченого (понад 150) є вагомим внеском в національну наукову скарбницю, а його учні серед яких академіки АН УРСР М. П. Кравчук, Д. О. Граве, М. М. Крилов, Г. В. Пфейффер, члени-кореспонденти Н. Х. Орлов, Ю. Д.Соколов, професори В. В. Добровольський,

О. С. Смогоржевський, В.О.Вірченко, В.Г.Кручиненко та багато інших, є гордістю української математики, небесної механіки та астрономії.

Experience of Recreation of Historical Tools of Astronomy and Navigation under the project "Master Terebrus"

V.S. Buravchenko

Kyiv National University of Construction and Architecture

Living history is a popular direction of research of realities of the past which unites archaeologists, craftsmen and volunteers from many countries. Results obtained through living history complement archeological and literature information on technologies, details of daily life, fashions and tactics of the past.

Though military aspects of living history are mostly known, other directions also exist, including recreation of the history of historical scientific instruments. The project started in 2016 from the objective of creation of a portable sundial of appropriate type which could be used in living history sailing campaigns using a recreated XVII century Ukrainian boat at Dnieper for tasks of time-telling and navigation.

By now over 40 types of historical scientific instruments were recreated and tested in the field under the Master Terebrus project ranging from ancient Roman sundials till XVII century astronomical analog computers modeling processes of geocentrical and heliocentrical models of Universe.

Though dependent on accuracy of used data, quality of measurements and their size, historical instruments provided surprising level of accuracy which was more than satisfied needs of scientists of Middle ages.

Олександр Кузьмич Осипов і Станція візуально-оптичних спостережень штучних супутників Землі за вивченням колекції Астрономічного музею

Л.В.Казанцева

Астроногмічна обсерваторія
Київського національного університету імені Тараса Шевченка

Наприкінці літа 2020 р. виповниться 100 років з дня народження О.К.Осипова, одного із співробітників і мешканців Київської університетської обсерваторії. Росіянин за походженням, випускник

Свердловського університету він фактично став співробітником Обсерваторії в часи Другої світової, коли колектив наукової установи працював в евакуації. І з того часу все його наукове і особисте життя проминуло на Київській Обсерваторній гірці. На жаль, його біографія не увійшла до університетських довідників, бо час, в який він працював, і обставини не дозволили свого часу Осипову стати професором, але декілька поколінь випускників кафедри астрономії до сьогодні вважають його своїм вчителем.

У період 1957-1989 рр Олександр Кузьмич незмінно очолював Станцію спостережень ШСЗ. Він стояв у витоків її створення, налагоджував перші спостереження, навчав і організовував спостерігачів, встановлював і досліджував обладнання, керував різними спостережними програмами та науковими темами зі спостережень супутників.

В той же час темою наукових інтересів О.К.Осипова з молодих років залишався Місяць, дослідження його руху і фігури. Він проводив багато фотографічних спостережень супутника Землі в різних фазах на фоні зір, організовував, збирав і публікував в Інформаційних повідомленнях АО спостереження покрить зірок і планет Місяцем на теренах країни, власноручно проводячи багатогодинні обчислення на механічній «машині Яковкіна», одним із перших у світі почав виїжджати з колегами в експедиції для спостережень дотичних покрить. Йому вдалося відкрити декілька тісних подвійних зірок зі спостережень явищ покрить.

Олександр Кузьмич був чудовим популяризатором астрономії, він проводив спостережні екскурсії для населення, свого часу вів ряд рубрик в місцевих газетах і журналах, виступав на радіо з просвітницькими програмами. Редагував науково-популярні видання, керував курсовими роботами студентів і був одним із головних «відповідачів» на листи аматорів в Обсерваторії.

Останнє десятиліття свого життя О.К. Осипов присвятив створенню Музею в Обсерваторії. Його зусиллями були започатковані музейні фонди і колекції. Зокрема, одна із найбільших з них присвячена роботі Станції візуально-оптичних спостережень ШСЗ. Саме Олександр Кузьмич зберіг всю документацію і матеріали роботи станції від оголошення про її створення до закриття. Це офіційні документи і розпорядження різних адміністративних і наукових структур, листування, наукові і популярні видання, рукописи результатів спостережень і фотоматеріали, інструменти і саморобні пристрої, публікації в ЗМІ, звіти станції за різними програмами, журнали спостережень і протоколи наукового семінару Станції,

навчальні плакати і стінні газети, поштові знаки та значки з тематики космонавтики. Все це дає можливість детально вивчити історію початку роботи маловідомої сторінки космонавтики, а саме наземного астрономічного супроводу.

В Музеї також зберігаються спогади вдячних учнів-спостерігачів ШСЗ, для яких робота на Станції була чудовою астрономічною практикою і можливістю детально вивчити зоряне небо. Зберігаються також і копії свідоцтв про присвоєння імені Олександра Кузьмича Осипова двом астероїдам, відкритим в Україні.

Проект «Музейна бібліотека» Астрономічного музею АО

Казанцева Л.В., Казанцев А.М.

Астрономічний музей Астрономічної обсерваторії
Київського національного університету імені Тараса Шевченка

Проект Астрономічного музею АО під умовною назвою «Музейна бібліотека» є першим кроком на шляху оцифровки музейних фондів, відкриття широкого доступу до них та створення віртуальних тематичних експозицій.

Колекції нашого музею складаються не тільки з інструментів, приладів, матеріалів, рідкісних та саморобних пристроїв, які використовували під час астрономічних спостережень та їх обробки, особистих речей співробітників, рукописів та фотографічного матеріалу. Зібрана й велика кількість різноманітних друкованих видань.

Цей тип музейних предметів, свого часу оприлюднений, не порушує авторських прав та інтелектуальної власності. Водночас він несе багато інформації, як біографічного змісту, так і стосується багатьох тем історії розвитку астрономії.

Представлено окремі і періодичні наукові видання, підготовлені в Обсерваторії, відбитки публікацій співробітників або подаровані їм колегами та учнями з автографами та присвятами, книги і статті в науково-популярних часописах та в ЗМІ, замітки, спогади та розширені огляди про Обсерваторію, її співробітників, описи астрономічних явищ та події та багато іншого.

Цікава збірка підручників та посібників з астрономічних та суміжних з ними дисциплін, довідників, зокрема різних астрономічних календарів. Зоряні карти і атласи, географічні мапи, навчальні плакати та таблиці, описи та інструкції з використання до інструментів,

буклети окремих музеїв, збірки та програми астрономічних конференцій, поштові знаки на астрономічну й космічну тематику та інше можна переглянути на сайті Астрономічного музею, Частина матеріалу вже виставлена, буде тривати доповнення матеріалів. Пошук можна вести за особистостями, тематикою та роками.

Джерела надходження цих друкованих матеріалів різні. В першу чергу це наукові архіви колишніх співробітників АО, передані Музею видання і публікації інших наукових і музейних установ. Велику частину збірки складають видання, зібрані свого часу Київським Відділенням Всесоюзного Астрономо-Геодезичного Товариства, яке довгий час базувалося в стінах АО і мало свою бібліотеку, фонди якої поповнювалися як з власних колекцій її членів, так і були придбані на кошти, зібрані через членські внески. Крім того, є декілька книг з бібліотеки Київського гуртка аматорів астрономії, що працював у місті у 1910-1924 рр, э й видання та публікації, подаровані відвідувачами Музею.

Майже кожен екземпляр «Музейної бібліотеки» є не просто книгою чи публікацією, а несе свою історію, належить до певної музейної колекції, виступає вже як музейний предмет і є об'єктом досліджень. Запропонований проект має на меті ознайомити з маловідомими експонатами Астрономічного музею, бути корисним історикам науки, краєзнавцям та всім зацікавленим.

Виробництво аерофотоплівок на ВО «Свема» у м. Шостка Сумської області

М.Г. Кокшайкін

Шосткинський краєзнавчий музей

Виробниче об'єднання «Свема» - флагман хіміко-фотографічної промисловості СРСР, який пройшов шлях від експериментально-дослідного виробництва «Мала кіноплівка» до ВАТ Акціонерна компанія «СВЕМА». Основною продукцією цього підприємства, з 1929 р. до кінця минулого сторіччя, був широкий асортимент кіно-фотоматеріалів і магнітних носіїв інформації для професійного та аматорського кіно і фотографії, медицини, науки та техніки, культури та інших сфер діяльності людини.

1 вересня 1928 року було укладено договір з французькою фірмою «Люм'єр» про будівництво радянської кіноплівочної фабрики потужністю 50 млн. погонних метрів за рік. Згідно договору, фірма

зобов'язалася надати СРСР технічну допомогу в організації виробництва всіх видів кінофотоплівок (кіноплівки, авіаплівки, рентгенплівки та ін.). Фірма зобов'язалася розробити проект фабрики, поставити необхідне устаткування та навчити кадри радянських фахівців з виробництва кінофотоплівки. Але, порушуючи умови договору, представники фірми «Люм'єр» затримували надання технічної документації, не допускали шосткинських інженерів до приготування емульсій та покинули Шостку перед початком монтажу обладнання нової фабрики. Тому монтаж був виконаний власними силами і 1 жовтня 1931 р. шосткинську фабрику кіноплівки № 6 було введено в експлуатацію. Спочатку фабрика виробляла лише позитивні кіноплівки, а вже у 1933-34 роках було опановано виробництво негативних кіноплівок та перших вітчизняних авіаплівок.

У 1940 р. колектив фабрики майже вдвічі збільшив її проектну потужність до 96,5 млн. п. м. та опанував масове виробництво близько 30 видів кіноплівок, серед яких СЧС-1 («светочувствительная советская» тип-1), СЧС-2, СЧС-4 та аероплівка «Тип-5» з чутливістю 250 Х и Д (*=11 од. ГОСТ).*

Після звільнення Шостки у 1943р. від нацистських окупантів, шосткинську фабрику №6 перейменували на фабрику №3 и почалося відновлення виробництва. У 1948 р. опановано випуск кольорових кіноплівок. Наприкінці 1954 року фабрикою були випущені перші в СРСР 3754 тис. метрів магнітної стрічки для звукозапису. А у 1955р. опановано випуск кіноплівок на вогнебезпечній триацетатній основі.

У 1950-ті роки Шосткинська фабрика №3 випускає панхроматичну аероплівку «тип-10», а пізніше Шосткинський філіал НДКФІ розробив та впровадив у виробництво на фабриці плівку «тип-17», а вже у 1960-ті роки розроблені ізопанхроматичні плівки «тип-22», «тип-25» та інші.

Розробка та впровадження нового апаратурного забезпечення технологічних процесів та досвід освоєння кольорових негативних та позитивних кіноплівок сприяли впровадженню спектрозональної фотографії та аерофотоплівок (*СН-2, СН-4, СН-5, а пізніше СН-6, СН-6М, СН-10, СН-15, СН-23*).

У зв'язку з необхідністю виготовлення довгометражних аероплівок довжиною до 3000 п.м., у 1985 р. на виробничому об'єднанні «Свема» було введено в експлуатацію «Технологічний комплекс спецплівок для детального та наддетального спостереження поверхні Землі та всіх видів аерофотозйомок».

Як «астрономічні зубри» врятували Полтавську Гравіметричну обсерваторію в 1934-1938 рр.

А.О. Корсунь[1], М.В. Лубков[2]

[1] Головна астрономічна обсерваторія НАНУ
[2]Полтавська гравіметрична обсерваторія Ін-ту геофізики ім. С.І. Субботіна НАНУ

Здавалося, що про видатного вченого Олександра Яковича Орлова, академіка УАН в 1919-1922рр., член-кор.АН СРСР з 1927 р., академіка АН УРСР з 1939 р., немало написано і його біографами, і учнями, і послідовниками вченого, і що немає таємних місць в біографії успішного вченого . Хоча все ж усі відмічали, що О.Я.Орлов, заснувавши Полтавську гравіметричну обсерваторію (ПГО) ще в 1926 році і організувавши її чітку і продуктивну роботу, як одного з успішних і важливих наукових закладів зі світовим визнанням, покинув Полтаву і Обсерваторію в 1934-1938 роках, переїхавши в Москву на роботу до Державного астрономічного інституту ім. П.К. Штернберга та читання лекцій в Геодезичному інституті.

Але чому стався переїзд? Ця подія переїзду О.Я.Орлова сприймалася авторами без усяких пояснень, а може цей факт просто замовчувався, бо такі тоді були сурові 30-ті роки в СРСР.

Найдений в архіві ПГО один документ, а саме – чернетка незакінченого рукопису О.Я.Орлова «Астрономічні зубри» (від 15 листопада 1938 року), пояснює ці доволі сумні причини далеких історичних подій. Про це і піде розповідь.

Popularization of astronomy in the language of national minorities in the Ukraine in 1920-1930s.

M. V. Lashko

Main Astronomical Observatory NAS of Ukraine

After the establishment of Soviet power, the Bolsheviks faced with hostility of the population and were forced to make certain concessions. One of them was the policy of national districts, which was pursued in the 1920 - 1930s and was aimed primarily at the introduction of the language of national minorities in places of their compact residence - in schools, in the press and other spheres of cultural life. Among them were astronomical

popular-scientific publications.

During the period from 1926 to 1937, four popular-scientific brochures (1 in Polish and 3 in German) by state publishing houses were published. First was N. Lebiediew's brochure "Kedy bedzie koniec swiata" (1926) (M. Lebedev. When the World Will End) which introduced readers with the modern theories of the universe, the origin of the solar system, and refuted myths and various versions of The End of the World.

The range of German-language brochures was somewhat wider. S. Waldhard's brochure "Gibt es leben auf anderen planeten" (S. Waldgart. Is there life on other planets) first appeared in 1930, brochure introduced readers to the climatic conditions on Earth, Venus, Mars and other planets in the solar system. The results of the study of Mars by Percival Lovell were also considered.

Next was M. Bronstein's brochure "Der Sonnenstoff" (1937) (M. Bronstein. Solar matter). Written by a prominent physicist, this brochure was a fascinating story of the discovery of helium, a substance first discovered on the Sun and only many years later on Earth.

The last was K. Bajew und W. Schischakow brochure "Die wahrheit uber den Himmel" (1937) (K. Baev, V. Shishakov. The truth about the sky), which told about the evolution of ideas about the structure of the universe. Also was given information about the essence of solar and lunar eclipses, about the Copernicus and Galileo ideas and discoveries. The book ended with a chapter about the infinity of the universe and the views of J. Bruno.

As we can see, these publications were diverse and aimed to widely promote astronomical knowledge among national minorities. In this publication, we have only briefly analyzed these publications. This will be discussed in more detail in further research.

Героические страницы из истории Киевской астрономической обсерватории

К.М. Ненахова

Главная астрономическая обверватория НАН Украины

Во время немецко-фашистской оккупации Киева (1941—1943 гг.) сотрудники Обсерватории не были отстранёнными созерцателями событий. В меру своих возможностей они оказывали сопротивление врагу, а некоторые даже погибли. В докладе представлены три страницы из 175-летней истории славного научного учреждения.

Первая часть («первая страница») посвящена жизни и деятельности

Николая Максимовича Остафова — аспиранта (1936—1939 гг.), а затем сотрудника Киевской астрономической обсерватории.

Во второй части («вторая страница») рассказывается об организации на территории Обсерватории приёма сводок Совинформбюро.

Третья часть («третья страница») повествует об укрывательстве лиц еврейской национальности.

Музеї Київського національного університету імені Тараса Шевченка на туристичній мапі Києва

Л.Г. Самойленко

Археологічний музей Київського національного університету імені Тараса Шевченка

Київ туристичний, як і годиться місту з більш як 1500-літньою історією, столиці європейської держави, має безліч принад: неповторна архітектура, особлива природа і топографія, безліч музеїв, галерей, виставок, культурних і освітніх закладів, які можуть зацікавити як киян, так і гостей міста.

А де у цьому розмаїтті культурного надбання місце нашого університету? Червоний корпус як архітектурна пам’ятка, пізнаваний і відомий за межами країни, може вважатися однією з емблем міста. Парк перед корпусом і ботанічний сад імені О. Фоміна, тісно пов’язані з історією університету і справедливо належать до унікальних пам’яток паркового мистецтва. Як заклад вищої освіти – належить до найстарших університетів в Україні, що веде свій літопис 185 років і посідає флагманські позиції у сучасних рейтингах.

Музейне надбання нашого університету теж можна вважати непересічним – він опікується найбільшою кількістю різнопрофільних музеїв у порівнянні з іншими університетами України, щоправда відомо про це доволі обмеженому колу зацікавлених осіб, тим паче, не позначено на туристичній мапі міста.

Кожен з наших музеїв має свою цікаву історію заснування і розвитку, тісно пов’язану як з освітнім процесом, так і з діяльністю наукових шкіл або вдатних діячів науки нашого університету. Майже всі музеї мають меморіальні розділи, або куточки, присвячені відомим діячам університетської освіти і науки та їх здобуткам. Та навіть у офіційних документах університету точної їх кількості годі й шукати.

Зараз на сайті університету у розділі «Музеї і музейні колекції» можна знайти інформацію про 9 музеїв, у звітах ректора налічують лише п'ять.

Спробуємо перерахувати більш прискіпливо. 1. Музеї історії університету; 2. Астрономічний музей; 3. Археологічний музей; 4. Ботанічний музей; 5. Геологічний музей; 6. Етнографічний музей; 7. Зоологічний музей; 8. Лінгвістичний музей; 9. Музей природи Канівського природного заповідника; 10. Музей історії ботанічного саду імені О.Фоміна а також й сам ботсад з його живими колекціями у оранжерейних комплексах можна вважати музеєм – 11; 12. Музей Олеся Гончара, наймолодший, відкрито 2018 р.. І нарешті ще два музеї, що від 2013 р. фігурують у офіційних довідниках серед музеїв університету, але які так і не прижилися у музейній родині – Музей квартира академіка А.Б. Сєвєрного і Музей астрономії Кримської астрофізичної обсерваторії. Отже, загалом – чотирнадцять.

Проте сучасна нормативно-правова база, яка регламентує діяльність музеїв у закладах вищої освіти України, не забезпечує їх повноцінне функціонування і охорону на гідному рівні. Музеї не згадуються у ЗУ «Про освіту» і «Про вищу освіту», хоч зберігають значну частину культурно-історичної спадщини України і мають розгалужену музейну мережу у своєму складі. Накази Міністерства освіти і науки, або Міністерства культури, що передбачали обов'язковий облік університетських музеїв та встановлювали певні процедури і стандарти забезпечення діяльності таких музеїв втратили чинність ще у 2014-2015 рр., а нові так і прийнято. Це гальмує розвиток наших музеїв через залишковий принцип у їх фінансуванні і недостатнє кадрове забезпечення, що у свою чергу робить їх маловідомими.

«Чорні скрині» і Космос

Ю.О. Шевела

Державний музей авіації ім. О.К. Антонова

Коли ми згадуємо історію перших космічних польотів, то перше, що згадується - Гагарінське «Поехали!» І ніколи не задумуємось, а яка апаратура донесла і зберегла для нас це коротке, і вже історичне слово? А між тим… Цю історію творили у Києві! А поштовхом для цього були… «ЧОРНІ СКРИНІ»! На жаль, тепер всім сумно відомі! Саме так, коли в кінці 50-х рр. минулого століття весь світ забезпечив

свої літаки бортовими самописцями і магнітофонами (котрі зараз знають як «чорні скрині»), виникла необхідність такого магнітофона і в СРСР. Базовою моделлю був невеличкий (не серійний) магнітофон «Ліра», створений у Київському п/я №1 (пізніше відоме в/о «Комуніст»). Для серійної розробки таких магнітофонів у 1959 році частину колективу перевели у новий п/я, спеціально для цього створений, - НДІ Електромеханічних приладів, котрий входив у об'єднання «Маяк»! І робота призупинилась, а причина, - Космос! У 1960 році у космічний політ відправились дві собачки «Бєлка» і «Стрелка» і, для запису їх «голосів» цим НДІ був створений перший космічний магнітофон «Звєзда»! Носієм магнітного запису був дріт (діаметром 0,03мм), котрий крутився по колу, і міг записувати до двох годин! А зовні, - звичайний залізний короб з роз'ємом, - прообраз «чорної скрині»! Розробка магнітофона для літаків був завершена тільки у 1961 році, він так і називався - МС-61 (Магнитофон Самолётный 1961г). Серійно вироблявся на Вільнюському підприємстві «Вільма», де його «вдягнули» у термоконтейнер, - перша «чорна скриня»! А магнітофон «Звєзда» був на борту всіх КК«Востоків» і «Восходів». Саме він і доніс до нас Гагарінське «Поєхали»! І вся розшифровка і перезапис на звичайні носії проводився у Києві, у НДІ ЕМП! У 1964 році був розроблений новий, модифікований дво-дорожечний магнітофон «Звєзда-64», котрий застосовувався на безпілотних супутниках.

У 1967 році, для висадки на Місяць був створений скафандр, а про магнітофон… Згадали вже тоді, коли скафандр був створений. Після деяких невдалих спроб, за розробку взявся Київський НДІ ЕМП, і, протягом місяця, був створений абсолютно унікальний магнітофон «Малиш»! Вагу мав всього 400гр, магнітний запис був на дроті, а для цього були розроблені касети, з магнітними головками всередині! І головне, - їх можливо було міняти навіть у рукавичках скафандра! Керівник Місячної прогами К.Феоктістов був у захваті від «Малиша» і миттєво підписав наказ про серійний випуск, але Місячну програму у тому ж 1967 році було закрито, великої серії не бкло. Магнітофони «Малиш», різних модифікацій, були на всіх КК«Союзах» (з 1-го по 18-й) і на всіх ДОС «Салют»!

Для польоту «Союз-Аполлон» магнітофон «Малиш» був модифікований, серійні називалися магнітофон «Пигмей», а пізніше, нова модель – «Гном». Ці магнітофони використовувались у всіх пілотованих космічних польотах (і на КС «Мир») до кінця існування СРСР!

Безпосередньо, до «чорних скриньок» НДІ ЕМП повернувся у 1966

році, - розроблений магнітофон «Марс». Модифіковані версії магнітофонів МС-61 і «Марс», різними підприємствами виробляються до сьогодення!

З усіма моделями і історією створення «чорних скриньок» та магнітофонами для космічних польотів (пілотованих і не пілотованих) можна ознайомитись у новій експозиції Державного Музею Авіації ім. О.К.Антонова.

Компаси Безарда: вікова історія

Ю.О. Шевела

Державний музей авіації ім. О.К. Антонова

У 1902 році Іоганом Ріттером фон Безардом (1871-1954) був запатентований компас абсолютно нової конструкції. У порівнянні з попередніми конструкціями компасів тих часів компас Безарда мав нову концепцію та приніс чимало інновацій. Нові функції були наступними: кришка мала дві прорізі з боків для забезпечення точності прицілювання; мав дзеркало, в якому можна було прочитати циферблат; циферблат спочатку був позначений червоними підписами «Схід/Захід»; на німецькій мові; мав дуже зручні мітки при використанні з картами; у кришці компаса був встановлений клінометр. Компас миттєво був прийнятий у Австрійській імперській армії а згодом і у німецькій. Винахідник продав дерев'яну модель компаса німецькому виробнику барометрів LUFFT. З 1917 року компас мав індивідуальну назву «Original Bezard» і мав два варіанта, - військовий і громадянський.

У період між Першою світовою війною і Другою патент на виробництво варіантів компасів Безарда придбали всі європейські країни а також США, Канада, Бразилія, Японія і навіть Російська імперія! Окрім військового і загальногромадянського варіанта були і варіанти спец. призначення: для мандрівників, астрономів (астролябія), тощо.

На основі компаса Безарда Ольгієром Якубовським у Польщі в 1933 році була розроблена нова система магнітного схилення

Країни, у які компанія LUFFT не експортувала свою продукцію, великі виробники виготовляли компаси Безарда, ставлячи на них свої імена і логотипи. Напр. Cornelius Knudsen у Данії, Gamma I MOM в Угорщині, OPTOS у Чехії, IOR у Румунії, FPM у ГДР (після Другої світової війни), Физелектроприбор у СРСР.

Після Другої світової війни компаси Безарда вироблялися і продовжують вироблятися у ФРН. Деякі країни східного блоку, виробляли незапатентовані варіанти – так звані імітації (напр. Чехословаччина, Румунія, Польща).